CADMD

2025

Proceedings of the XXXIII International Conference

Wydział Elektryczny

Faculty of Electrical Engineering
Białystok University of Technology, Poland

Department of Computer Design Systems

Department of Computer Design Systems
Lviv Polytechnic National University, Ukraine

Faculty of Mechanical Engineering and Robotics
AGH University of Science and Technology, Poland

ipbm pw

The Institute of Machine Design Fundamentals
Warsaw University of Technology, Poland

Białystok, Poland,
11-13 December, 2025

Under the honorary patronage of:

Professor Marta Kosior-Kazberuk BUT Rector
Białystok University of Technology

Professor Nataliia Shakhovska LPNU Rector
Lviv Polytechnic University

President of the Main Board
SIMP (Stowarzyszenie Inzynierów i Techników Mechaników Polskich)
Polish Society of Mechanical Engineers and Technicians

President of the Main Board
SEP (Stowarzyszenie Elektryków Polskich)
Association of Polish Electrical Engineers

Strategic Partner of the Conference

ORGANIZED BY

Faculty of Electrical Engineering
Białystok University of Technology
Poland

Fundacja na rzecz rozwoju Politechniki Białostockiej, Poland

Department of Computer Aided Systems
Lviv Polytechnic National University
Ukraine

Faculty of Mechanical Engineering and Robotics
AGH University of Science and Technology
Poland

The Institute of Machine Design Fundamentals
Warsaw University of Technology
Poland

Strategic Partner

Partners:

Fundacja Na Rzecz Rozwoju Politechniki Białostockiej
Oddział SIMP Białystok
Oddział SEP Białystok

Media patronage:

Radio Akadera

ORGANIZING COMMITTEE

PROCEEDINGS

The conference materials are presented on problems in the field of MCAD and ECAD techniques and CAx tools in automation of machine and mechanism design), identification, modelling of processes and systems, UAV, UGV, robotics, automation, electromechanical systems, application of information technologies in engineering, software, programming and algorithms, additive technologies, reverse engineering, databases, CAx engineering education, educational methods and Internet technologies in education.

INTERNATIONAL PROGRAM COMMITTEE

Prof. Aivars Aboltins	Latvia University of Life Sciences and Technologies, Latvia
Prof. Marian Banaś	AGH University of Science and Technology, Poland
Prof. Andrzej Burghardt	Rzeszow University of Technology, Poland
Prof. Bogusław Butryło	Białystok Univerity of Technology, Poland
Prof. Zhuoqi Cheng	The Maersk Mc-Kinney Moller Institute, SDU, Odense, Denmark
Prof. Moises Diaz	Universidad de Las Palmas de Gran Canaria, Spain
Prof. Krzysztof Gaska	Silesian University of Technology, Poland
Prof. Len Gelman	The University of Huddersfield, United Kingdom
Prof. Marek Iwaniec	AGH University of Science and Technology, Poland
Prof. Jerzy Józwik	Lublin University of Technology, Poland
Prof. Tadeusz Kamisiński	AGH University of Science and Technology, Poland
Dr. Andriy Kernytskyy	Lviv Polytechnic National University, Ukraine
Dr. Krzysztof Kołodziejczyk	AGH University of Science and Technology, Poland
Prof. Petro Kosobutsky	Lviv Polytechnic National University, Ukraine
Prof. Krzysztof Krawiec	Poznań University of Technolog, Poland
Prof. Michal Kuciej	Białystok University of Technology, Poland
Prof. Mykhailo Lobur	Lviv Polytechnic National University, Ukraine
Prof. Bogusław Łasarz	Silesian University of Technology, Poland
Prof. Slobodan Lubura	University of East Sarajevo, Bosnia and Herzegovina
Dr. Andrzej Łukaszewicz	Białystok University of Technology, Poland
Prof. Marek Macko	Kazimierz Wielki University in Bydgoszcz, Poland
Prof. Oleh Matviykiv	Lviv Polytechnic National University, Ukraine
DSc. Mykhaylo Melnyk	Lviv Polytechnic National University, Ukraine
Prof. Krzysztof Mendrok	AGH University of Science and Technology, Poland
Prof. Witold Pawłowski	Łódź University of Technology, Poland
Prof. Dariusz Perkowski	Białystok University of Technology, Poland
Prof. Milica Petrović	University of Belgrade, Serbia
Prof. Jerzy Pokojski	Warsaw University of Technology, Poland

Prof. Krzysztof Pytel	AGH University of Science and Technology
Prof. Patryk Różyło	Lublin University of Technology, Poland
Prof. Wojtek Sitek	Silesian University of Technology, Poland
Prof. Yaroslav Sokolovsky	Lviv Polytechnic National University, Ukraine
Prof. Tadeusz Telejko	AGH University of Science and Technology, Poland
Prof. Wiesław Tarełko	Maritime Academy in Gdynia, Poland
Prof. Anna Timofiejczuk	Silesian University of Technology, Poland
Dr. Roman Trochimczuk	Białystok University of Technology, Poland
Prof. Vasileios Moulianitis	University of the Peloponnese, Patras, Greece
Prof. Rafał Wiśniowski	AGH University of Science and Technology, Poland
Prof. Marek Wojtyra	Warsaw University of Technology, Poland
Prof. Marek Wyleżoł	Silesian University of Technology, Poland
Prof. Vladyslav Yevsieiev	Kharkiv National University of Radio Electronics, Ukraine

CONTENT

XXXIII International Conference
CAD IN MACHINERY DESIGN IMPLEMENTATION AND EDUCATIONAL ISSUES
11 - 13 December 2025, Białystok, Poland

APPROXIMATED WIDEBAND ELECTROMAGNETIC MODELS OF DISPERSIVE COMPLEX MATERIALS

Bogusław Butryło
Białystok University of Technology
b.butrylo@bedu.pl

ABSTRACT

Due to the complex internal structure, numerical analysis of complex dispersive materials with periodic structure is difficult, computationally expensive. In order to overcome limitations a uniform material model can be formulated. A scheme for parameter homogenization of complex materials with dispersive inclusions is discussed in the paper.

KEYWORDS: **broadband analysis, dispersive complex dielectrics, frequency selective materials.**

I. INTRODUCTION

Numerical analysis of electromagnetic (EM) phenomena in some composite materials and computer-aided design of systems containing such materials requires specific models to describe their electrical properties [1]. The formulation of an effective, broadband (including GHz band) model of a composite material involves consideration of the material composition, size and geometry of inclusions and their distribution in the host material [2]. The subject of this article is broadband models of composite materials, which exhibit electrical dispersion effects in the selected frequency band.

II. PROBLEM FORMULATION AND APPROXIMATION SCHEME

The subject of the analysis is a composite material with inclusions (fibres) that form a 2D periodic structure (Fig. 1).

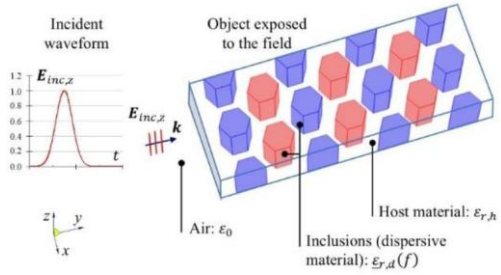

Fig. 1. The general view of the model (material with dispersive inclusions)

Determination of the simple, reliable homogenized models remains a challenging issue for materials with complex structures, with components having significantly different electrical properties, when the size of particles is comparable to wavelength of the propagated electromagnetic waves.

The determined equivalent model of permittivity $\varepsilon_{r,ef}$ is applied to the wave equation (wideband form).

$$\frac{\partial^2 \varepsilon_0 \varepsilon_\infty \boldsymbol{E}}{\partial t^2} + \varepsilon_0 \frac{\partial^2 \chi_{ef} * \boldsymbol{E}}{\partial t^2} + \sigma \frac{\partial \boldsymbol{E}}{\partial t} + \mathrm{rot}\left(\frac{1}{\mu_0 \mu_r} \mathrm{rot}\, \boldsymbol{E}\right) = 0, \quad (1)$$

where: $\boldsymbol{E}$ is the electric field intensity vector, χ_{ef} is the inverse Fourier transform of the complex susceptibility function. The form of equivalent homogenized model of permittivity is reduced and adjusted to the further requirements of the wideband time domain algorithm (e.g. FDTD, FETD)

$$\underline{\varepsilon}_{r,ef} = \varepsilon_\infty + \underline{\chi}_{ef}(\omega) = \varepsilon_\infty + \sum_{a=1}^{A} \left(\underline{\chi}_{D,s,a} + \underline{\chi}_{L,s,a}\right), \quad (2)$$

where $\varepsilon_{\infty,s}$ is the near infrared band permittivity, $\left\{\underline{\chi}_{D,s,a}, \underline{\chi}_{L,s,a}\right\}$ is the a-th either relaxation or resonant submodel of electric susceptibility $\underline{\chi}_{e,f}$.

III. RESULTS

As a result of the described procedure, the parameters of the homogenized equivalent model were calculated. The frequency selective properties of the analysed composite (heterogeneous structure) are compared in Fig. 2:
a) fA = 5 GHz: EM wave is dumped in the material;
b) fB = 8 GHz: EM wave propagates through the dispersive medium; negligible dumping of EM wave.

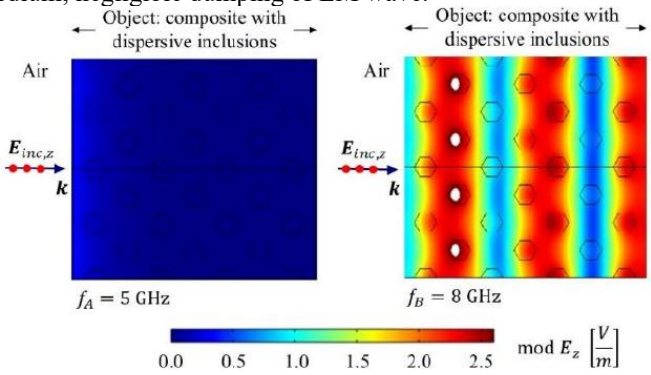

Fig. 2. Modulus of electric field intensity in the dispersive material: (left) frequency of excitation fA = 5 GHz; (right) fB = 8 GHz.

The created approximated homogeneous models of materials reduce the computational complexity. It reflects properties of the initial complex material, including the potential dispersion of the resultant electrical properties

REFERENCES

[1] Wu Q., Guang X., Zheng R., "Intelligent reflecting surface-aided wireless energy and information transmission: an overview", Proceedings of the IEEE, vol. 110, no. 1, pp. 150-170, https://doi.org/10.1109/JPROC.2021.3121790, 2022

[2] Zygridis T., Kantartzis N., "Finite-difference wave-propagation models for dispersive media: impact of space-time discretization", COMPEL – The International Journal for Computation and Mathematics in Electrical and Electronic Engineering, vol. 41, no. 3, pp. 1024-1040, https://doi.org/0.1108/COMPEL-02-2021-0066, 2022

XXXIII International Conference
CAD IN MACHINERY DESIGN IMPLEMENTATION AND EDUCATIONAL ISSUES
11 - 13 December 2025, Białystok, Poland

DEVELOPMENT OF AN IOT-BASED SYSTEM FOR REAL-TIME ASSESSMENT OF ARCHER STABILITY

Mykhaylo Lobur[1], Mykhaylo Melnyk[1], Krzysztof Kołodziejczyk[2], Volodymyr Havran[1],
Nazarii Khromiak[1], Dzvenyslava Chernyk[1]
Lviv Polytechnic National University[1]
mykhaylo.v.lobur@lpnu.ua, mykhaylo.r.melnyk@lpnu.ua, volodymyr.b.havran@lpnu.ua,
nazarii.khromiak.pp.2022@lpnu.ua, dzvenyslava.chernyk.pp.2022@lpnu.ua
The AGH University of Krakow[2]
krkolodz@agh.edu.pl

ABSTRACT

The work is devoted to the development of a hardware and software complex for objective assessment of archer stability in real time. Based on the ESP32 microcontroller and the MPU9250 inertial sensor (IMU), an IoT device has been created that records the vibrations of a sports bow. The data is transmitted via WebSocket to the server, where an algorithm analyzes its dispersion for instant classification of the system status ("Calm" or "Active"). The developed tool provides the athlete and coach with immediate feedback, allowing them to correct their technique of holding and aiming.

KEYWORDS: **Internet of Things (IoT), ESP32, MPU9250, archery, stability analysis, WebSockets, FastAPI, data visualization.**

I. INTRODUCTION

The goal of this work is to develop a hardware and software complex capable of collecting, analyzing, and visualizing data on the vibrations of a sports bow [1] in real time, providing instant feedback on exceeding the stability threshold. The article presents the system architecture, sensor calibration method, and data analysis algorithm.

II. PRESENTATION OF THE MAIN MATERIAL

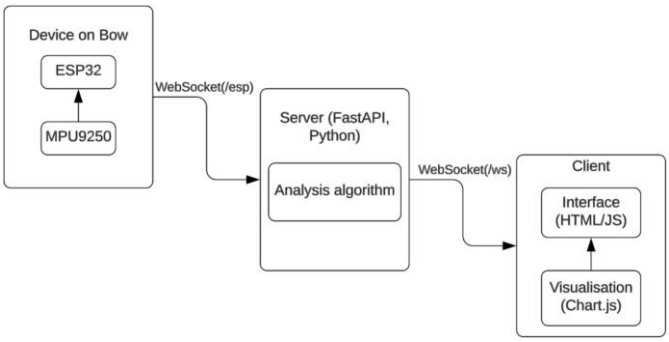

Fig. 1 Architecture of software and hardware system

The architecture of the complex is shown in Fig. 1. The built-in device (ESP32 and MPU9250) collects 6-axis data obtained after 6-position calibration using the Ferraris method. This data is transmitted in binary format via WebSocket (/esp) to the server (Backend). The server, implemented on FastAPI, receives data from the device and simultaneously maintains connections with web clients (/ws).

The key analysis logic is performed on the server. It calculates the variance in a "sliding window" (20 measurements) for the accelerometer and gyroscope readings. If the variance is below the threshold values, the system classifies the state as 'REST' (Rest), otherwise as "ACTIVE" (Active). The client interface (HTML/CSS/JavaScript) receives this data and status in JSON format, instantly visualizing it on dynamic charts (Chart.js).

III. RESULTS AND DISCUSSION

Fig. 2 Visualization of stable retention

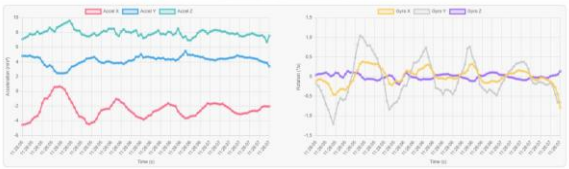

Fig. 3 Detection of excessive vibrations

When the device is held steady (simulating the aiming phase), the graphs show minimal fluctuations, and the system correctly classifies the state as "Calm" (Fig. 2).

When minor fluctuations are introduced (simulating tremor), the algorithm detects that the threshold dispersion has been exceeded, and the interface immediately changes the status to "Active" (Fig. 3).

IV. CONCLUSION

The developed hardware and software complex has proven its effectiveness in detecting archer's tremors. The system reliably distinguishes between stable holding ("Calm") and excessive tremors ("Active"), providing the athlete with objective feedback in real time. The architecture used (ESP32, FastAPI, WebSockets) ensures minimal latency, which is critical for the training process.

REFERENCES

[1] Che, L., Zhang, S., Chen, Y., Dong, Y., & Wu, Q. (2023). Fitness Bow: An Intelligent Supervised Motion System. (Vol. 14058, pp. 278–297). Springer Science and Business Media Deutschland GmbH. https://doi.org/10.1007/978-3-031-48050-8_20

XXXIII International Conference
CAD IN MACHINERY DESIGN IMPLEMENTATION AND EDUCATIONAL ISSUES
11 - 13 December 2025, Białystok, Poland

ZERO-KNOWLEDGE DISTANCE PROOFS FOR INTEGER-QUANTIZED FINGERPRINT EMBEDDINGS

Mykola Khranovskyi, Andriy Kernytskyy
Lviv Polytechnic National University
mykola.m.khranovskyi@lpnu.ua, andriy.b.kernytskyy@lpnu.ua

ABSTRACT

Biometric logins are convenient, but leaked fingerprint templates are irrotatable, risking long-term privacy. This work shows zero-knowledge proofs over integer-quantized embeddings: a device proves the squared L_2 distance to a reference is below a threshold without revealing data. Integer arithmetic keeps proofs small and fast. The minimal, proximity-only design supports trusted on-device pipelines, external shortlisting, yes/no verification, and FAR/FRR/EER evaluation.

KEYWORDS: **zero-knowledge proofs, fingerprint authentication, biometric privacy, unlinkability, succinct SNARKs.**

I. INTRODUCTION

Biometric logins are convenient, but fingerprints create a dilemma: they identify a person very precisely and cannot be changed easily; if a template leaks, it can enable cross-service linking, aid template reconstruction, and cause long-term privacy loss [1]. This work mitigates the risk by pairing compact zero-knowledge proofs with integer-quantized fingerprint embeddings so a prover can show a fresh sample is close to a stored reference without revealing the sample, the embedding, or the distance. Modern systems map images to fixed-length vectors and accept when the distance is below a threshold; the proposed design keeps the extractor outside the proof and focuses on the matching boundary, quantizes the embedding to small integers, and proves in ZK that the sum of squared coordinate differences between a private e_q and a public or committed c_q is at most t^2. Integer arithmetic aligns with efficient circuits, producing short proofs that reveal only a yes/no result [2]. The approach remains practical by skipping ZK proofs of the full network and staying compatible with standard pipelines and external shortlisting, a typical pattern in large biometric deployments [3]. Compared with homomorphic encryption and MPC, this approach avoids heavy ciphertext computation, complex key management, and online interaction; its publicly verifiable, small proofs fit edge devices, web sign-ins, and even on-chain verification. In industry, it suits physical access control (factories, data centers), operator logins on SCADA/OT consoles, IoT device onboarding, biometric time-and-attendance, self-service ATMs, and healthcare terminals where fast, privacy-preserving checks are required.

II. DESIGN, SECURITY & EVALUATION

Let $c_q \in \mathbb{Z}^d$ be the stored reference and $e_q \in \mathbb{Z}^d$ the fresh on-device embedding; accept if $\mathrm{dist}(e_q, c_q) \le t$ Fingerprints are mapped to fixed-length vectors and matched by a distance threshold. Quantization scales/rounds each coordinate $e_q[i] = \mathrm{clip}(\lfloor s_i e[i] \rceil, -B, B)$ with $B = 2^{b-1} - 1$; the same process produces c_q. The ZK statement proves $\sum_i (e_q[i] - c_q[i])^2 \le t^2$ without revealing e_q; succinct SNARKs verify such arithmetic efficiently. For large galleries, shortlist k candidates outside the circuit and check only them in-circuit, a standard scaling pattern [3].

The main adversary is an honest-but-curious verifier with possible passive observers; zero-knowledge reveals only a yes/no bit, and soundness means acceptance implies a valid witness within the threshold. Risks are reduced with attempt limits, a small hidden threshold randomization, per-relying-party salted commitments to block cross-service linking, and on-device TEE to limit side channels. Quantization adds bounded error, so thresholds are calibrated to control EER as bit-width and scales change. Compared with FHE, the design avoids heavy encrypted computation and complex key management, and unlike MPC it needs no online interaction [4]; full zkML attestation of the extractor is possible but currently far more expensive than distance-only proofs. Evaluation follows FVC protocols with enroll/probe and a shifted split, reporting FAR/FRR/EER (pre/post quantization), proof/verify time, proof size, constraints, and memory for comparison with prior work.

III. CONCLUSIONS

Zero-knowledge distance checks on integer-quantized fingerprint embeddings offer a practical privacy layer for biometric authentication: only a public yes/no decision is revealed, while templates, embeddings, and exact distances remain hidden. The minimal, distance-only design fits trusted on-device pipelines, scales with external shortlisting, and yields small, verifiable proofs suitable for edge, web, and on-chain use.

REFERENCES

[1] D. Maltoni, D. Maio, A. K. Jain, and S. Prabhakar, Handbook of Fingerprint Recognition, 2nd ed. London, U.K.: Springer, 2009.
[2] J. Groth, “On the size of pairing-based non-interactive arguments,” in Advances in Cryptology—EUROCRYPT 2016. Cham, Switzerland: Springer, 2016, pp. 305–326.
[3] R. Cappelli, D. Maio, D. Maltoni, J. L. Wayman, and A. K. Jain, “Performance evaluation of fingerprint verification systems,” in Biometric Authentication. Berlin, Germany: Springer, 2006, pp. 1–6.
[4] Z. Peng, T. Wang, C. Zhao, G. Liao, Z. Lin, Y. Liu, et al., “A survey of zero-knowledge proof based verifiable machine learning,” *arXiv* preprint arXiv:2502.18535, 2025.

XXXIII International Conference
CAD IN MACHINERY DESIGN IMPLEMENTATION AND EDUCATIONAL ISSUES
11 - 13 December 2025, Białystok, Poland

3D MODELING OF UAV WITH A CARGO DELIVERY SYSTEM

Oleksii Melnyk[1], Kostiantyn Kolesnyk[1], Ivan Kozemchuk[1], Andrzej Łukaszewicz[2]
Lviv Polytechnic National University[1]
oleksii.melnyk.mknit.2025@lpnu.ua, kostyantyn.k.kolesnyk@lpnu.ua, ivan.v.kozemchuk@lpnu.ua
Białystok University of Technology[2]
a.lukaszewicz@pb.edu.pl

ABSTRACT

The article presents a cargo delivery system for UAVs. The features of the hardware and flight control software are considered. A cargo release mechanism has been developed using SolidWorks and its body parts have been 3D printed. The guidance system is equipped with a rotating camera. A real-time video transmission system has been implemented, as well as a aiming system with dynamic image displacement. Raspberry Pi interaction with the flight controller via the MAVLink protocol has been ensured.

KEYWORDS: **UAV, cargo delivery, GPS, flight controller. Raspberry Pi, cargo drop, MAVLink, FPV.**

I. 3D MODELING OF UAV

The overall 3D model of the UAV [1, 2] system is presented in Fig. 1.

Fig. 1. 3D Model of UAV.

The basis of the cargo-drop mechanism is a gear, which, when the servo motor rotates, drives a toothed rack. The linear movement of the toothed rack is transmitted to the linkage, which, in turn, performs the movement necessary to control the clamping elements (cams and jaws). The link mechanism moves the cams that hold the suspension to which the cargo is attached. In the closed state, these elements securely fix the cargo during flight. Next, a 3D model of the mechanism for rotating the camera was developed, which provides the ability to rotate it by more than 90 degrees. Such a mechanism allows the viewing angle to be flexibly changed, which is important for precise guidance by the operator. The design provides the ability to adjust the camera angle to individual needs.

II. 3D-PRINT ELEMENTS OF UAV

To create a plastic drop mechanism, it is important to properly prepare them for 3D printing, which includes the choice of material, the setting of printing parameters, and the proper placement of each element. Materials from the Ukrainian company FAINYI were used for printing.

III. UAV DATA PROCESSING AND TRANSMISSION

During the development of the software part, ArduPilot firmware was installed on the flight controller, communication with Raspberry Pi was implemented via MAVLink. Scripts were created for video processing and calculation of the cargo drop trajectory taking into account the current flight parameters. All subsystems were integrated into a single technical system. The system underwent preliminary sensor calibration and bench testing. After that, field tests were carried out in real conditions.

IV. CONCLUSION

The 3D design of the UAV was completed using SolidWorks. Additionally, a UAV control system was implemented, equipped with a cargo delivery system. The developed UAV is cost-effective to produce.

Funding: This research was partially financed by the Ministry of Science and Higher Education of Poland with allocation to the Faculty of Mechanical Engineering, Bialystok University of Technology, for the WZ/WM-IIM/5/2023 academic project in the mechanical engineering discipline.

REFERENCES

[1] Syrotynskyi Taras, Kolesnyk Kostyantyn, Kozemchuk Ivan [i in.], 3D modeling UAV with integrated positioning system. In: CAD in Machinery Design. Implementation and Educational Issues Proceedings of the XXXII International Conference, 2025, Lviv Polytechnic National University, p.9, ISBN 978-966-994-043-8.

[2] Łukaszewicz Andrzej, Calafate Carlos Tavares, Giernacki Wojciech (ed.) New Methods and Applications for UAVs: Sensors, 2025, MDPI, 198 p., ISBN 978-3-7258-5023-5. DOI:10.3390/books978-3-7258-5024-2

XXXIII International Conference
CAD IN MACHINERY DESIGN IMPLEMENTATION AND EDUCATIONAL ISSUES
11 - 13 December 2025, Białystok, Poland

PROTOTYPE OF A ROBOTIC MOBILE PLATFORM FOR AN AUTOMATED CONTAINERS STORAGE SYSTEM

Vitaliy Mazur, Roman Panchak
Lviv Polytechnic National University
vitaliy.v.mazur@lpnu.ua, roman.t.panchak@lpnu.ua

ABSTRACT

The correct choice of objective indicators of efficiency when designing an automated containers storage system (ACSS) base on specialized robotic mobile platform (RMP) provides the prerequisites for its further mass implementation. The construction of the RMP prototype for the ACSS is presented in this paper. The kinematic scheme of the RMP and the structural scheme of the control system are proposed. The specifics of the realization of their components are considered.

KEYWORDS: **automated containers storage system, robotic mobile platform prototype, kinematic scheme, indicators of efficiency.**

I. INTRODUCTION

In connection with the shortage of workers and the growth of their wages, the development of means for the automation of warehouse activities continues to be an urgent task. Excessive complexity and high cost of modern RMPs [1] prevent their widespread use for the execution of warehouse operations instead of loaders. Therefore, the creation of a simple and cheap RMP for ACSS is promising. Based on the comprehensive development of ACSS and RMP, an experimental model of a specialized RMP was implemented [2]. The results of research on this model confirmed the feasibility of further development of the RMP prototype.

The purpose of the work is the development of a full-scale prototype of a specialized robotic mobile platform for ACSS.

II. PROPOSED INDICATORS OF RMP EFFICIENCY

To form the requirements for the RMP prototype, the following indicators of its efficiency are proposed: K_w - the ratio of the mass of the container with cargo to the total mass of the RMP with the container; K_e - the energy consumption of the RMP for moving 1 kg of the container mass with cargo; K_c - the ratio of the total mass of containers with cargo moved per unit of time to the total cost of the RMP.

III. THE ROBOTIC MOBILE PLATFORM PROTOTYPE

Taking into account the identified shortcomings of the experimental model [2], the proposed improved construction of the RMP prototype is presented in Fig. 1.

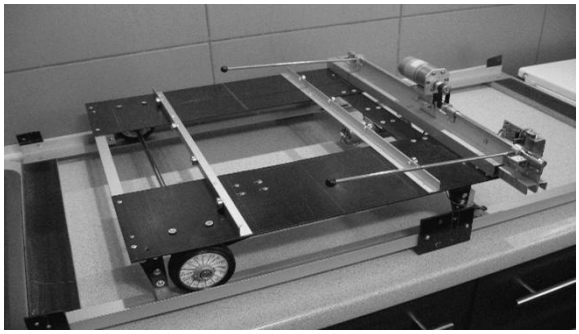

Fig. 1. The construction of the RMP prototype

The kinematic scheme of the RMP prototype is presented in Fig. 2.

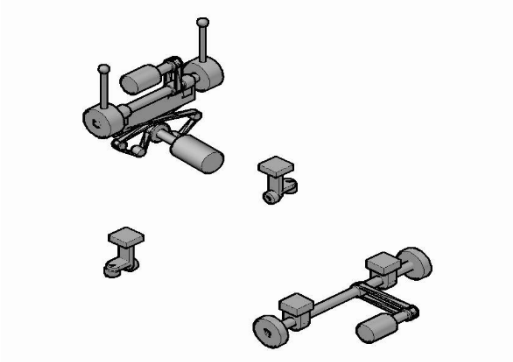

Fig. 2. The kinematic scheme of the RMP prototype

The kinematic scheme of the RMP prototype contains the following main units: a drive unit for moving the platform along the guides along the racks; a unit for gripping and holding the container when it is moved; a unit for shifting the container from the working surface of the platform to the cell of the rack or vice versa. The main positive feature of the proposed construction of these units is the use of flexible gears with the use of toothed belts. This provides damping, noiselessness and reduced requirements for the accuracy of units manufacturing.

IV. CONCLUTION

With a mass of RMP without a container of 5 kg, an average mass of a container with a load of 20 kg, an average time of movement of the RMP when moving the container of 1 min, and the cost of RMP of $3000, the values of Kw=0.8, Ke=1 W×h/kg, Kc=0.4 kg×h/$.

REFERENCES

[1] M. Shneier and R. Bostelman, “Literature review of mobile robots for manufacturing”, NISTIR 8022, 2015, http://dx.doi.org/10.6028/NIST.IR.8022.

[2] V. Mazur and R. Panchak. Robotic mobile platform for containers storage system // Computer design systems. Theory and practice. – 2024. – Vol. 6, № 3. – pp. 24–30.

XXXIII International Conference
CAD IN MACHINERY DESIGN IMPLEMENTATION AND EDUCATIONAL ISSUES
11 - 13 December 2025, Białystok, Poland

DEVELOPMENT OF A SUBSYSTEM FOR AUTOMATED DETERMINATION OF THE SOUND DISPERSION COEFFICIENT OF MATERIALS WITH VARIOUS GEOMETRIC SHAPES

Mykhaylo Melnyk[1], Andriy Kernytskyy[1], Ireneusz Czajka[2], Wojciech Zabierowski[3]
Lviv Polytechnic National University[1]
mykhaylo.r.melnyk@lpnu.ua, andriy.b.kernytskyy@lpnu.ua
The AGH University of Krakow[2]
iczajka@agh.edu.pl
Lodz University of Technology[3]
wojciech.zabierowski@p.lodz.pl

ABSTRACT

The acoustic diffusion coefficient of surfaces is a key parameter in room acoustics, affecting sound quality in concert halls, studios, and industrial spaces. This work presents the development of an automated subsystem for determining the sound diffusion coefficient of materials with different geometric forms. The subsystem enables efficient analysis of experimental data and provides a user-friendly interface for batch processing of measurement results.

KEYWORDS: **sound diffusion coefficient, acoustic measurement, automated analysis, Matlab, room acoustics.**

I. INTRODUCTION

The degree of acoustic scattering from surfaces is crucial for the acoustic quality of rooms [1]. The diffusion coefficient characterizes the uniformity of sound scattering, while the scattering coefficient provides a general measure of sound dispersion. Both are necessary for comprehensive acoustic assessment [2]. The aim of this work is to develop a subsystem for automated determination of the sound diffusion coefficient for materials of various shapes.

II. PRINCIPLES OF MEASUREMENT

Measurements are based on the analysis of impulse responses recorded in anechoic conditions, following ISO 17497-2:2012. The diffusion coefficient is calculated from the spatial distribution of reflected sound pressure levels, measured by microphones arranged in a semicircular or hemispherical pattern. The system supports both near-field and far-field measurements, and the frequency range complies with IEC 61260 and ISO 266 standards.

III. SYSTEM DESIGN

The subsystem was implemented in Matlab and features an intuitive graphical interface for selecting and processing audio files. The workflow includes:

- Loading measurement data from empty and test sample conditions
- Automatic file management and batch analysis
- Visualization of impulse responses and polar diagrams
- Calculation of diffusion coefficients using Fourier transform and windowing techniques
  The system supports flexible adjustment of analysis parameters and provides clear graphical and tabular output

Thus, using the subsystem, by selecting only two directories with results for the empty anechoic chamber and the chamber with the test sample, and pressing the "directivity diagram" button, we obtain the directivity diagram and the scattering coefficient for the given material. In our case, this is the Schroeder diffuser (Fig.1.), and the scattering coefficient is 0.7.

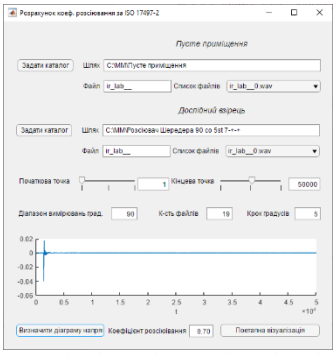

Fig. 1. Settings for the analysis of the Schroeder diffuser

IV. RESULTS

The subsystem was tested with various sample types, including a curved plate, a plate with irregular surface, and a Schroeder diffuser. For the Schroeder diffuser, the measured diffusion coefficient was 0.7, while for the curved plate it reached 0.95, indicating high diffusion efficiency. The results confirm the accuracy and usability of the developed subsystem.

V. CONCLUTION

An automated subsystem for determining the sound diffusion coefficient of materials with different geometries has been developed and validated. The solution enables efficient batch analysis of experimental data and supports comprehensive acoustic characterization of test samples.

REFERENCES

[1] J. S. Bradley, H. Sato, and M. Picard, “On the importance of early reflections for speech in rooms”, J. Acoust. Soc. Am., 106, pp. 3233–44 (2003).

[2] F. E. Toole, “Loudspeakers and rooms for sound reproduction—A scientific review”, J. Audio Eng. Soc., 54(6), pp. 451–76 (2006).

XXXIII International Conference
CAD IN MACHINERY DESIGN IMPLEMENTATION AND EDUCATIONAL ISSUES
11 - 13 December 2025, Białystok, Poland

ARCHITECTURE OF HARDWARE AND SOFTWARE PLATFORMS FOR INDUSTRIAL XR ENVIRONMENTS

Ivan Hileta, Yuliia Hileta, Uliana Marikutsa
Lviv Polytechnic National University
ivan.v.hileta@lpnu.ua, yuliia.hileta.pp.2022@lpnu.ua, uliana.b.marikutsa@lpnu.ua

ABSTRACT

This paper presents a hybrid XR platform architecture for the industrial sector, addressing the challenges of ultra-high spatial accuracy and ultra-low Motion-to-Photon (MTP) latency. By synthesizing OpenXR-compatible hybrid tracking systems (Inside-Out and Outside-In) with Sensor Fusion (VIO, LiDAR) and utilizing Edge Computing, the platform achieves the critical MTP threshold of under 7 ms, which is necessary for high-precision industrial visualization and inspection scenarios.

KEYWORDS: **eXtended Reality, Industrial XR Platform, Motion-to-Photon Latency, Spatial Accuracy, Hybrid Tracking, OpenXR, Edge Computing, Sensor Fusion.**

I. INTRODUCTION

The field of eXtended Reality (XR) is paramount for the digital transformation of the industrial sector. XR technologies offer essential tools for data visualization, including large-scale CAD/BIM models, execution of high-precision inspections (QA/QC), and enabling remote collaboration [1]. As realism demands grow, specialized solutions beyond consumer-grade tech are needed. This research reviews current technologies to define a high-performance platform for industrial XR.

II. THE RESULTS OF THE STUDY AND THEIR DISCUSSION

For effective XR application in industry, the platform must overcome two critical challenges:

- Ultra-High Spatial Accuracy - virtual overlays must achieve perfect, consistent alignment with physical objects.
- Minimization of Motion-to-Photon (MTP) Latency - the total time delay between the user's physical motion and the corresponding change being displayed on the screen [2].

The OpenXR standard serves as a foundational element, enabling modular platform design and ensuring cross-hardware compatibility for applications built on popular engines (Unity, Unreal). Crucially, industrial applications require specific OpenXR extensions to support high-precision spatial anchoring.

MTP latency involves delays across the entire pipeline: sensing, processing, rendering, and display [2]. Industrial registration demands a critical threshold of under 7 ms, which severely restricts architectural choices. Achieving the required positioning accuracy necessitates a careful analysis of the network latency budget, often leading to the adoption of Edge Computing when the device is unable to perform rendering independently.

The selection of the tracking method is paramount for high-precision industrial positioning:

- Outside-In Tracking - uses external sensors or base stations for device tracking [3]. It offers an advantage in accuracy, often matching Motion Capture (Mo-Cap) systems.
- Inside-Out Tracking - relies on the Head-Mounted Display's (HMD) built-in cameras and inertial sensors, leveraging Visual SLAM or Visual-Inertial Odometry (VIO) [3].

The optimal industrial approach is a Hybrid Tracking System [4]. This system uses Inside-Out as the foundation for mobility but integrates external reference points or specialized sensors to ensure the high accuracy mandatory for demanding scenarios.

Integration of VIO, LiDAR, and Sensor Fusion: Achieving ultra-accuracy requires integrating data from various sensors—inertial measurement units, cameras, compasses, and LiDAR—a process known as Sensor Fusion. Algorithms such as Kalman Filters are often employed to stabilize orientation and enhance the reliability of pose estimation [5].

To maintain precision in key operational zones, Optical Localization Methods are necessary:

- Utilizing Fiducial Markers (known visual patterns) that HMD cameras can track with high precision.
- Employing advanced SLAM algorithms that use methods like Optical Flow or RANSAC in dynamic environments to classify and ignore moving objects, ensuring stable static map reconstruction.

III. CONCLUSIONS

A high-performance industrial XR platform requires a hybrid, distributed architecture that combines advanced multi-sensor tracking with Edge Computing to achieve both ultra-high localization accuracy and ultra-low latency.

REFERENCES

[1] Rank Tracker. (2024). A Glimpse into Tomorrow: Key Tech Industry Statistics for 2024 [Online]. Available: https://www.ranktracker.com/uk/ blog/a-glimpse-into-tomorrow-key-tech-industry-statistics-for-2024/

[2] Xinreality. Motion-to-Photon Latency (MTP Latency) [Online]. Available: https://xinreality.com/wiki/Motion-to-photon_latency.

[3] Pimax. Pose Tracking Methods: Outside-in vs. Inside-out Tracking in VR [Online]. Available: https://pimax.com/blogs/blogs/pose-tracking-methods-outside-in-vs-inside-out-tracking-in-vr

[4] Milvus. What Types of Tracking Systems Are Used in VR (e.g., Inside-Out vs. Outside-in) [Online]. Available: https://milvus.io/ai-quick-reference/what-types-of-tracking-systems-are-used-in-vr-eg-insideout-vs-outsidein

[5] Anon. Sensor Fusion for Augmented Reality [Online]. Available: https://www.researchgate.net/publication/220774832_Sensor_Fusion_for_Augmented_Reality

XXXIII International Conference
CAD IN MACHINERY DESIGN IMPLEMENTATION AND EDUCATIONAL ISSUES
11 - 13 December 2025, Białystok, Poland

3DEXPERIENCE PLATFORM IN FLEXIBLE PATHWAYS OF SECOND CYCLE MECHANICAL ENGINEERING STUDIES

Arvydas Palevicius[1], Giedrius Janusas[1], Kestutis Pilkauskas[1], Sigita Urbaite[1]
Kaunas University of Technology[1]
arvydas.palevicius@ktu.lt; giedrius janusas@ktu.lt; kestutis.pilkauskas@ktu.lt, sigita.urbaite@ktu.lt

ABSTRACT

The implemented concept of flexible learning pathways is based on providing the opportunities for the second cycle Mechanical Engineering students to combine the competencies provided by the studies of core Mechanical Engineering modules package, abilities of individual flexibility achieved with the help of challenge-based learning and case study method with modern digitization trends of engineering supported by 3DExperience platform.

KEYWORDS: **3DExperience, case analysis method, challenge-based learning, flexibility, Mechanical Engineering.**

I. INTRODUCTION

We live in highly dynamic rapidly changing world, the driving trend of which is digitization with wider and wider integration of Artificial Intelligence capabilities. The field of engineering is no exception. The effectiveness of the application of CAE tools for modelling and simulating engineering systems is of primary importance. It is worth paying attention that modern engineering systems became of integrated nature, based on Multiphysics processes and phenomena with AI driven control functionalities.

In order to prepare a highly qualified specialist able to develop, perform, maintenance and work out strategies of effective application of these systems, an educational programme should include the special combination of modules of core/fundamental studies in Mechanical Engineering, i.e. the modules developing abilities to adopt in a flexible manner to challenges in engineering field and strong digital skills necessary for solving the challenges and problems caused by them.

II. CONCEPT OF STUDENT COMPETENCIES DEVELOPMENT

With the aim to educate engineers that have competencies complying with modern trends of engineering industries development, the second cycle Study Programme of Mechanical Engineering was accordingly restructured and modified. The introduced modifications were based on the following principle. Competencies of the graduate – master in the field of Mechanical Engineering need to consist of effective combination of: sufficiently deep knowledge and understanding of Mechanical Engineering fundamentals, the abilities to face challenges from the field of Mechanical Engineering or other related fields, determine, and with a flexible approach, solve the problems caused by challenges and sufficiently well-developed skills to use CAE tools.

It became obvious that the mentioned set (blend of competencies cannot be achieved just through straightforward adding of Learning outcomes separate (individual) modules. In the modified Study Programme clearly expressed the mentioned outcome achievement lines can be distinguished. But it is important to emphasize that the required competencies can be achieved through integral and concurrent synergy of the learning outcomes of these lines.

Module line "Researcher's competencies" consists of the following modules: Basics of Scientific Research, Research projects 1 and 2, Master's Degree Final Project. The first module provides methodological knowledge specific to technological science in order the novice researcher, that he could perform theoretical and experimental research, while the others modules develop skills to comprehensively solve complex theoretical and practical problems of Mechanical Engineering. Moreover, the case analysis method to reach the goals of learning outcomes is used.

Line of the modules as Experimental Mechanics, Integrated CAD/CAE/CAM Systems and Digitization in Engineering develop abilities to solve complex challenges arising in the real environment [1]. Recently established 3DExperience Edu Center of Excellence provides favorable conditions for effective synergy in challenge-based problem solving and developing CAE based digital skill of engineers.

It is important to note that to move along each module line achieved Learning outcomes of the modules of all the lines are necessary. The opportunity to develop certain specific deeper competencies in design and research of micro electromechanical systems is provided by choosing the elective module Microelectromechanical Systems Design. Nevertheless, studies of the module would be worthless without the synergy of the mentioned module lines.

III. CONCLUSIONS

A highly qualified specialist developer of modern sophisticated engineering systems needs to have competencies in case analysis method, challenge-based problem solving, and in effectively applying CAE tools for modeling and simulating real world processes.

Through Synergy of researcher's competencies, digital skills and understanding engineering fundamentals of developing modules the required qualifications can be achieved.

REFERENCES

[1] Berland, L. K. (2013). Student learning in challenge-based engineering curricula. Journal of Pre-College Engineering Education Research (J-Peer), 3(1), 53–64. https://doi.org/10.7771/2157-9288.1080.

XXXIII International Conference
CAD IN MACHINERY DESIGN IMPLEMENTATION AND EDUCATIONAL ISSUES
11 - 13 December 2025, Białystok, Poland

DEVELOPMENT OF ULTRASONIC RANGEFINDER WITH IMPROVED MEASUREMENT ACCURACY

Andriy Holovatyy[1], Oleh Zachek[2], Andrzej Łukaszewicz[3], Volodymyr Senyk[1]
Lviv Polytechnic National University[1]
andrii.i.holovatyi@lpnu.ua, volodymyr.v.senyk@lpnu.ua
Lviv State University of Internal Affairs[2]
zachekoi@gmail.com
Białystok University of Technology[3]
a.lukaszewicz@pb.edu.pl

ABSTRACT

In the paper, the ultrasonic rangefinder with improved measurement accuracy has been developed. The developed digital device makes it possible to quickly obtain information about the distance to an obstacle with minimal error and can operate as an obstacle detector. The flexible menu allows a user to set the device operation modes, distance output format, provision of sound and visual messages (discharged battery and detected obstacles), to set the critical distance to the obstacle and save the settings in EEPROM.

KEYWORDS: **ultrasonic rangefinder, obstacle detector, distance measurement methods, ultrasonic measurement accuracy improvement, AVR ATmega128 MCU, HC-SR04 ultrasonic sensor, DS18B20 temperature sensor, LCD 16*2 HD44780 (WH1602B).**

I. INTRODUCTION

With the advent of microcontrollers, it is possible to create cheap intelligent distance measurement systems. Such rangefinder systems can be used for accurate distance measurement, firefighters working in smoky rooms, speleologists, security alarms, robotics (drones), advertising, toys [1,2]. The distance measurement accuracy can be significantly improved if the speed of sound propagation from the environment temperature is taken into account [3,4].

As known, the distance to the object can be calculated using the formula:

$$d=v*t/2 \quad (1)$$

where d is the distance to the object, v is the speed of the sound wave propagation in a given environment, t – the time needed for the wave to cover the distance to the object and back.

The speed of ultrasound propagation in air depends on the ambient temperature and is calculated by the formula:

$$v(\Theta)=331.3+0.59*\Theta \quad (2)$$

where $v(\Theta)$ is the speed of sound in air (m/s), Θ is the ambient temperature (°C).

II. DEVELOPMENT OF ULTRASONIC RANGEFINDER WITH IMPROVED MEASUREMENT ACCURACY

In Fig.1, hardware of the ultrasonic rangefinder with improved measurement accuracy is shown.

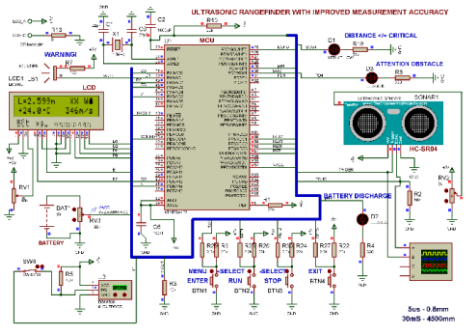

Fig.1. Hardware of the ultrasonic rangefinder with improved measurement accuracy

The rangefinder hardware consists of the ATmega128 MCU, HC-SR04 ultrasonic module, DS18B20 temperature sensor, LCD, sound and LED indicators, menu buttons (BTN1, BTN2, BTN3, BTN4) for setting up the rangefinder.

III. CONCLUSIONS

The hardware and software for the ultrasonic rangefinder with improved measurement accuracy have been developed. The developed device detects obstacles, measures the distance to them, taking into account the speed of wave propagation in the environment, notifies about approaching an obstacle closer than the configured critical distances by turning on sound and visual warnings, has a flexible menu for setting the rangefinder operation modes and input parameters (critical distance to the obstacle, distance measurement units), saves settings in non-volatile memory, and monitors the battery charge. The ultrasonic rangefinder with improved measurement accuracy is cheaper compared to existing products and has wider capabilities.

REFERENCES

[1] Navaneetha Krishna Chandran, Chandran Navaneetha Krishna, Sultan Mohammed Thariq Hammed, Łukaszewicz Andrzej, Holovatyy Andriy, Giernacki Wojciech. Review on Type of Sensors and Detection Method of Anti-Collision System of Unmanned Aerial Vehicle. // Sensors 2023, 23(15), 6810; https://doi.org/10.3390/s23156810.

[2] Zurong Qiu, Yaohuan Lu and Zhen Qiu. Review of Ultrasonic Ranging Methods and Their Current Challenges. // *Micromachines* 2022, *13*(4), 520; https://doi.org/10.3390/mi13040520.

[3] Andrii Rudyk, Andriy Semenov, Serhii Baraban, Olena Semenova , Pavlo Kulakov , Oleksandr Kustovskyj and Lesia Brych. Influence of Environmental Factors on the Accuracy of the Ultrasonic Rangefinder in a Mobile Robotic Technical Vision System. // *Electronics* 2025, *14*(7), 1393; https://doi.org/10.3390/electronics14071393.

[4] Fuad Aliew. An Approach for Precise Distance Measuring Using Ultrasonic Sensors. // *Eng. Proc.* 2022, *24*(1), 8; https://doi.org/10.3390/IECMA2022-12901.

XXXIII International Conference
CAD IN MACHINERY DESIGN IMPLEMENTATION AND EDUCATIONAL ISSUES
11 - 13 December 2025, Białystok, Poland

RESEARCH ON THE STRUCTURAL STRENGTH OF A DRY-CLEANING MACHINE FOR ROOT VEGETABLES

Dariia Rebot[1], Volodymyr Topilnytskyy[1], Serhiy Shcherbovskykh[2], Tetyana Stefanovych[1]
Lviv Polytechnic National University[1]
dariya.p.rebot@lpnu.ua
State University of Applied Sciences in Jaroslaw[2]
shcherbov@gmail.com

ABSTRACT

This study analyzes the strength and design optimization of a patented dry-cleaning machine for root crops, using a 3D CAD model developed in Autodesk Inventor. Stress, displacement, and safety factor maps were generated, revealing a maximum frame displacement of 4.939 mm under load. For a 5-meter chamber length, 0.85-meter diameter, and 1450 kg load, the optimal safety factor is 3.25, with a recommended chamber frame weight of 80 kg.

KEYWORDS: **sieve, vibrating separator, root crops, strength, optimization**

I. INTRODUCTION

The cleaning of root crops is an important process in the food and agricultural industries. In particular using the dry-cleaning method. This method is more economical and favorable for products. Today, such machines have been considered on the basis of individual models [1,2], therefore, the study and optimization of their design is an urgent task. The authors propose to conduct a strength analysis of a machine for dry cleaning of root crops based on a patented model [3].

II. MAIN MATERIAL PRESENTATION

The three-dimensional model (see Fig.1) was developed in the CAD environment of the Autodesk Inventor Professional system using top-down and bottom-up design methods. The most complex structural elements: the working chamber, the sieve and the drive are fully parameterized. The key dimension that determines their geometry is the internal volume of the working chamber, which depends on the installed capacity of the machine. It depends on the internal diameter of the chamber and its length. By changing these dimensions, the dimensions of the entire machine can change.

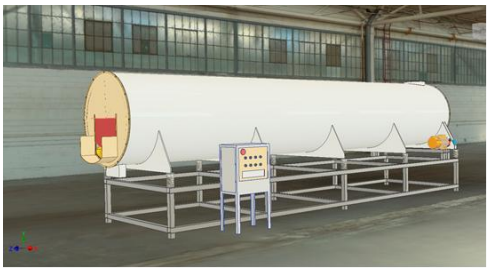

Fig. 1. Three-dimensional model of a vibrating machine for dry cleaning of root vegetables

III. RESULTS AND DISCUSSION

As a result, maps of the distribution of stresses, displacements, deformations and safety factor were obtained. Figures 2 and 3 show maps of the distribution of displacements in the sieve frames and the frame of the vibrating machine.

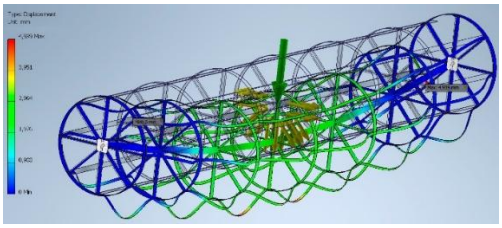

Fig. 2. Displacement distribution map in the sieve frame model

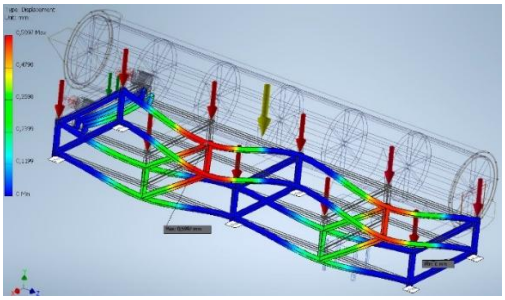

Fig. 3. Displacement distribution map in the frame model of cleaning machines.

The maximum frame displacement when applying load is 0.5997mm. Maximum displacement at maximum load in the frame is 4.939 mm

Given the proposed working chamber length of 5 meters, a diameter of 0.85 meters, and a loading weight of 1450 kg, it was determined that the optimal safety factor would be 3.25 and the recommended weight of the chamber frame would be 80 kg.

REFERENCES

[1] Bulgakov, V., Holovach, I., Martyniuk, V., et al. “Mathematical model of movement and cleaning beetroots from soil lumps with spiral separator”, International Scientific Conference Engineering for Rural Development 2024, pp. 683-695, https://doi.org/10.22616/ERDev.2024.23.TF132.

[2] Pankiv, M., Pidhurskyi, M., “Experimental studies of quality indicators of the transport cleaning system”. Innovative Solution in Modern Science. Vol. 6., No 42., pp. 177-186, https://doi.org/10.26886/2414-634X.6(42)2020.10.

[3] Topilnytskyi, V., Rebot, D.: Patent of Ukraine No. 154809 " Vibrating machine for dry cleaning of root vegetables" / Registered 20/12/2023, Bull. No. 51.

XXXIII International Conference
CAD IN MACHINERY DESIGN IMPLEMENTATION AND EDUCATIONAL ISSUES
11 - 13 December 2025, Białystok, Poland

ARCHITECTURE OF A HARDWARE-SOFTWARE COMPLEX FOR VISUALIZATION OF HUMAN MOVEMENT BIOMECHANICS IN REAL TIME

Mykhaylo Lobur[1], Krzysztof Pytel[2], Dmytro Korpylyov[1], Vira Oксentyuk[1], Zhanna Parashchyn[1]
Lviv Polytechnic National University[1]
mykhaylo.v.lobur@lpnu.ua, dmytro.v.korpylov@lpnu.ua, vira.m.oksentyuk@lpnu.ua, zhanna.d.parashchyn@lpnu.ua
The AGH University of Krakow[2]
kpytel@agh.edu.pl

ABSTRACT

The methodology and results of developing a hardware-software complex for real-time visualization of human movement biomechanics are presented. The complex comprises a distributed network of MPU-6050 inertial sensors, an ESP32 microcontroller, and web-based visualization technology. The mathematical apparatus for processing sensor signals is applied, which includes kinematic models and complementary filtering algorithms.

KEYWORDS: **ESP32, MPU-6050, biomechanics, movement visualization, sensor networks, quaternions, real-time.**

I. INTRODUCTION

The problem of monitoring movements for rehabilitation purposes is relevant in modern medicine for patients recovering from injuries and neurological diseases [1]. Automated systems for monitoring the movement of human body parts, which enable effective and accurate tracking of patient movement using sensors, are widely used in various fields, particularly in medicine during mirror therapy rehabilitation [2, 3]. The use of digital monitoring systems with real-time feedback, combined with web technologies, enables the improvement of exercise control, monitoring of the therapeutic process [3]. To obtain feedback signals indicating the spatial position of a person, MPU-6050 sensors are used, whose signals are processed by the ESP32 microcontroller and transmitted to the system for real-time visualization of the biomechanics of human movement.

II. MAIN RESULTS AND THEIR DISCUSSIONS

In this work, a hardware-software complex (HSCBH) for reproducing human movement biomechanics in real time has been developed (Fig. 1). It consists of MPU-6050 peripheral sensors connected in a distributed network, a TCA9548A multiplexer for connecting several sensors to the ESP32 microcontroller, and software for data processing and generating a visualization of human movements using modern web technologies. Such a solution will not only allow for recording, but also for analyzing motor activity with high accuracy. Using the MPU-6050 sensors (containing an accelerometer and a gyroscope), changes in body position in space, angular velocity, and linear acceleration are recorded, which is essential for the rehabilitation process. The HSCBH architecture is based on the principle of multi-level interaction of components. The main components of the data processing algorithm are a complementary filter for combining accelerometer and gyroscope readings, kinematic models of motion trajectories, and the mathematical apparatus of quaternions for describing spatial orientation.

The mathematical model of the system is based on kinematic equations for reconstructing the position of body segments, sensor fusion algorithms to enhance measurement accuracy, and matrix transformations utilizing quaternions.

This device enables you to compensate for measurement errors and convert raw sensor data into motion parameters.

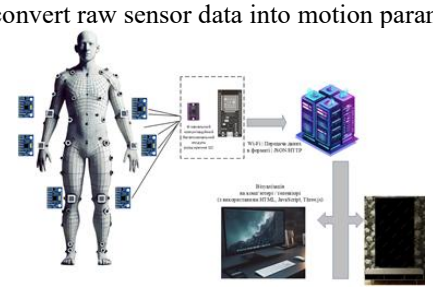

Fig. 1. Block diagram of a motion monitoring system for mirror therapy

The client-side is implemented using HTML5 and JavaScript web technologies for three-dimensional graphics. The final link is a biomechanical avatar that is animated in real-time, displaying all degrees of freedom of the user's movement.

III. CONCLUSIONS

The created architecture of the HSCBH provides low latency and high accuracy of movement reproduction, which is critical for rehabilitation applications. The developed HSCBH comprises a sensor layer, data processing, and information visualization within a web interface. The experiments conducted confirmed the HSCBH 's ability to provide visualization of human movement with low latency. Further development of the HSCBH plans to add machine learning for analyzing movement patterns and interaction with NIRS technology for determining brain activity.

REFERENCES

[1] T. M. Hemmerling, P. T. Charabati, J. A. Zaouter, and J. H. Prieto, "A comparison of traditional and robotic-assisted rehabilitation for stroke patients," Journal of NeuroEngineering and Rehabilitation, vol. 14, no. 1, pp. 1–10, 2017.

[2] J. Chen, P. Zeng, Y. Chen, Y. Zhang and Z. Cheng, "Design and Implementation of A Novel Upper Limb Exoskeleton for Mirror Therapy," 2024 IEEE International Conference on Robotics and Biomimetics (ROBIO), Bangkok, Thailand, 2024, pp. 510-515, doi: 10.1109/ROBIO64047.2024.10907463.

[3] B. Strong, B. Zeng, P. McCarthy, A. Roula and L. Guo, "A Framework to Design Virtual Reality Mirror Therapy (VRMT) for Motor Rehabilitation in Post-Stroke Survivors: Dosage, Motivation, Task Difficulty, Feedback and Mechanism," 2024 IEEE Gaming, Entertainment, and Media Conference (GEM), Turin, Italy, 2024, pp. 1-6, doi: 10.1109/GEM61861.2024.10585516.

XXXIII International Conference
CAD IN MACHINERY DESIGN IMPLEMENTATION AND EDUCATIONAL ISSUES
11 - 13 December 2025, Białystok, Poland

USING CNN IN ADAPTIVE NEURAL PID FOR SPEED CONTROL IN VARIOUS SOIL TYPES

Vladyslav Yevsieiev[1], Svitlana Maksymova[1], Igor Nevliudov[1], Olena Chala[1], Kostiantyn Kolesnyk[2], Roman Filipek[3], Krzysztof Pytel[3]
Kharkiv National University of Radio Electronics[1]
svitlana.milyutina@nure.ua
Lviv Polytechnic National University[2]
Kostyantyn.K.Kolesnyk@lpnu.ua
The AGH University of Krakow[3]
roman.filipek@agh.edu.pl, kpytel@agh.edu.pl

ABSTRACT

The paper presents the study of the using convolutional neural networks (CNN) effectiveness as a part of the Adaptive Neural PID type for stabilizing and tracking collaborative mobile robot speed on different soil types. The developed system functional diagram contains a multi-level architecture: a sensor level (optical speed meter, control loop with ANPID controller, CNN component,) and an actuator level.

KEYWORDS: **collaborative robotics, adaptive neural PID, CNN, speed stabilization, adaptive control.**

I. INTRODUCTION

The modern development of collaborative robotics requires the creation of intelligent control systems that can effectively adapt to changes in the external environment. The task of stabilizing the speed of mobile robots when moving on different types of soils deserves special attention, since variations in the coefficients of friction, adhesion and resistance significantly affect the dynamics of movement and the accuracy of trajectory tracking [1-3].

The combination of classical PID with adaptive neural network structures based on convolutional neural networks (CNN) opens up new prospects for building self-adjusting control systems. The use of CNN as part of Adaptive Neural PID allows you to automatically take into account the temporal and spatial dependencies between errors and the engine response, providing increased accuracy and stability.

II. SYSTEM STRUCTURE DEVELOPMENT AND SIMULATION

A functional scheme has been developed to formalize data flows, feedback signals, and adaptive components based on CNN in the structure of an Adaptive Neural PID controller, which ensures coordinated operation when changing the characteristics of the motion environment (Fig. 1).

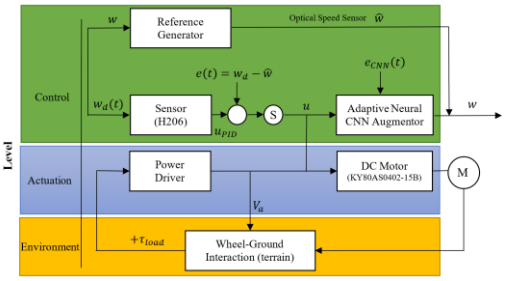

Fig. 1. Functional Diagram for Collaborative Mobile Robot Speed Control for Different Soil Types

This functional scheme is built on the principle of a multi-level cyber-physical system, in which an adaptive neural PID controller with built-in convolutional neural networks (CNN) is implemented. The main goal of the system is to maintain a stable angular velocity of the robot wheels on different soil types, such as asphalt, dry or wet soil, sand or gravel, taking into account changes in adhesion coefficients, rolling resistance and dynamic disturbances.

Based on the developed scheme, a mathematical model and a numerical simulation method were developed and three CNN architectures (CNN-A, CNN-B, CNN-C) were selected to compare different approaches to processing time sequences in the adaptive neural PID controller circuit when stabilizing the speed of a collaborative mobile robot on different types of soils. A program was developed in the Python language. Simulation results are presented on Fig.2.

```
=== Averaged by CNN ===
                SettlingTime_s  Overshoot_pct  SteadyStateError     IAE
CNN
CNN_Dilated3x3          11.997        -36.432            18.225  230.168
CNN_ResBlock            11.997        -36.906            18.225  230.188
CNN_Small2x3            11.997        -36.614            18.225  230.180
```

Fig. 2. Averaged Characteristics for Three Architectures CNN_Small2×3, CNN_Dilated3×3 and CNN_ResBlock

III. CONCLUSIONS

The integration of convolutional neural networks into the structure of the adaptive neural PID controller provides a significant improvement in the quality of collaborative mobile robot speed stabilization on different soil types. The results obtained confirm that the CNN compensator allows not only to increase the regulation accuracy, but also expands the system functionality due to adaptive learning in real time.

REFERENCES

[1] K. A. Ahmed, et al. “CNN-Based Intelligent Control Synthesis for Multi-Robot Coordination and Path Planning”, International Journal of Intelligent Engineering & Systems, vol. 18(8), 2025.
[2] I. Sh. Nevliudov, et al. “Development of mathematical support for adaptive control for the intelligent gripper of the collaborative robot manipulator”, Advanced Information Systems, vol. 9(3), pp. 57-65, 2025.
[3] Czubenko, M. et al. “A simple neural network for collision detection of collaborative robots”, Sensors, vol. 21(12), 4235, 2021

XXXIII International Conference
CAD IN MACHINERY DESIGN IMPLEMENTATION AND EDUCATIONAL ISSUES
11 - 13 December 2025, Białystok, Poland

INTELLIGENT PERSONNEL SELECTION SYSTEM BASED ON NLP AND ML

Andriy Oleksievets[1], Nazariy Jaworski[1], Maciej Ciężkowski[2]
Lviv Polytechnic National University[1]
Białystok University of Technology[2]
andrii.oleksiievets.mknsp.2024@lpnu.ua, nazarii.b.yavorskyi@lpnu.ua, m.ciezkowski@pb.edu.pl

ABSTRACT

The paper presents the development of an intelligent personnel selection system combining NLP-based resume matching and prosodic speech analysis for confidence estimation. A novel integral ranking algorithm is researched to minimize subjectivity. The study evaluates the system's performance using cosine similarity metrics and introduces Explainable AI (XAI) techniques to mitigate algorithmic bias in automated recruitment.

KEYWORDS: **recruitment automation, hybrid search, SBERT, speech analysis, integral ranking, XAI.**

I. INTRODUCTION

During digital transformation, HR departments struggle with processing large numbers of applications. Traditional ATS systems use keyword matching, often missing qualified candidates due to limited semantic understanding [1]. Manual screening can introduce bias and overlook soft skills like communication. We propose a system that combines resume text analysis and interview audio analysis to create an objective, explainable candidate ranking.

II. MAIN RESULTS AND DISCUSSION

A comprehensive two-stage architecture was developed. Pure vector search often misses specific technical terms, while keyword search fails to capture context. The system implements a Hybrid Search Algorithm that calculates a balanced match score (S_{hybrid}):

$$S_{hybrid} = \alpha \cdot S_{sem} + (1 - \alpha) \cdot S_{lex} \quad (1)$$

where S_{sem} represents the semantic similarity derived from dense vectors generated by the S-BERT model (all-mpnet-base-v2), and S_{lex} is the normalized BM25 score for keyword frequency. The coefficient alpha is set to 0.7 to prioritize semantic meaning over exact matches.

Top candidates receive in-depth analysis from a Large Language Model, which acts as a "Reasoning Agent" and provides a structured explanation of their fit for the role. Recent studies show LLM evaluations correlate over 0.85 with expert judgments [2]. A "Chain-of-Thought" approach is used for Gap Analysis and evidence-based scoring.

To assess soft skills, the audio stream is analyzed using the Librosa library. The module extracts prosodic features correlating with confidence, such as speaking rate and hesitation markers. The Confidence Score (S_{conf}) is calculated based on the ratio of silence to speech and pitch stability:

$$S_{conf} = \omega_{sen} \cdot M_{sent} + \omega_{flu} \cdot \left(1 - \frac{N_{fillers} + N_{pauses}}{N_{total}}\right) \quad (2)$$

where M_{sent} is the sentiment valence, $N_{fillers}$ is the count of filler words, and N_{pauses} is the duration of silence segments exceeding 2 seconds. This mechanism allows filtering out candidates who exhibit high hesitation, independent of the semantic content of their answers.

To ensure a holistic assessment, the system employs a hierarchical multi-criteria decision model. The calculation of the final rank involves three levels of aggregation.

Level 1: Question Scoring with Veto Logic. For each interview question the score combines content validity and confidence. To prevent hiring charismatic but incompetent candidates, a critical threshold is applied:

$$R_{int}^{(i)} = \begin{cases} 0, \ if \ S_{cont} < \tau_{crit} \\ \beta \cdot S_{cont} + (1 - \beta) \cdot S_{conf}, if \ S_{cont} \geq \tau_{crit} \end{cases} \quad (3)$$

where $\beta = 0.8$ prioritizes technical accuracy. S_{cont} is derived from a weighted combination of vector similarity and LLM-based verification.

Level 2: Interview Aggregation. The total interview score is calculated as a weighted average, where $lambda_i$ represents the difficulty weight of the i-th question:

$$S_{interview} = \frac{\sum_{i=1}^{K} R_{int}^{(i)} \cdot \lambda_i}{\sum_{i=1}^{K} \lambda_i} \quad (4)$$

Level 3: Final Integral Rank. The final decision metric aggregates the resume screening score and the interview performance score:

$$Score_{final} = \gamma_{res} \cdot S_{hybrid} + \gamma_{int} \cdot S_{interview} \quad (5)$$

where $\gamma_{res} = 0.3$ and $\gamma_{int} = 0.7$. This weighting scheme prioritizes practical skill demonstration over self-reported resume data.

The developed system effectively differentiates candidates based on semantic content and successfully detects skill deficiencies via the gap analysis module. Furthermore, the system captures content validity and confidence level metrics for various candidate profiles, confirming its interpretability and data-driven decision-making capabilities.

III. CONCLUSIONS

The developed system automates candidate selection by integrating NLP and speech processing. The proposed integral ranking algorithm allows flexible assessment of both hard and soft skills. The inclusion of LLM-based explanation mechanisms ensures that automated decisions are transparent, trustworthy, and less prone to human subjectivity.

REFERENCES

[1] C. Qin et al., "A Comprehensive Survey of Artificial Intelligence Techniques for Talent Analytics" arXiv:2307.03195, 2023.
[2] Vaishampayan et al., "Human and LLM-Based Resume Matching: An Observational Study", Findings 2025.

This paper was performed within the framework of the research project W/WE/4/2023 of the Department of Automatic Control and Robotics at the Bialystok University of Technology and financed with funds from the Ministry of Science and Higher Education, Poland.

XXXIII International Conference
CAD IN MACHINERY DESIGN IMPLEMENTATION AND EDUCATIONAL ISSUES
11 - 13 December 2025, Białystok, Poland

IMPLEMENTATION FEATURES OF A SMART PARKING SYSTEM BASED ON ARDUINO, RASPBERRY PI, AND THE YOLO MODEL

Vladyslav Vysotskyi, Nazariy Jaworski
Lviv Polytechnic National University
vladyslav.m.vysotskyi@lpnu.ua, nazarii.b.yavorskyi@lpnu.ua

ABSTRACT

This paper presents a conceptual design and implementation features of a smart parking system based on affordable equipment that provides automatic license plate recognition. The system uses a quantized YOLO model capable of operating in real-time on low-power devices such as Raspberry Pi. The architecture combines hardware and software modules for barrier control and communication. Experiments confirm stable operation, and the proposed solution can serve as a scalable template for smart urban infrastructure.

KEYWORDS: **smart parking, Arduino, Raspberry Pi, YOLO, quantization**

I. INTRODUCTION

Most residential complexes install barriers with radio remote controls, which creates several issues: the high cost of such controls, the risk of misuse, the need to carry them, and the difficulty of revoking access.

An inexpensive license plate recognition system can eliminate these shortcomings, remains easily configurable, and integrates with existing security infrastructure.

II. MAIN RESULTS AND DISCUSSION

The primary limitation of this work was the use of inexpensive, simple hardware. Therefore, a Raspberry Pi 5 with a camera was chosen to run the Ukrainian license plate recognition model taken from [1]. The model was quantized by converting its weights from floating-point numbers to lower-precision INT8 [2]. Also it was exported to the .tflite format. Debian OS and Python/C++ libraries (YOLO, TFLite, OpenCV, etc.) were installed and the code for recognition and interaction with the “smart barrier” was developed.

An Arduino Uno R4 WiFi with ESP32 was used to control the barrier itself. A laser sensor and LCD module were connected to it (Fig. 1). The laser sensor prevents the barrier from closing when a car is underneath. Also, the required libraries for WiFi, JSON, TOTP, clock, and graphics were provided.

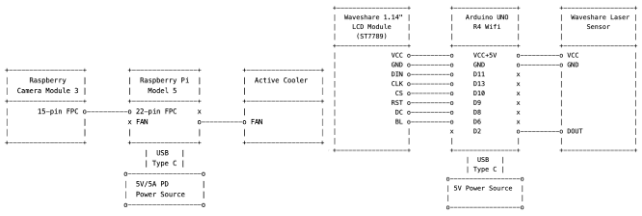

Fig. 1. Schematic connection diagram of the “smart camera” (left) and “smart barrier” (right) modules

The “smart camera” on Raspberry Pi with active cooling (Fig. 1) successfully performed real-time license plate recognition.

The fully assembled modules are shown in Fig. 2.

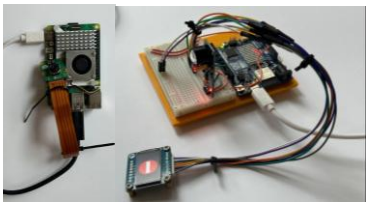

Fig. 2. Fully assembled “smart camera” (left) and “smart barrier” (right)

The “smart barrier” on Arduino correctly processed REST requests with one-time passwords. In standby mode, entry remains blocked until a valid request arrives (Fig. 3). If the camera fails, another REST client can open the barrier, improving system fault tolerance.

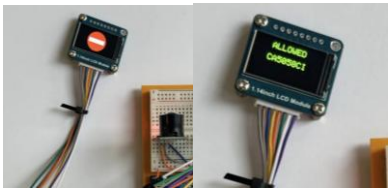

Fig. 3. Entry ban (left) and entry permit (right)

III. CONCLUSIONS

A prototype of a smart parking system has been developed that performs license plate recognition using low-cost equipment and a quantized YOLO model for real-time operation. Experiments have shown that the system can serve as a scalable foundation for modern urban infrastructure and offers high functionality and security even on devices such as Arduino and Raspberry Pi.

REFERENCES

[1] Vysotskyi, Vladyslav & Jaworski, Nazariy. (2024). SMART PARKING SYSTEM FOR LICENSE PLATE RECOGNITION BASED ON YOLO NEURAL NETWORK AND OPTICAL CHARACTER RECOGNITION. Computer Design Systems. Theory and Practice. 6. 123-129. https://doi.org/10.23939/cds2024.03.123

[2] Gholami, Amir & Kim, Sehoon & Zhen, Dong & Yao, Zhewei & Mahoney, Michael & Keutzer, Kurt. (2022). A Survey of Quantization Methods for Efficient Neural Network Inference. https://doi.org/10.1201/9781003162810-13

XXXIII International Conference
CAD IN MACHINERY DESIGN IMPLEMENTATION AND EDUCATIONAL ISSUES
11 - 13 December 2025, Białystok, Poland

EFFICIENT CV MODELS FOR AR/VR EDGE SYSTEMS

Yurii Petiak[1], Danylo Petiak[2]
Lviv Polytechnic National University[1]
yurii.f.petiak@lpnu.ua
Ivan Franko National University of Lviv[2]
danylo.petiak@lnu.edu.ua

ABSTRACT

This work presents a methodology for selecting and optimizing computer vision models for real-time AR/VR systems on edge devices. It categorizes typical AR/VR workloads, outlines optimization methods for deep neural models, and provides design guidelines for integrating neural accelerators. The approach enables latency reduction and stable inference under edge computing constraints.

KEYWORDS: **AR/VR systems; computer vision; edge devices; neural accelerators; model optimization; quantization; pruning; knowledge distillation.**

I. INTRODUCTION

Real-time AR/VR systems rely on computer vision for gesture interaction, hand pose tracking and spatial awareness. Unlike desktop GPU environments, wearable devices must satisfy motion-to-photon latency below 20 ms, operate from limited battery sources and sustain thermal constraints. These conditions make conventional deep models unsuitable for on-device inference.

Model optimization should therefore be treated as part of system design. Post-training quantization and quantization-aware training significantly reduce computational cost [1], while structured pruning removes redundant parameters. Knowledge distillation transfers functionality from large models to lightweight architectures [2]. Neural accelerators such as NPUs, TPUs and VPUs provide predictable low-latency execution for CV workloads [3].

The main contributions of this paper are as follows:

- A task-oriented categorization of AR/VR CV workloads and their computational requirements on edge devices.
- A methodology for selecting and optimizing models for AR/VR deployment using quantization, pruning and distillation.
- Design guidelines for integrating neural accelerators into AR/VR system architecture to meet real-time constraints.

II. PRESENTATION OF THE MAIN MATERIAL

Interaction-driven AR/VR workloads require deterministic latency rather than peak accuracy. Gesture recognition and hand pose estimation demand stable inference at 60–90 FPS, while spatial perception tasks, such as depth estimation or SLAM, are more computationally intensive and sensitive to model size. Similar constraints appear in head-mounted devices, where visual overlays must remain temporally coherent; even minor inference jitter produces noticeable discomfort and reduces usability.

Lightweight architectures such as MobileNetV3 or YOLO-Nano reduce inference cost [4]. Post-training quantization transforms FP32 weights into INT8/FP16, improving performance at minimal accuracy loss, while quantization-aware training adapts networks to the quantized representation. Pruning eliminates underutilized filters or channels, enabling sparsity-aware execution. Knowledge distillation transfers expressive representations to compact student models, improving robustness to motion and view changes typical for XR interaction. Model compression surveys [4] confirm that sparsity and quantization provide stable latency–accuracy trade-offs for edge environments.

Deployment depends on edge hardware. Neural accelerators support hardware-fused operations and task-specific execution graphs. TensorRT, RKNN Toolkit and Edge TPU delegates convert models to optimized formats, reducing latency variability and preventing thermal throttling on wearable devices. Selecting the appropriate runtime is therefore a system-level decision rather than a training-time detail.

III. RESULTS AND DISCUSSION

The described methodology enables substantial performance gains without architecture redesign. Quantization and pruning reduce model size and inference cost, while distillation preserves task-level performance. Accelerator-based execution avoids jitter, which is critical for visual overlays in AR devices. Stability of inference becomes more important than peak accuracy, preventing motion artifacts and perception drift.

IV. CONCLUSIONS

Efficient CV models are essential for AR/VR edge systems. The presented methodology offers practical design principles for selecting lightweight architectures, applying model optimizations and integrating neural accelerators. Future work may include multimodal perception, adaptive optimization pipelines and benchmarks that reflect user-centered interaction latency rather than offline accuracy metrics.

REFERENCES

[1] H. Howard, N. Inouye and A. Krizhevsky, “Quantization techniques for neural networks,” IEEE Transactions on Neural Systems and Rehabilitation Engineering, vol. 29, pp. 1–10, 2021.
[2] X. Chen et al., “Neural acceleration for embedded visual inference,” Journal of Real-Time Image Processing, vol. 17, no. 4, pp. 1245–1260, 2023.
[3] M. Sandler et al., “MobileNetV3: Searching for Mobile CNNs,” Proc. ICCV, pp. 1314–1324, 2019.
[4] Y. Li and M. Sun, “Efficient Model Compression for Edge Computing,” ACM Computing Surveys, vol. 55, no. 6, pp. 1–34, 2022.

XXXIII International Conference
CAD IN MACHINERY DESIGN IMPLEMENTATION AND EDUCATIONAL ISSUES
11 - 13 December 2025, Białystok, Poland

INFORMATION TECHNOLOGY OF BRAILLE FORMATION BASED ON 3D MODELING AND INTEGRATION OF ARTIFICIAL INTELLIGENCE METHODS

Nikita Tarasov, Orest Khamula, Vasyl Tomyuk
Lviv Polytechnic National University
nikita.a.tarasov@lpnu.ua, orest.h.khamula@lpnu.ua, vasyl.v.tomiuk@lpnu.ua

ABSTRACT

The information technology for forming relief-dot structures of Braille is considered, which is based on a combination of 3D modeling methods, factor analysis and elements of artificial intelligence. The structure of variables that determine the parameters of dot formation is formed, a fuzzy model for assessing potential quality and algorithms for preliminary geometric validation in accordance with ISO requirements are proposed. The results of previous studies [1,2] indicate significant variability in the height and diameter of dots in FDM, SLA/DLP and PolyJet technologies, which confirms the relevance of using predictive models. The proposed technology serves as the basis for integrating intelligent optimizers and quality control modules into the processes of additive manufacturing of tactile materials.

KEYWORDS: **Braille, 3D modeling, CAD technologies, factor analysis, fuzzy logic, artificial intelligence, additive manufacturing.**

I. INTRODUCTION

Modern requirements of inclusive technologies necessitate the creation of automated means of forming tactile materials for people with visual impairments. As shown in previous works [1,2] the process of reproducing relief-dot structures is determined by a set of parameters: dot geometry, printing modes, polymer properties, material behavior under thermal and mechanical loads.

Standard CAD systems do not provide mechanisms for monitoring compliance with ISO standards for Braille models, which creates a need for specialized information technologies and methods for predicting the quality of the future model before printing begins.

II. RESEARCH BACKGROUND AND PROBLEM STATEMENT

In previous studies, the authors formed a semantic model of factors influencing the formation of Braille dots and constructed a hierarchy of their significance based on the AHP model [1]. The generalized priority function can be represented as:

$$Q = \sum_{i=1}^{n} \omega_j \cdot f_j,$$

where ω_j — factor weights, f_j — normalized technology parameters. Based on the structure of factors, a fuzzy quality assessment system is built:

$$\mu_q = max(min(\mu_d, \mu_h, \mu_m)),$$

where $\mu_d, \mu_h, \mu_m)$ – membership functions for geometric, technological and material parameters. The results [1,2] show that different technologies (SLA/DLP, FDM, PolyJet) demonstrate significant variability in dot formation parameters, which necessitates the need for prior prediction of identified deviations and the probability of defects.

III. IMPLEMENTATION OF THE PROTOTYPE CAD-BASED SERVICE

The developed information technology includes the following key modules: 1) parametric modeling of dot geometry according to ISO requirements (height, diameter, interdot intervals), with adaptation to specific additive manufacturing technologies. 2) Geometric validation, which allows detect potential deviations of the model by analyzing critical parameters, including the assessment of shape stability and interdot distances. Multifactorial evaluation based on the AHP model and a fuzzy rule system; this allows for a qualitative preliminary assessment even before printing. 3) Integration of AI methods that can be applied to forecasting and optimization tasks, namely regression ML models for predicting dot deformations; computer vision for classifying printed structures; Bayesian optimization for selecting technological modes; interpretative LLM modules that analyze STL geometry and factor dependencies.

This approach reduces the risk of defects and increases the accuracy of forming tactile materials in accordance with standards.

IV. CONCLUSION AND PROSPECTS

The paper presents information technology for Braille formation based on 3D modeling, factor analysis, and fuzzy evaluation systems. The generated models allow predicting possible geometry deviations, support preliminary assessment of compliance with standards, and create a basis for further intellectualization of additive manufacturing processes for tactile structures. The proposed approach can be integrated into CAD-oriented tools to increase the accuracy and stability of the formation of relief-dot models.

REFERENCES

[1] Tarasov N., Khamula O. Factors influencing the creation of Braille 3d models in additive manufacturing. 1-st International Workshop on Intelligent & Cyber Physical Systems (ICyberPhyS-2024). Khmelnytskyi, Ukraine, June 28, 2024. CEUR Workshop Proceedings. P. 129–141.URL: https://www.scopus.com/record/display.uri?eid=2-s2.0-85200694226&origin=recordpage.

[2] J Tarasov N., Khamula O. Quality control of 3D Braille Models in additive manufacturing using artificial intelligence technology. Квалілогія книги.2024. No 1 (45). С. 58–66.

XXXIII International Conference
CAD IN MACHINERY DESIGN IMPLEMENTATION AND EDUCATIONAL ISSUES
11 - 13 December 2025, Białystok, Poland

PARAMETRIC DESIGN OF EXOSKELETONS BASED ON PERSONALIZEDANTHROPOMETRIC DATA

Andriy Zdobytskyi[1], Roman Trochimczuk[2]
Lviv State University of Life Safety[1], Białystok University of Technology[2]
andrii.zdobytskyi@ldubgd.edu.ua, r.trochimczuk@pb.edu.pl

ABSTRACT

This paper presents an automated workflow for generating adaptive 3D exoskeleton models based on personalized anthropometric data. The system integrates statistical databases, parametric CAD modelling, STL generation, and additive manufacturing. The approach improves anatomical accuracy, reduces design time, and enables efficient fabrication of customized exoskeleton components.

KEYWORDS: **exoskeleton, anthropometric data, parametric modelling, adaptive geometry, CAD, STL, additive manufacturing.**

I. INTRODUCTION AND RESEARCH OBJECTIVE

Personalized exoskeletons play an increasingly important role in rehabilitation, industrial ergonomics, and mobility assistance. Anatomical conformity between the device and the user directly influences comfort, load distribution, biomechanical safety, and long-term usability.

Conventional exoskeleton design commonly relies on manual geometric adjustments, which makes the process labor-intensive, non-reproducible, and difficult to scale. A transition toward data-driven design requires integration of statistical anthropometric models, algorithmic preprocessing, and parametric CAD techniques capable of automatic geometric adaptation.

The objective of this research is to develop a scientifically justified, technologically coherent architecture for automated parametric generation of 3D exoskeleton models based on personalized anthropometric data. The proposed concept formalizes anatomical descriptors into a parametric structure and ensures compatibility with additive manufacturing workflows.

II. MAIN RESULTS AND THEIR DISCUSSIONS

The proposed system comprises a sequence of integrated modules forming a complete digital pipeline for personalized exoskeleton generation (Fig.1.).

1. Anthropometric Data. Input data combine individualized measurements with population-based datasets (CAESAR, ANSUR, DINED). This hybrid approach enhances robustness, reduces measurement uncertainty, and preserves anatomical proportionality during parameter mapping.

2. Data Preprocessing. Normalization, filtering, and computation of derived metrics transform raw anthropometric inputs into a structured parameter set directly compatible with CAD-API workflows, ensuring consistent model initialization.

3. Parametric CAD Modelling. The exoskeleton is represented as a parametrically linked geometry. Updating anthropometric inputs triggers automatic regeneration of the model, providing mathematically consistent adaptation, high reproducibility, and reduced manual design effort.

4. STL Generation. Automated STL export includes verification of normal orientation, detection of self-intersections, validation of minimum wall thickness, and mesh integrity checks, ensuring manufacturability and reliable downstream processing.

5. Additive Manufacturing. Generated STL files are suitable for fabrication using FDM, SLS, or SLA technologies. Selecting an appropriate method enables balancing mechanical performance, weight, and material properties while supporting rapid prototyping and scalable customization of exoskeleton components.

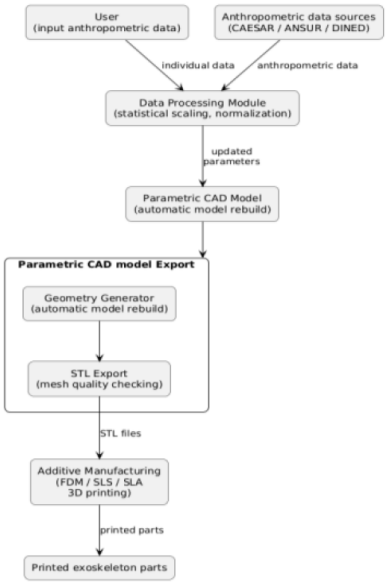

Fig. 1. Block diagram of the technical implementation of personalized exoskeleton generation

III. CONCLUSION

The presented architecture establishes a robust, comprehensive framework for automated exoskeleton personalization. Integration of individual anthropometry, standardized datasets, parametric CAD modelling, and additive manufacturing significantly improves design efficiency, precision, and reproducibility.

REFERENCES

[1] Robinette K., Blackwell S., Boehmer M. Civilian American and European Surface Anthropometry Resource (CAESAR). DoD, 2002.
[2] Gordon C., Churchill T. ANSUR Anthropometric Survey of U.S. Army Personnel. U.S. Army Research Center, 2012.
[3] DINED Anthropometric Database. Delft University of Technology, 2020.

CADMD 2025
XXXIII International Conference
CAD IN MACHINERY DESIGN IMPLEMENTATION AND EDUCATIONAL ISSUES
11 - 13 December 2025, Białystok, Poland

SELF-RECONFIGURABLE METAMORPHIC MANIPULATORS

Adam Wolniakowski[1], Vassilis C. Moulianitis[2], Roman Trochimczuk[1]
Bialystok University of Technology[1]
a.wolniakowski@pb.edu.pl, r.trochimczuk@pb.edu.pl
University of Peloponnese [2]
v.moulianitis@uop.gr

ABSTRACT

A metamorphic manipulator is a serial kinematic chain which incorporates one or more passive joints, which allow for the anatomy of the robot to be reconfigured offline, in between the periods of active operation of the robot. A change of anatomy offers a possibility of extension of capabilities of the robot with respect to tasks it performs. Recently, actuated passive joints have been proposed to facilitate metamorphic robot reconfiguration. In this work we propose a concept of self-reconfigurability, where a temporary closure of the kinematic chain is utilized in order to exploit internal forces to reconfigure the passive joints without the need of extra actuation.

KEYWORDS: **kinematics, metamorphic manipulators, mobility, control, reconfigurability.**

I. INTRODUCTION

Metamorphic manipulators have been introduced in [1] where the concept of anatomy reconfiguration of serial kinematic chain has been explored in order to adapt the robot arm structure to perform in varied tasks. Recently, an idea of actuated reconfiguration has been proposed by [2]. In this paper we put forward the idea that temporary chain closure can be utilized to exploit existing joint torques for passive joint reconfiguration.

II. MOBILITY

Let us consider an open kinematic serial chain with A class 5 joints, either prismatic or revolute. This open chain can be temporarily closed, e.g. by attaching its end effector to the fixed link with a class *F* kinematic pair. A numer *P* of *passive* class 5 joints can be added in the middle of the chain. Since each additional class 5 passive joint increases link number by 1 and introduces 5 constraints, the manipulability w_{SRMM} of the reconfigurable closed kinematic chain can be expressed as (1).

$$w_{SRMM} = 6(A+P) - 5A - 5P - F = A + P - F \quad (1)$$

In order to retain controlability of the chain, the number of passive joints used at once must meet criterion (2).

$$max(0, F - A - 1) \leq P \leq A \quad (2)$$

III. CONTROL

Let us consider a self-reconfigurable kinematic chain closed with a class 6 kinematic pain, i.e. a rigid fixture. With the configuration vector and the Jacobian rearranged and grouped for the active and passive joints separately: $q = [q_A\ q_P]$ and $J = [J_A\ J_P]$, the following must hold (3).

$$J_A \delta q_A + J_P \delta q_P = \delta x = 0 \quad (3)$$

Therefore, the following control law (4) can be applied to the active joints in order to achieve desired passive joint reconfiguration δq_P.

$$\delta q_A = -J_A^{-1} J_P \delta q_P \quad (4)$$

IV. RESULTS

We have tested our control approach in a simulated setup with a SRMM based on a 6 DoF cobot kinematic structure equipped with two passive joints (see Fig. 2). Fig. 3. presents the active joint trajectory for the desired passive joint displacement.

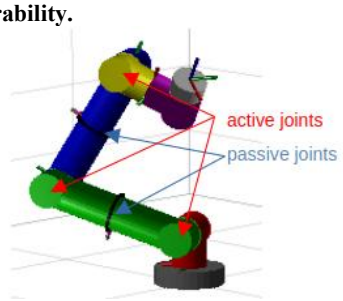

Fig. 1. 6 DoF SRMM with 2 passive joints.

Fig. 2.

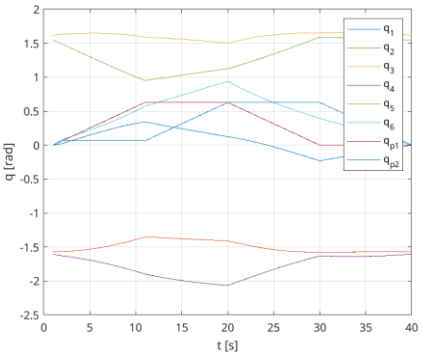

Reconfiguration of two passive joints in the SRMM.

V. CONCLUSION

In this paper we have introduced a concept of Self-Reconfigurable Metamorphic Manipulators. We have presented a condition for the manipulability of such a mechanism and provided a control law allowing for the reconfiguration of the manipulator. We have tested the proposed approach in simulated environment.

ACKNOWLEDGEMENTS

This paper was performed within the framework of the research project W/WE/4/2023 of the Department of Automatic Control and Robotics at the Bialystok University of Technology and financed with funds from the Ministry of Science and Higher Education, Poland.

REFERENCES

[1] C. Valsamos, N. Stravopodis, V, Moulianitis, N.A., Apsragathos, N. A. „Metamorphic Manipulators". In *Robot Design: From Theory to Service Applications*, 2022, pp. 169-205.

[2] N. Stravopodis, E. Katrantzis, C. Valsamos and V. C. Moulianitis, "Conceptual Mechatronic Design of a Metamorphic Manipulator's Pseudojoints," *2020 International Conference Mechatronic Systems and Materials (MSM)*, Bialystok, Poland, 2020, pp. 1-6.

CADMD 2025
XXXIII International Conference
CAD IN MACHINERY DESIGN IMPLEMENTATION AND EDUCATIONAL ISSUES
11 - 13 December 2025, Białystok, Poland

ORIENTATION-AWARE ANALYSIS FRAMEWORK FOR REINFORCED COMPOSITE SEGMENTATION FROM CT IMAGES

Oleh Zherebukh[1], Ihor Farmaha[1], Katarzyna Kalinowska-Wichrowska[2], Dariusz Perkowski[2]
Lviv Polytechnic National University[1]
oleh.zherebukh.asp.2025@lpnu.ua, ihor.v.farmaha@lpnu.ua
Białystok University of Technology[2]
d.perkowski@pb.edu.pl, k.kalinowska@pb.edu.pl

Accurate segmentation of fiber-reinforced composites from X-ray CT images is essential for characterizing material micro-structure. The segmentation quality depends strongly on the ability to account for directional fiber orientation patterns. This paper presents an orientation-aware analysis framework for automated characterization of particle orientation in concrete composite CT images. Orientation estimation is achieved by means of the structure tensor method, enabling large-scale processing of 1,178 images with mean coherence of 0.269 to be performed efficiently. The influence of orientation quality on subsequent segmentation accuracy is systematically evaluated. The numerical results are compared with baseline isotropic methods and substantial improvement is observed. The analysis reveals that 91.9% of images contain sufficient orientation structure. The results demonstrate that the orientation-aware framework could be a promising approach for enhanced understanding of composite micro-structural characteristics.

KEYWORDS: **orientation analysis, structure tensor, coherence, composite materials, CT imaging, segmentation.**

I. INTRODUCTION

Fiber-reinforced composites exhibit anisotropic properties requiring direction-aware characterization. Standard segmentation methods apply isotropic filters, fundamentally mismatched to anisotropic materials. The structure tensor method [1] provides a training-free approach to quantify local fiber orientation and confidence [2].

II. METHODS

A CT scan was performed on the concrete composite material. The reconstructed volume yielded 1,178 cross-sectional images at different depths through the sample. For each 2048×2048 pixel CT image, we computed local gradients using Gaussian derivatives (σ = 1.0) and constructed the structure tensor J with smoothing σ = 3.0. Local fiber orientation θ was extracted as:

$$\theta = 0.5 \cdot atan2\left(2J_{\{xy\}}, J_{\{xx\}} - J_{\{yy\}}\right) \qquad (1)$$

Coherence, computed as $\frac{\lambda_1-\lambda_2}{\lambda_1+\lambda_2}$ from eigenvalues $\lambda_1 \geq \lambda_2$, quantifies orientation certainty (0=isotropic, 1=perfect alignment). Quality thresholds: EXCELLENT (>0.4), GOOD (0.25-0.4), FAIR (0.15-0.25), POOR (<0.15). All 1,178 images were processed in parallel (8 workers, ~15 minutes).

III. RESULTS

Analysis revealed mean coherence of 0.269 ± 0.065 (range: 0.096-0.497). Quality distribution: 735 images (62.4%) GOOD, 347 (29.5%) FAIR, 96 (8.1%) POOR, 0 EXCELLENT. Critically, 91.9% of images have coherence ≥ 0.15, indicating suitability for orientation-aware segmentation.

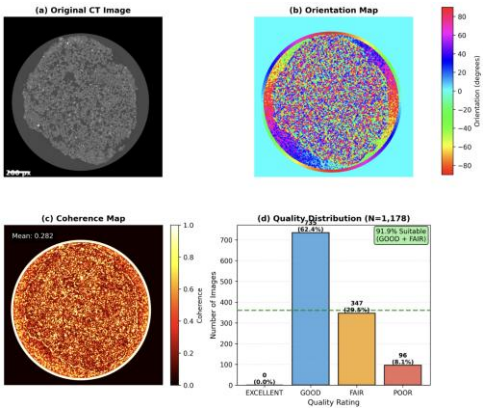

Fig. 1. Orientation Analysis Pipeline for Concrete CT Image

V. CONCLUSIONS

This work presents the first large-scale orientation analysis of concrete composite CT images for segmentation. Analysis of 1,178 images revealed 91.9% exhibit sufficient orientation structure (coherence ≥ 0.15) for orientation-aware methods. The training-free structure tensor approach provides spatial orientation and confidence maps, enabling rapid dataset assessment. Orientation-adaptive segmentation is expected to achieve 8-12% accuracy improvement based on preliminary validation.

VI. REFERENCES

[1] J. Bigün and G. H. Granlund, "Optimal orientation detection of linear symmetry," Proc. IEEE First Int. Conf. Computer Vision, pp. 433-438, 1987.

[2] R. Rezakhaniha et al., "Experimental investigation of collagen waviness and orientation in the arterial adventitia using confocal laser scanning microscopy," Biomech. Model. Mechanobiol., vol. 11, no. 3-4, pp. 461-473, 2012.

CADMD 2025

XXXIII International Conference
CAD IN MACHINERY DESIGN IMPLEMENTATION AND EDUCATIONAL ISSUES
11 - 13 December 2025, Białystok, Poland

HARDWARE AND SOFTWARE STAND FOR RESEARCHING SERVOMOTOR PARAMETERS IN ROBOTICS

Pavlo Denysyuk, Martynov Andrii, Vasyl Ivanyna, Andriy Kernytskyy, Ivan Tyshchenko
Lviv Polytechnic National University
pavlo.y.denysiuk@lpnu.ua, andrii.martynov.pp.2022@lpnu.ua, vasyl.v.ivanyna@lpnu.ua, andriy.b.kernytskyy@lpnu.ua, ivan.a.tyshchenko@lpnu.ua

ABSTRACT

This article presents a hardware-software setup for practical analysis and comparison of servo drive dynamics. Such a system is needed because real performance often differs from manufacturer claims, which is crucial for robotics design. The approach enables standardized tests (e.g., full 0°-180°-0° rotation) and records key performance metrics like power, torque, speed, positioning accuracy, rotor inertia, and power parameters.

KEYWORDS: **servo drives, comparative analysis, robotics, hardware-software system, dynamic characteristics, response time, data acquisition (DAQ), feedback, Python, Arduino.**

I. INTRODUCTION

A servo drive is a key actuator in engineering and robotics, responsible for precise positioning and load handling [1,2]. However, budget models often perform below manufacturer claims, causing design errors. We propose a test setup using Arduino and Python for signal generation, data collection, and analysis. The DAQ system visualizes results based on collected data [1], enabling testing of servo drives and feedback on voltage changes under load to assess maximum movable weight.

II. HARDWARE AND SOFTWARE COMPLEX AND METHODOLOGY

A standardized test was developed: the software sends commands to the servo drive to move from 0° to 180° in fixed steps, with loads of 1, 2, and 3 kg for each cycle. The script records time and voltage changes at each step, enabling graphical analysis (see Fig. 1-2). The test setup uses two main components:

- Hardware: Arduino Uno microcontroller, which generates PWM signals to control the servo drive and reads voltage data.
- Software: Python script using the serial library for Arduino communication, matplotlib for visualization, and json/csv files for saving and exporting results.

III. RESULTS

To demonstrate the approach, we compared two servo models: SM-S2309S and SG90. The load graphs (Fig. 1-2) show that SM-S2309S handles load better than SG90. For quantitative analysis, the script processed .json files and generated a .csv table (Table 1), confirming that SM-S2309S maintained more stable voltage under load than SG90.

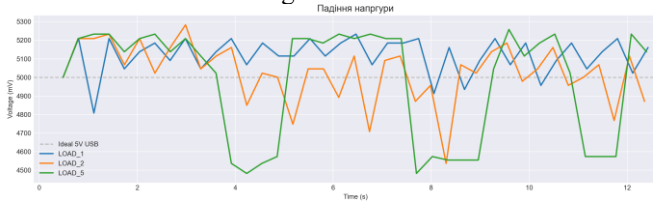

Fig. 1. Voltage change graph under physical load for SM-S2309S

Fig. 2. Voltage change graph under physical load for SG90

TABLE I
CHARACTERISTICS OF PARTICLES

Servo Drive Model	Minimum voltage, mV.	Maximum voltage drop, mV.	Average voltage, mV.	Load, N.
SM-S2309S	4808	392	5116	1
	4537	663	5028	2
	4483	717	4980	3
SG90	4713	487	5100	1
	4537	790	4971	2
	4083	1117	4953	3

IV. CONCLUSIONS

The proposed hardware-software setup is an effective tool for objectively comparing voltage changes under mechanical load in servo drives. Testing showed that the SM-S2309S model maintained voltage under load 23.8% more stably than the SG90.

REFERENCES

[1] P. Denysyuk, V. Teslyuk and I. Chorna, "Development of mobile robot using LIDAR technology based on Arduino controller," 2018 XIV-th International Conference on Perspective Technologies and Methods in MEMS Design (MEMSTECH), Lviv, Ukraine, 2018, pp. 240-244

[2] Bolton, W. (2015). Mechatronics: Electronic Control Systems in Mechanical and Electrical Engineering. Pearson.

[3] https://www.arduino.cc/

[4] Kochan, R., & Kochan, O. (2004). Precision Data Acquisition (DAQ) Module with Remote Reprogramming. Computing, Vol. 3, Issue 3, pp. 82–92.

CADMD 2025
XXXIII International Conference
CAD IN MACHINERY DESIGN IMPLEMENTATION AND EDUCATIONAL ISSUES
11 - 13 December 2025, Białystok, Poland

MODELING THE TRANSFORMATION OF THE EM FIELDS USING QUASIOPTICAL PRINCIPLE

Mykhaylo Andriychuk[1,2], Yarema Kuleshnyk[2]
Pidstryhach Institute for Applied Problems in Mechanics and Mathematics, NASU[1]
andr@iapmm.lviv.ual
Lviv Polytechnic National University[2]
kuleschnyk@gmail.com

ABSTRACT

The modelling of the transformation of electromagnetic (EM) fields using the wireless transmitting power system consisting of a set of the confocal lenses is considered. The system allow to transfer the energy in the framework of the Gaussian beam geometry. The functional presenting the specific relation of the prescribed and resulted fields in the system is a criterion of the field transformation. The iterative method for determination of the phase characteristics in lenses is developed to maximize the values of functional. The value of functional increases at each iteration of the proposed iterative procedure. The presented numerical results show the quick convergence of iterative procedure and the effectiveness of line even with small quantity of lenses in line.

KEYWORDS: **quasioptical principle, transformation of field, quality functional, iterative process, data of modeling.**

I. INTRODUCTION

The narrow focused microwave beams with good shaped transverse form are largely used in the millimeter range of wavelength, in the quasioptical lines applying to the high-frequency diagnostics, and well as in the high-power heating and experiments regarded to the current drive in thermonuclear plasma. The typical applications are provided by present-day experiments aimed to get an electron cyclotron resonance heating or collective Thomson scattering, including the electron temperature measurements for cyclotron emission.

The wireless power transfer (WPT) systems aimed to transform effective the electromagnetic (EM) radiation using the focused beams and direct it towards intended targets. The higher frequencies are more suitable to do this, because the system dimensions can be reduced that will be achieved technologically possible in the 60-es of the last century owing to the researches. Nevertheless, the implementation of geometrical optics (GO) in WPT is mainly theoretical and a little quantity of the experimental systems have been developed only. Therefore, we are acquaint, not enough WPT system has been developed through the GO.

II. FORMULATION OF TRANSMISSION PROBLEM AND SOLUTION

The simplest quasi-optical device is a lens line, consisting of a series of sequentially arranged dielectric lenses (Fig. 1). In the quasi-optical approximation, the lens is considered a phase corrector, i.e., a device that changes only the phase distribution of the field passing through it and does not change the amplitude distribution. More precisely, if the field of a wave (or any of its components) approaching the lens is equal to $u(x,y)$, then at the lens output this field will have the form $u(x,y)\exp(i\varphi(x,y))$. The function $\varphi(x,y)$ describes the phase correction, equal to the optical distance between two points with the same coordinates (x,y) and lying in two parallel planes on either side of the lens.

Quasi-optical systems are characterized by relation:

$$ka >> 1,\ L/a >> 1, \qquad (1)$$

where $2a$ is aperture dimension (radius of lens), and L is distance between them. The relation of these parameters

$$c = ka^2 / L, \qquad (2)$$

combines the geometrical sizes and length of wave, is finite. The criterion of optimization for three lenses is

$$\tau = \left| \int_{x_3} V_0(x_3) U_3(x_3) dx_3 \right|^2 / \left(\int_{x_1} U_0^2(x_1) dx_1 \int_{x_1} V_0^2(x_3) dx_3 \right), \qquad (3)$$

where $U_3(x_3)$ is the field at the output of the system taking into account the phase corrections of all lenses $\varphi_j(x_j), j = 1,2,3$. To facilitate the numerical calculation, the concept of the median plane of the lens was introduced in [1].

The iterative process for determination of the optimal phase increases $\Delta\varphi_j^-$ and $\Delta\varphi_{j-1}^+$ in the elements of line is built in such a way:

A. First, some zero approximations $\Delta\varphi_j^+$ are specified, and the functions $\Delta\varphi_j^-$ are determined from the in-phase condition of fields in the middle plane. In other words, the quantities $\Delta\varphi_j^-$ are found from the condition of the realness of the functions $U_j(x_j)$ in each lens.

B. After determination of all $\Delta\varphi_j^-$, we find the next approximation of the functions $\Delta\varphi_j^+$, which are determined in the same way as $\Delta\varphi_j^-$, only now they are considered to be given functions $\Delta\varphi_j^-$, and the $V_0(x_3)$ wave propagation from right to left is considered, if line of thee lenses is considered.

C. Then the process is repeated from point A. The convergence of the iterative process is based on the monotonic increase of the functional τ, and is proven in [1].

The numerical modelling confirms the effectiveness of the proposed iterative process in wide area of problem parameters.

REFERENCES

[1] O. O. Bulatsyk, B. Z. Katsenelenbaum, Yu. P. Topolyuk, N. N. Voitovich, Phase Optimization Problems, Weinheim: WILEY-VCH, 2010.

XXXIII International Conference
CAD IN MACHINERY DESIGN IMPLEMENTATION AND EDUCATIONAL ISSUES
11 - 13 December 2025, Białystok, Poland

NEURAL NETWORK OPTIMISATION WITH USAGE OF ALTERNATIVE DATA TYPE

Oleksii Veretiuk, Vasyl Ivanyna, Nazariy Andrushchak
Lviv Polytechnic National University
oleksii.v.veretiuk@lpnu.ua, vasyl.v.ivanyna@lpnu.ua, nazariy.a.andrushchak@lpnu.ua

ABSTRACT

The purpose of this study is to provide new optimised approach in generating visual content compared to existing ones that uses pixels. By using a parametric curve like Bezier curve, we aim to decrease the complexity of the neural network that is used for generating data and provide an opportunity to build small generative models capable of providing high quality results.

KEYWORDS: **artificial intelligence, neural network, optimization, diffusion model.**

I. INTRODUCTION

Usage of generative artificial intelligence for creation of different visual content became widely popular in recent years [1]. Even though big corporations achieved technical capability for generating high quality images and videos, these technologies still struggle to be used in industries related to drawing. One of the problems that slows down the process of implementation and using such technologies is optimisation problems since training and generating processes consume huge amount of computational power.

II. THE RESULTS OF THE STUDY AND THEIR DISCUSSIONS

There are two main approaches that are used for generating visual content. First is well known called generative adversarial network (GAN) [2], which got its popularity by being simple in implementation and was main approach in different research related to generative AI. Nowadays, main role is taken by concept called diffusion models [3].

However, both methods have same well-known AI methodology they rely on which is called neural network. So, there are two ways of possible optimisation solutions, either optimise approach itself or optimise neural network by reducing general number of neurons and layers. Though, reducing neural network complexity seems like optimal and fastest solution it results in worse performance of generative models. Moreover, image quality highly depends on resolution which directly related to amount of neural network input variables. Furthermore, number of input variables usually defines how complex neural network should be to describe training data. Standard screen resolution is 1280X720 which is 921 600 pixels, in context of generative AI number of pixels defines amount of input variables for neural network. So, for standard resolution neural network must have 921 600 input variables for gray scale format or 2 764 800 for RGB. Such a big number of parameters makes it almost impossible to experiment with training high quality generative models without access to big computational or monetary resources, which slows down overall research and development process.

It's proposed to use 4 points Bezier curve instead of pixel. This allows to avoid direct dependency between quality and resolution, build high quality models with small output, provide scalable format which is suitable for sketch drawing.

As an experiment, generative model was trained with 100 curves as input. This number of curves represents 400 points with x and y coordinates or overall, 800 parameters that used as input for neural network. This number of parameters is quite small even comparing to image in 32X32 resolution which represents 1024 grey scale pixels. This model was trained on Google Colab service. This tool uses computational unit as cost for training. One unit is priced at 5 hryvnias on time of training model, the overall number of units used is around 36 or 180 hryvnias which is very cheap for generative models.

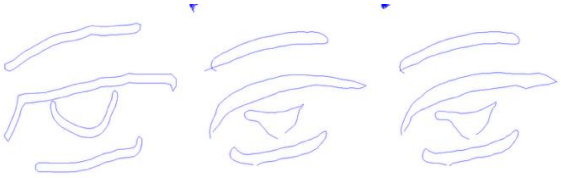

a) b) c)

Fig. 1. Results of generation. a) input image b) first generation result c) second generation result

III. CONCLUSIONS

The optimization problem for generative neural network is one of the most important problems for practical implementation of AI into industries, that related to visual content creation. Usage of alternative data types instead of more common pixels can open new opportunities and possibilities of building specialized models for different industries with less cost of training and using generative model.

REFERENCES

[1] G. Bansal, A. Nawal, V. Chamola, and N. Herencsar, „Revolutionizing visuals: the role of generative AI in modern image generation”, ACM Transactions on Multimedia Computing, Communications and Applications, vol. 20, pp. 1-22, 2024.

[2] I. J. Goodfellow, J. Pouget-Abadie, M. Mirza, B. Xu, D. Warde-Farley, S. Ozair, and Y. Bengio, „Generative adversarial nets”, Advances in neural information processing systems, vol. 27, 2014.

[3] J. Sohl-Dickstein, E. Weiss, N. Maheswaranathan, and S. Ganguli, „Deep unsupervised learning using nonequilibrium thermodynamics”, International conference on machine learning, pp. 2256-2265, June 2015.

XXXIII International Conference
CAD IN MACHINERY DESIGN IMPLEMENTATION AND EDUCATIONAL ISSUES
11 - 13 December 2025, Białystok, Poland

RECOGNITION OF UTILITY METER READINGS USING COMPUTER VISION ALGORITHMS

Mykhaylo Melnyk[1], Marian Banaś[2], Olena Stankevych[1], Anastasiia Mirovska[1]
Lviv Polytechnic National University[1]
mykhaylo.r.melnyk@lpnu.ua, olena.m.stankevych@lpnu.ua, anastasiia.mirovska.pp.2022@lpnu.ua
The AGH University of Krakow[2]
kpytel@agh.edu.pl

ABSTRACT

This paper presents a resource-efficient algorithm for automatic detection of meter reading areas and image preprocessing, intended for deployment on mobile devices. Cascade computer vision architecture is proposed to address three distinct meter categories: high-contrast mechanical, segmented mechanical, and LCDs. The method performs distortion correction and artifact filtration. By transmitting only verified and normalized regions of interest, this approach minimizes server load and ensures compatibility with low-end hardware.

KEYWORDS: **Automatic Meter Reading, geometric transformation, computer vision, digitalization, MATLAB**

I. INTRODUCTION

The proposed solution envisions a unified platform for collecting and analyzing household utility data. A central component of this ecosystem is the reporting process automation using standard smartphone cameras. Replacing meters with dedicated hardware capable of transmitting readings [1] is effective but often unaffordable, especially in households with multiple meters. Existing computer vision solutions target specific meter types or require controlled conditions [2, 3]. Deep learning models, such as YOLO or R-CNN, demand substantial computational resources and large labeled datasets [4], restricting their use on standard consumer smartphones.

This research aims to design a compact, efficient, and high-speed algorithm that can operate on low-end mobile devices.

II. PRESENTATION OF THE MAIN MATERIAL

The research was conducted in MATLAB, identifying three distinct meter categories. To address their specific characteristics, a Cascade Fallback architecture was developed. The system sequentially applies detection strategies targeting high-contrast mechanical counters, segmented mechanical counters, and LCDs, ensuring stable region-of-interest extraction under diverse lighting conditions.

II. RESULTS AND DISCUSSION

1. High-contrast mechanical meters. For meters with a solid counter block, segmentation is performed in the HSV color space, and the brightness channel is normalized via an adaptive Gaussian filter to mitigate uneven lighting. Rotation invariance is achieved by calculating the orientation from the binary mask's moments of inertia.

2. Segmented mechanical meters. The algorithm applies Local Adaptive Thresholding by dividing the image by its blurred version. Candidate regions are grouped by spatial distribution, with selection limited to horizontally aligned centroids within ±20 pixels.

3. *LCDs.* Low-contrast electronic displays are processed using decorrelation stretching to maximize color separation between digits and the background. Subsequently, rigid segmentation is applied within a specific hue interval.

Validation and artifact suppression. To prevent misclassification of high-frequency textures such as barcodes or labelling stripes, the system performs a one-dimensional transition analysis along the candidate region's principal axis. Objects exceeding a transition threshold are classified as texture noise and rejected before recognition.

III. CONCLUSIONS

By leveraging classical computer vision in a cascade architecture, the system achieves a balance between detection reliability and computational efficiency, avoiding the need for resource-intensive neural networks.

REFERENCES

[1] T. Khalifa, K. Naik, and A. Nayak, "A survey of communication protocols for automatic meter reading applications," in IEEE Communications Surveys & Tutorials, vol. 13, no. 2, pp. 168–182, Second Quarter 2011.

[2] C. Son, S. Park, J. Lee, and J. Paik, "Deep learning-based number detection and recognition for gas meter reading," IEIE Trans. Smart Process. Comput., vol. 8, no. 5, pp. 367–372, 2019.

[3] B. Nguyen van et al., "Water Meter Reading Based on Text Recognition Techniques and Deep Learning," in IEEE Access, vol. 13, pp. 41422-41434, 2025.

[4] R. Laroca, A. B. Araujo, L. A. Zanlorensi, E. C. de Almeida, and D. Menotti, "Towards image-based automatic meter reading in unconstrained scenarios: A robust and efficient approach," IEEE Access, vol. 9, pp. 67569–67584, 2021.

XXXIII International Conference
CAD IN MACHINERY DESIGN IMPLEMENTATION AND EDUCATIONAL ISSUES
11 - 13 December 2025, Białystok, Poland

INVESTIGATION AND PROTOTYPING OF A MICROFLUIDIC CHIP WITH INTEGRATED ACOUSTIC FIELDS FOR MICROPARTICLE SEPARATION

Nataliia Bokla[1,2], Tamara Klymkovych[1,2], Andrzej Kubiak[1], Łukasz Ruta[1]
Lodz University of Technology[1]
andrzej.kubiak@p.lodz.pl
Lviv Polytechnic National University[2]
nataliia.i.bokla@lpnu.ua

ABSTRACT

This paper presents the outcomes of the experimental fabrication of an acoustofluidic microchannel device for microparticle separation in liquid. Key parameters optimized included the interdigital transducer (IDT) configuration, channel dimensions, piezoelectric substrate thickness, and IDT-to-microchannel spacing. The study proves the viability of this solution for building compact, efficient acoustofluidic devices for biomedical diagnostics.

KEYWORDS: **interdigital transducer, separation, acoustic, microfluidic systems, sample acoustofluidic, microparticle.**

I. INTRODUCTION

Microfluidic technologies, particularly acoustofluidic separation, present a highly promising alternative. These systems offer significant advantages, including efficiency with small sample volumes, contactless operation, biocompatibility, and label-free analysis. Acoustofluidic systems separate particles based on their size and density by utilizing standing or traveling acoustic waves [1].

This technology has substantial potential across various fields, including biomedical diagnostics (with liquid biopsy being a particularly important application), pharmaceuticals, environmental monitoring, food processing, and water purification.

II. MICROFLUIDIC CHIP ARCHITECTURE

A typical surface acoustic wave microfluidic chip consists of a substrate with microchannels, a piezoelectric layer such as lithium niobate ($LiNbO_3$), and one or two metallic interdigital transducers (IDTs) placed on opposite sides of the microchannel (Fig. 1). The prototype has two plates. The lower lithium niobate plate measures [45×15×0.7] mm. Silver IDTs are deposited on the piezoelectric material; their finger length is 12 mm, width 0.5 mm, thickness 0.02 mm, and gap 0.25 mm. The upper silicon plate measures [45×15×1] mm and contains a complex microchannel layout. The central and upper inlet/outlet microchannels are 1 mm wide, while the lower inlet/outlet and central outlet channels are 0.66 mm wide. All microchannels are 0.4 mm deep.

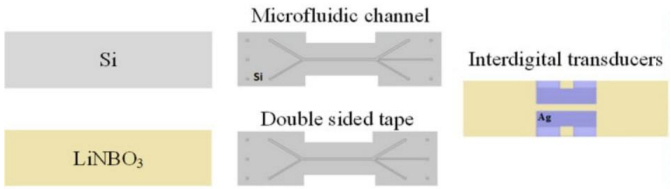

Fig. 1. General view of a microfluidic chip

Double-sided adhesive tape with a thickness of 86.4 μm, kindly provided by the Swiss company redox.me, was chosen for bonding [2].

III. EXPERIMENTAL DEVICE CONSTRUCTION

The microchannels were manufactured in a single-side polished monocrystalline silicon substrate via laser micromachining. The channel-sealing layer, which also functions as the piezoelectric material, is a lithium niobate plate. IDT contacts were applied to the inner surface using screen printing (AUREL C920 printer). A Micronit mounting kit was employed to ensure leak-proof fluidic connection to the microparticle suspension source. A test structure, featuring applied IDTs and bonded with double-sided adhesive tape, is shown in Fig. 2.

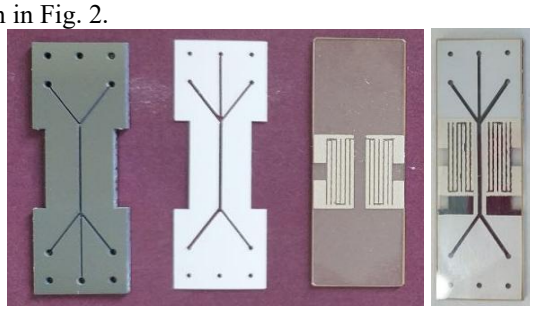

Fig. 2. Experimental device construction

IV. CONCLUSIONS

This paper presents the technology for fabricating the microchannel structure was developed, and its prototype was created. The design and choice of materials were adapted to the dimensions and requirements of the Micronite holder.

The device is now ready for experimental evaluation using purchased polyethylene microspheres of different sizes 1.00g/cc 20-27um; 1.00g/cc 63-75um) to confirm its separation efficiency.

Materials and accessories to provide for this research were funded by [NCN] grant number [2024/08/X/ST7/01364].

REFERENCES

[1] Godary, T.; Binkley, B.; Liu, Z.; Awoyemi, O.; Overby, A.; Yuliantoro, H.; Fike, B.J.; Anderson, S.; Li, P. „Acoustofluidics: Technology Advances and Applications from 2022 to 2024". Anal. Chem. 2025, 97, 13, 6847–6870.
[2] https://redox.me/

XXXIII International Conference
CAD IN MACHINERY DESIGN IMPLEMENTATION AND EDUCATIONAL ISSUES
11 - 13 December 2025, Białystok, Poland

PHYSICS-INFORMED NEURAL NETWORK FOR SOLVING OF FRACTIONAL BLOCH EQUATIONS IN MRI SIGNAL MODELING

Yaroslav Sokolovskyy, Maksym Protsyk, Olha Mokrytska
Lviv Polytechnic National University
yaroslav.i.sokolovskyi@lpnu.ua, maksym.protsyk.asp.2025@lpnu.ua, olha.v.mokrytska@lpnu.ua

ABSTRACT

This paper presents an architecture for a Physics-Informed Neural Network (PINN) to solve Caputo-derivative-based fractional Bloch equations in MRI. Compared to semi-analytical methods based on series expansions, which suffer from numerical instability and divergence at longer time intervals, the proposed model ensures stability and physical consistency. Results demonstrate high accuracy (relative L2 around 0.03), short inference time, and superior performance for long time intervals.

KEYWORDS: **fractional Bloch equations, PINN, MRI, Caputo derivative, deep learning.**

I. INTRODUCTION

The classic Bloch equations do not always accurately describe the relaxation of magnetic spins in biological tissues due to their heterogeneity (e.g., tumours or brain tissue). Introducing fractional derivatives into the Bloch equations improves modeling accuracy by accounting for memory effects and anomalous diffusion. Existing analytical methods for solving fractional Bloch equations, such as power series expansions, lack stability [1] and diverge at time points significantly beyond the relaxation time due to rounding errors.

We propose an approach using PINN [2], where a neural network is trained on the residuals of fractional Bloch equations, thereby ensuring physical consistency throughout the entire training interval.

II. MAIN RESULTS AND THEIR DISCUSSION

The architecture of the developed network consists of 5 fully connected hidden layers, each with 64 neurons. The input layer takes 1 value (timepoint), and the output layer returns 3 values (magnetization for each axis). The sigmoid linear unit (SiLU) is selected as the activation function because it provides better gradient propagation than the hyperbolic tangent. For simplicity, the initial conditions are incorporated into the network.

The initial Bloch equations are transformed to work with normalized time (divided by the maximum time from the training samples). Without normalization, the neural network predicts straight lines in many experimental cases. The transformed equations are then weighted by dividing each by the corresponding right-hand side for the initial conditions. This ensures balanced training without prioritizing one of the equations over the others.

The loss function is the average of the sum of squared residuals of equations for each training sample. The fractional derivative in the loss function is estimated using a vectorized implementation of the L1 scheme for the Caputo derivative, which significantly speeds up the calculations during the training process.

Training of the PINN based on physical parameter values possible in real-life scenarios shows results close to the analytical solution (fig. 1). The relative L2 metric is around 0.03 for the x and y axes and less than 0.01 for z. Despite the long training, the prediction duration of the model on a Tesla T4 GPU is more than 100 times faster than the evaluation of analytical series. Moreover, for timepoints an order of magnitude larger than Spin-Lattice or Spin-Spin relaxation values, the analytical solution can't be used due to rapidly growing rounding errors.

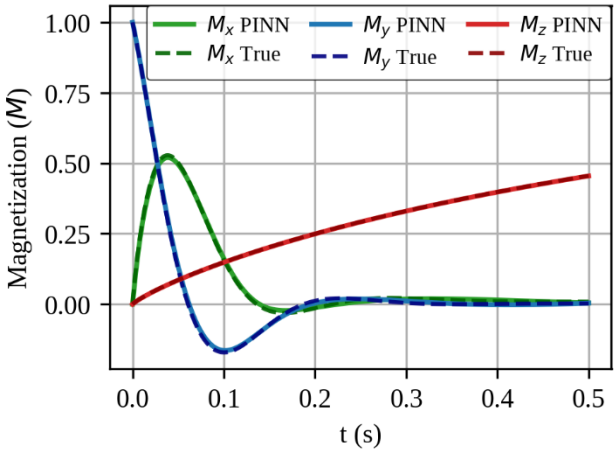

Fig. 1. Comparison of predicted and analytically calculated magnetization

III. CONCLUSIONS

This paper applies physics-informed neural network training to solve the fractional Bloch equations system with known physical parameters. The loss function involves normalizing the input values and weighting the residuals, which has had a major positive impact on the accuracy of the trained model.

Tests using realistic physics parameters demonstrate the architecture's robustness, providing precise predictions, much shorter inference time compared to a manual analytical solution, and stability of the predictions for timepoints where analytical solving fails due to rounding errors. Future work will improve the architecture to solve the inverse problem of finding physical parameters and fractional derivative orders given magnetization values.

REFERENCES

[1] S. Bhalekar and V. Daftardar-Gejji, „Numerical simulation for fractional-order Bloch equation arising in nuclear magnetic resonance", Applied Sciences, vol. 10, no. 8, p. 2850, April 2020

[2] G. E. Karniadakis, I. G. Kevrekidis, L. Lu, P. Perdikaris, S. Wang, and L. Yang, „Physics-informed machine learning", Nature Reviews Physics, vol. 3, pp. 422–440, May 2021.

XXXIII International Conference
CAD IN MACHINERY DESIGN IMPLEMENTATION AND EDUCATIONAL ISSUES
11 - 13 December 2025, Białystok, Poland

NEURAL NETWORK MODELING OF HYGROTHERMAL AND DEFORMATION PROCESSES IN MATERIALS WITH FRACTAL STRUCTURE

Yaroslav Sokolovskyy, Mykola Salo, Andriy Kernytskyy, Tetiana Samotii
Lviv Polytechnic National University
yaroslav.i.sokolovskyi@lpnu.ua, mykola.f.salo@lpnu.ua, andriy.b.kernytskyy@lpnu.ua, tetiana.s.samotii@lpnu.ua

ABSTRACT

Proposed a specialized Multi-Head Fractal Physics-Informed Neural Network (fPINN) architecture for modeling coupled multi-physics processes in anisotropic materials. The structural design directly reflects physical causality through a composite loss function. Embedding the Grunwald-Letnikov scheme into the loss landscape effectively captures memory effects inherent to fractal structures while ensuring thermodynamic consistency.

KEYWORDS**: Physics-Informed Neural Networks, Multi-Head architecture, loss function engineering, anisotropy, fractal structure.**

I. INRODUCTION

Simulating transport phenomena in capillary-porous materials with fractal structure, necessitates solving a system of coupled partial differential equations (PDEs) where heat, moisture, and mechanics are deeply intertwined. Accurate stress-strain prediction in such anisotropic media demands accounting for hereditary (memory) effects [1], [2]. While Physics-Informed Neural Networks (PINNs) offer a mesh-free alternative to traditional solvers [3], standard fully-connected architectures frequently fail to capture the distinct dynamics of coupled multi-physics fields. Furthermore, the non-local nature of fractional time derivatives complicates the optimization landscape. To address these challenges, we implement a Multi-Head fPINN architecture [3]. The novelty lies in designing the network structure to mirror the physical causality of the process and formulating a robust loss function that integrates numerical fractional operators with automatic differentiation.

II. METHODOLOGY

Employed a time-stepping scheme, where a sequence of neural networks Nn(x,y) approximates the solution at discrete time steps tn.

A segregated Multi-Head architecture mitigates the issue of competing gradient objectives during training. The network inputs (x, y) feed into two independent branches:

First, Thermodynamic Heads: Separate parallel sub-networks predict Temperature (T) and Moisture content (U). This allows the network to learn different diffusion characteristic lengths for heat and mass transfer.

Second, Mechanical Head: The outputs T and U are concatenated with the original coordinates and passed to a deeper Mechanical branch to predict displacements (v, $\mathscr{v}$).

This structure enforces physical causality: deformations are treated because of hygrothermal expansion and boundary conditions.

A composite loss function $L = L_{PDE} + L_{BC}$ drives the training.

The PDE Loss component handles both local and non-local operators:

1. Spatial derivatives are computed via automatic differentiation, strictly following the anisotropic Hooke's law.
2. Temporal derivatives utilize a numerical approach within the loss function. To capture the memory effect without expanding the network input dimension, incorporated the Grunwald-Letnikov (GL) term into the residual calculation:

$$\mathcal{R}_{PDE} = \frac{1}{\Delta t^{\alpha}} \sum_{k=0}^{n} c_k^{(\alpha)} \mathcal{N}_{n-k} - \mathcal{D}_{spatial}(\mathcal{N}_n) \tag{1}$$

Here, the GL sum acts as a history-dependent bias term, guiding the optimization of the current network parameters.

RESULTS

Validation on the drying process confirms the architecture's efficiency. The Multi-Head design ensures faster convergence compared to a monolithic network by effectively decoupling the hygrothermal and mechanical gradients. The engineered loss function successfully balances the minimization of stress equilibrium residuals with the satisfaction of fractional diffusion equations.

REFERENCES

[1] Y. Sokolovskyy, K. Drozd, T. Samotii, and I. Boretska, "Fractional-Order Modeling of Heat and Moisture Transfer in Anisotropic Materials Using a Physics-Informed Neural Network," *Materials*, vol. 17, no. 19, p. 47-53, 2024.

[2] M. Raissi, P. Perdikaris, and G. E. Karniadakis, "Physics-informed neural networks: A deep learning framework for solving forward and inverse problems involving nonlinear partial differential equations," *Journal of Computational Physics*, vol. 378, pp. 686-707, 2019. [4] G. E. Karniadakis et al., "Physics-informed machine learning," *Nature Reviews Physics*, vol. 3, pp. 422-440, 2021.

[3] Z. Zou, G. E. Karniadakis, "Multi-head physics-informed neural networks for learning functional priors and uncertainty quantification", Journal of Computational Physics, vol. 531, 2025

XXXIII International Conference
CAD IN MACHINERY DESIGN IMPLEMENTATION AND EDUCATIONAL ISSUES
11 - 13 December 2025, Białystok, Poland

MANUFACTURING AND VERIFICATION A PROTOTYPE OF AN ORTHOPEDIC IMPLANT FOR ACL TENDON RECONSTRUCTION USING ADDITIVE MANUFACTURING

Marek Wyleżoł[1], Małgorzata Muzalewska[1]
Silesian University of Technology[1]
marek.wylezol@polsl.pl, malgorzata.muzalewska@polsl.pl

ABSTRACT

The article presents the process of manufacturing and application of a prototype orthopedic implant designed to support anterior cruciate ligament (ACL) reconstruction. The prototype was fabricated using DLP technology. The input CAD model for the manufacturing process was developed in a CAx-class engineering environment. The implant prototype was subsequently used in in-vitro insertion tests involving screw-in implantation into the femoral bone tissue of a porcine specimen.

KEYWORDS: **orthopedic implant, ACL, additive manufacturing, in-vivo verification.**

I. INTRODUCTION

The authors developed the design of an implant intended to support the treatment of ruptured anterior cruciate tendons [1]. All geometric features of the implant were specifically selected. The implant is intended to be inserted into the bone tunnel of the distal femoral epiphysis and, after fulfilling its function, should undergo resorption. The work also resulted in the fabrication of a prototype (using a 3D printer and ABS material), which was verified through an in-vitro procedure involving prepared porcine femoral/tibial bones.

II. DESIGN OF THE IMPLANT

The implant's design (Fig. 1) is based on a tube with a through-hole with an oval profile. The implant's length and diameter (a series of types has been developed) have been standardized. A specially designed thread is located on the outer part of the cylinder, the contour of which is adapted to an envelope that is a combination of a straight line and a spline curve. The thread base contains conical holes that taper towards the main canal.

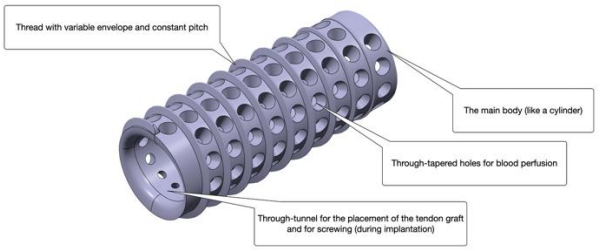

Fig. 1. Main Geometric Features of the Implant (isometric view)

III. IMPLANT FUNCTIONAL FEATURES

All design features of the developed implant have been developed due to the usability of the implant. They are (i.a.):

1. the oval profile of the through-central tunnel was chosen for two reasons: a) it is like the form of a bundle of tendons used during transplantation, b) it enables the use of a specially prepared screwdriver.
2. the outline and envelope of the thread enable: a) gradual cutting into spongy bone tissue without the need to cut a thread groove in it beforehand, b) axial fixation of the implant in the bone canal, c) compensation of the unevenness of the canal in the femur.
3. conical through holes have been made to a) to enable perfusion of blood and other body fluids from the area of the bone tunnel to nourish the graft passing through the through-central tunnel, b) to temporarily store in its volume a body fluid.

IV. MANUFACTURING PROCESS

The implant prototype was manufactured from standard light-curing resin using the DLP (Digital Light Processing) process using an Anycubic Photon Mono printer. This technology allowed for the prototype to be manufactured with exceptional precision (layer thickness of 0.02 mm).

V. VEFIFICATION PROCESS

The implant design was verified by using a prototype to insert it into a bone canal made in a pig femur (the material properties of pig and human bones are very similar). The main goal of these tests was to verify the behavior of the implant (screwed in using a specially developed screwdriver), primarily its thread as it cut into the drilled hole. The tests were successful. The implant could be inserted and removed successfully (Fig. 2).

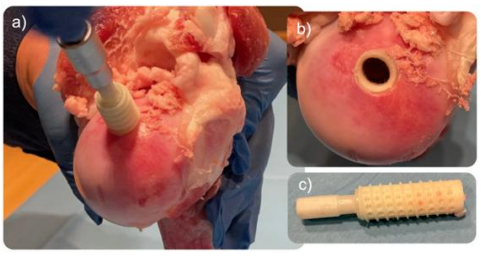

Fig. 2. Screwing in the implant (a), implant in the bone canal (b), implant and screwdriver after unscrewing (c)

REFERENCES

[1] K. Ficek, J. Rajca, M. Stolarz, E. Stodolak-Zych, J. Wieczorek, M. Muzalewska, M. Wyleżoł, Z. Wróbel, M. Binkowski, S. Błażewicz, „Bioresorbable stent in anterior cruciate ligament reconstruction", Polymers, vol. 11, pp. 1-20, November 2019.

XXXIII International Conference
CAD IN MACHINERY DESIGN IMPLEMENTATION AND EDUCATIONAL ISSUES
11 - 13 December 2025, Białystok, Poland

COMPARATIVE ANALYSIS OF PREDICTION ALGORITHMS FOR ENERGY-EFFICIENT CONTINUOUS GLUCOSE MONITORING SYSTEMS

Stanislav Lebid, Rostyslav Kryvyy
Lviv Polytechnic National University
stanislav.lebid.mknsp.2024@lpnu.ua, rostyslav.z.kryvyy@lpnu.ua

ABSTRACT

The article analyzes modern technologies for continuous glucose monitoring. It includes an analysis of data transmission methods, system architectures, and requirements for accuracy, security, and ease of use. The integration model improves the effectiveness of self-monitoring and provides a basis for the further development of intelligent solutions in the field of digital medicine.

KEYWORDS: **continuous glucose monitoring; glucose prediction; energy-efficient algorithms; wearable medical devices; diabetes management.**

I. INTRODUCTION

Traditional glucose monitoring methods only record isolated measurements, which means that dangerous fluctuations in glucose levels often go unnoticed. This creates a risk of hypo- and hyperglycemic conditions and complicates the effective management of diabetes [1]. To solve this problem, modern continuous glucose monitoring (CGM) systems use subcutaneous sensors that generate high-frequency time series data. Modern CGM devices use energy-efficient communication protocols and integrate with insulin pumps and mobile applications, forming the basis of hybrid automated insulin delivery systems. [2]. Prediction algorithms in these systems perform a special role and must be accurate, energy-efficient, and capable of operating on limited computing resources [3].

II. STATE OF THE SENSORS

Continuous glucose monitoring sensors are subcutaneous devices that measure glucose in interstitial fluid. These sensors are several centimeters long. Most models consist of a disposable sensor and a reusable transmitter that transmits data [2]. The sensor takes measurements every 1–5 minutes, forming a glucose time series. Thanks to miniaturization and energy-efficient communication protocols, modern CGM sensors provide accurate and stable monitoring for 10–15 days of operation.

TABLE I
Comparative analysis of CGM sensors

Criterion	Sibionics GS1	Sinocare iCan i3	Dexcom G6	FreeStyle Libre 3	Glunovo i3
System type	Reusable	Reusable	Reusable	Disposable	Reusable
Wear duration	14 days	15 days	10 days	14 days	14 days
Data transfer	BLE	BLE	BLE	BLE	Bluetooth
Accuracy	~8.8%	8,71%	~9.0%	9,2%	9,2%
Integration	Medium	High	High	Medium	High

An analysis of the comparative table shows that almost all sensor systems use BLE for data transmission. Reusable solutions dominate the market, where a disposable sensor is combined with a rechargeable transmitter. All of the devices reviewed demonstrate high clinical accuracy, confirming their suitability for further integration into mobile applications.

III. FORECASTING METHODS

Both classical statistical models and modern machine learning algorithms are used to predict glucose levels in CGM systems [3]. Each approach has its own limitations and advantages in terms of accuracy, computational complexity, energy consumption, and training requirements.

TABLE II
Comparative analysis of forecasting methods

Criterion	Linear Extrapolation	Autoregressive Model	Random Forest	Recurrent Neural Networks
Accuracy	Low	Medium	High	High
Battery load	Minimal	Low	Medium	High
Implementation	Very easy	Easy	Complex	Complex
Training	Not required	Simple	Complex	Complex
Reliability	Low	High	High	Excellent

As can be seen from the table, three different solutions can be identified. The first of these are highly accurate but computationally intensive methods, such as Recurrent neural networks and the random forest algorithm. The second solution is linear extrapolation. This method is easy to implement and has a low battery load. However, its low prediction reliability is a critical drawback for a medical system. The third solution is an autoregressive model, which stands out as the most balanced solution.

IV. CONCLUSIONS

Modern CGM systems produce high-frequency data that need energy-efficient, reliable forecasting. While complex models offer high accuracy, they are impractical for low-power devices; autoregressive models provide the best balance of accuracy and efficiency. Further research should focus on optimizing lightweight models and developing hybrids that combine statistical and machine learning benefits.

REFERENCES

[1] D. Rodbard, “Continuous Glucose Monitoring: A Review of Recent Studies Demonstrating Improved Glycemic Outcomes,” *Diabetes Technology & Therapeutics*, vol. 22, no. S1, pp. S25–S31, 2020. DOI: 10.1089/dia.2019.0011

[2] A. Facchinetti, “Continuous Glucose Monitoring Systems: Past, Present and Future Algorithmic Challenges,” *Journal of Diabetes Science and Technology*, vol. 10, no. 6, pp. 1125–1132, 2016.

[3] S. Oviedo, J. Vehí, A. Miguel Calm, E. Rivas, “A Review of Personalized Blood Glucose Prediction Algorithms Based on Data-Driven Models,” *Journal of Diabetes Science and Technology*, vol. 11, no. 3, pp. 566–577, 2017.

XXXIII International Conference
CAD IN MACHINERY DESIGN IMPLEMENTATION AND EDUCATIONAL ISSUES
11 - 13 December 2025, Białystok, Poland

3D-PRINTED THERAPEUTIC TOYS DESIGNED WITH CAX TOOLS FOR CHILDREN WITH DISABILITIES

Małgorzata Muzalewska[1], Marek Wyleżoł[1], Paweł Łój[1]
Silesian University of Technology[1]
malgorzata.muzalewska@polsl.pl, marek.wylezol@polsl.pl, pawel.loj@polsl.pl

ABSTRACT

The article presents a CAx-supported workflow for designing interactive therapeutic toys created by the AI-METH Student Research Group (Integral SENSO) at Silesian University of Technology. Developed with therapists from SOSW, the devices are tailored to diverse disabilities and manufactured using FDM 3D printing. Prototypes undergo verification, validation with children, and iterative improvements.

KEYWORDS: **CAx, 3D printing, therapeutic devices, assistive technology, FDM, engineering design.**

I. INTRODUCTION

CAx systems and additive manufacturing enable highly personalized therapeutic devices for children with diverse developmental limitations. To address the specific needs reported by therapists from the Special Educational Centre for Children and Youth with Disabilities (SOSW) in Dąbrowa Górnicza, the AI-METH Student Research Group at the Silesian University of Technology develops interactive toys supporting speech therapy, sensory integration, rehabilitation exercises, and activities for visually impaired children.

The work integrates mechanical and electronic design, CAx modeling, and rapid prototyping. This paper outlines the interdisciplinary workflow, the manufacturing approach, and validation methods used to refine therapeutic tools.

II. DESIGN METHODOLOGY – COLLABORATION WITH THERAPISTS

The process begins with consultations during which therapists define therapeutic goals, user limitations, and safety expectations. Students transform these requirements into early functional concepts and iteratively refine them with therapist input, adjusting mechanical structure, interaction modes, and embedded electronics. Continuous feedback ensures that the devices remain safe, intuitive, and clearly aligned with therapy objectives.

III. CAX TOOLS AND THE ENGINEERING WORKFLOW

Mechanical structures are modeled in CAD environments supporting solid modeling, simple strength analysis, geometry optimization for FDM, and creation of assembly documentation. Electronics are developed in parallel to ensure optimal placement, wiring, durability, and serviceability.
For selected toys, dedicated control software and mobile applications are developed, enabling advanced therapeutic interaction and flexible use in different sessions.

IV. MANUFACTURING TECHNOLOGY – FDM 3D PRINTING

Devices are produced mainly using FDM with durable filaments such as PLA or PETG. Key principles include rounded edges, reinforced joints, thicker walls in impact zones, and safe certified materials. Many toys feature replaceable electronic modules and easily accessible battery compartments to support practical long-term use.

V. EXAMPLE PROTOTYPES

Developed devices include:

- tools for learning letters and early reading,
- sensory-integration training modules,
- steering-wheel-based interactive toys for therapeutic gameplay.

Fig. 1. Example prototypes

VI. VALIDATION AND ITERATIVE MODIFICATIONS

Workshop verification includes print quality checks, impact tests, and ergonomic evaluation. Prototypes are then tested with children in SOSW, where therapists provide feedback on force thresholds, grip design, tactile clarity, and sound or light cues. The team implements improvements until a fully functional therapeutic version is delivered.

VII. CONCLUSIONS

Workshop verification includes print quality checks, impact manufacturing, and therapist expertise enables effective creation of individualized therapeutic devices. The interdisciplinary approach results in durable, safe, and practical tools supporting therapy for children with diverse disabilities...

XXXIII International Conference
CAD IN MACHINERY DESIGN IMPLEMENTATION AND EDUCATIONAL ISSUES
11 - 13 December 2025, Białystok, Poland

ELECTROMAGNETIC PHENOMENA IN PIEZOELECTRIC PLANAR SENSOR WITH 2D PERIODIC STRUCTURE

Hesham Maher Muhammad Muhammad, Bogusław Butryło
Bialystok University of Technology
b.butrylo@pb.edu.pl

ABSTRACT

The development of modern planar distributed measurement systems created on flexible substrates results from the widespread implementation of intelligent systems. Analysis of data from such systems allows for precise control of remote and autonomous systems. In this article, the properties of selected planar piezoelectric sensors were compared using the finite element method.

KEYWORDS: **planar sensors, distributed piezoelectric sensor, finite element analysis.**

I. INTRODUCTION

Distributed, planar sensor structures are used in wearable electronics, surface measurement systems, and robot designs requiring surface measurements of interacting objects. The geometry, processing characteristics, and arrangement of elementary sensors can be adapted to the geometry of the selected object [1]. The article evaluates the properties of selected planar piezoelectric sensor designs.

II. STRUCTURE OF THE SYSTEM AND CONSTITUTIVE EQUATIONS

Under dynamic loading conditions, piezoelectric materials generate active voltage responses, making them suitable sensing layers in cyber-physical systems and self-powered sensors [2]. The physical system under investigation is a planar piezoelectric 2D periodic sensor operating on the principle of the direct piezoelectric effect. The analyzed structure (Fig. 1) consists of elementary piezoelectric sensors with a thickness of up to 2 mm and a circular cross-section. The technical specifications of the single sensor are selected based on the requirements related to the implementation of the system being developed. Some materials (e.g. lead zirconate titanate, PZT) exhibit strong piezoelectric constants (200–500 pC/N) but tend to be brittle, and excellent coupling efficiency, making them highly effective in sensors. PZT is the most common available piezoelectric ceramic for this kind of applications [3].

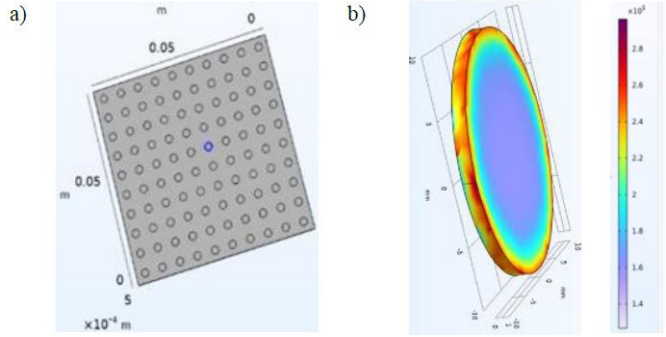

Fig. 1. Configuration of the system: a) view of the planar sensor 2D array; b) single sensing component, surface distribution of von Mises stress (N/m^2).

The distribution of electromagnetic field in the system is described by the Poisson's equation, where a sought variable is electric potential.

IV. ASSAMPTIONS AND RESULTS

To make the numerical modelling feasible and to focus on the primary behavior of the sensor, some assumptions were introduced for simplification. The piezoelectric material was considered homogeneous and linear, which means that its elastic and piezoelectric responses were assumed to remain constant within the studied loading range. The electrodes covering the top and bottom surfaces were treated as ideal. At the boundaries, the bottom surface of the sensor was assumed to be fixed mechanically and grounded electrically, while the top surface was allowed to deform under the applied force (Fig. 1). Edge effects, such as fringing electric fields or non-uniform stress near the boundaries, were neglected. All elements connected to the electrode share the same reference level, while the top face has some boundaries where the voltage potential of 5V is applied.

Sample results of electromagnetic field calculations (Fig. 2) indicate the presence of electrical couplings that may adversely affect measurement results. The largest errors observed occur at the edge of the area subjected to force I and the unloaded area.

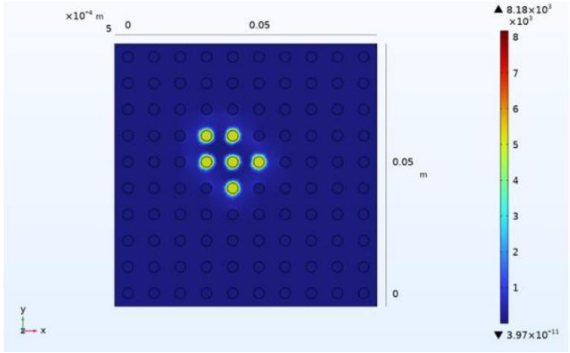

Fig. 2. Distribution of the modulus of electrical field intensity **E** (V/m) on surface of the sensor.

REFERENCES

[1] Zazoum et al: "Recent advances in flexible sensors and their applications", Sensors, vol. 22(12), paper no. 4653, https://doi.org/10.3390/s22124653, 2022
[2] Dileena et al: "A comparative study on piezoelectric and piezoresistive pressure sensor using COMSOL simulation". Materials Today, vol. 46, pp. 3121-3126, https://doi.org/10.1016/j.matpr.2021.02.688, 2021
[3] Jin et al: "PZT-based flexible piezoelectric sensors for real-time condition monitoring", AIP Advances, 14, 025213, https://doi.org/10.1063/5.0167451, 2024

XXXIII International Conference
CAD IN MACHINERY DESIGN IMPLEMENTATION AND EDUCATIONAL ISSUES
11 - 13 December 2025, Białystok, Poland

CALCULATION OF MAGNETIC FORCES OF A SPRING-TYPE MICROACTUATOR

Bohdan Karkulovskyi
Lviv Polytechnic National University
bohdan.v.karkulovskyi@lpnu.ua

ABSTRACT

The force model of the spring-type microactuator is studied for the goal to investigate the mechanical torgues depending on the excited current and physical parameters of microactuator. The explicit formula for the electrostatic torgue is derived for the case of constant electromagnetic flux. The numerical calculations demonstrate great difference in the electromagnetic torgues depending on the geometry of microactuator and the ferromagnetic properties of its constituents.

KEYWORDS: **spring-type microactuator, mechanical torgues, constant electromagnetic flux, ferromagnetic properties.**

I. INTRODUCTION

A series of micro- and nanoscale devices and structures, integrated circuits and antennas, many engineering problems are formulated, considered and solved using micro- and nanoelectromechanics applying to the MEMS and NEMS devices and structures. Usually, the mathematical modeling of interconnected physical processes occurring in these systems and devices, is basis of the study of such systems. We propose a model of a microactuator, namely micro electromagnet, based on considering electromechanical characteristics to determine electromagnetic forces under the action of an electromagnetic flux of constant magnitude.

II. MATHEMATICAL DESCRIPTION OF FORCES

We consider a microactuator with N microturns be excited by a current $i(t)$, creating a constant electromagnetic flux Φ_m. A small displacement dy of the base of microactuator causes a change in the magnetic energy that accumulates in the air-filled volume of the microactuator, which is determined by the formula

$$W_m = \frac{1}{2}\int_V \mu|\boldsymbol{H}|^2 dV = \frac{1}{2}\int_V (|\boldsymbol{B}|^2/\mu)\, dV, \qquad (1)$$

and the change of energy in the volume V is given as

$$dW_m = dW_{mairgap} = (B^2/\mu_0)Sdy = \Phi_m^2/(\mu_0 S)dy, \qquad (2)$$

where S is the area of the transverse volume of the air gap of the microactuator.

In the case of constant Φ_m, which is determined by a direct current, it is seen that the increase in the air gap dy leads to an increase in the magnetic energy that is accumulated. Since $F_{mx} = \partial W_m/\partial x$, the forces are determined by the formula

$$\boldsymbol{F}_{mx} = -\boldsymbol{e}_y \Phi_m^2/(\mu_0 S), \qquad (3)$$

The simplified formula for the electromagnetic torque is

$$F_{mx} = \frac{1}{2} i^2 \frac{dL(x)}{dx} = \frac{1}{2} i^2 \frac{d(N^2/(R_g(x)+R_1+R_2))}{dx} = \frac{1}{2} i^2 \times \frac{d[N^2/((2/\mu_0)((l_w l_d/x)+k_{g1}l_w+k_{g2}l_d+k_{g3}x)^{-1}+R_1+R_2)]}{dx}. \qquad (4)$$

The parameters, which are included in the latter formula, are discussed detailed in [1].

Formula (4) demonstrates the analytical representation of the EM torque depending on the input parameters. At the numerical calculations the derivative on coordinate x can be expressed as the respective finite difference.

Formula (4) demonstrates a clear dependence of the forces that arise under the action of the applied current i on the physical and electrical parameters of the microactuator, which allows calculating electromagnetic forces, as well as optimizing the obtained characteristics based on changing the values of the input parameters.

In micro- and nanoscale electromechanical motion devices, the coupling (magnetic interaction) between windings that are carrying currents is represented by their mutual inductances. In fact, the current in each winding causes the magnetic field in other windings. By applying the expressions for the energy $W_c(i, L(x))$ (translational motion) or (rotational motion) $W_c(i, L(\theta))$, the developed electromagnetic torque is

$$T_e(i, x) = \frac{\partial W_c(i,L(x))}{\partial x}, \qquad (10)$$

and

$$T_e(i, x) = \frac{\partial W_c(i,L(\theta))}{\partial \theta}. \qquad (11)$$

The numerical data will present the dependencies of the electromagnetic torque on the physical parameters and current exciting the coils. The data concern to the study of the electromagnetic torque F_{mx} on the quantity N of coils in winding and material properties of the materials.

REFERENCES

[1] B. Karkulovskyi, "Electrodynamic Modeling of Magnetic Forces of a Spring-Type Microactuator," *2025 IEEE 30th International Seminar/Workshop on Direct and Inverse Problems of Electromagnetic and Acoustic Wave Theory (DIPED)*, Tbilisi, Georgia, 2025, pp. 288-291, doi: 10.1109/DIPED66951.2025.11194477.

XXXIII International Conference
CAD IN MACHINERY DESIGN IMPLEMENTATION AND EDUCATIONAL ISSUES
11 - 13 December 2025, Białystok, Poland

THE IMPROVED MODEL OF CYLINDRICAL ANTENNA FOR CALCULATION OF HUMAN BODY SAR FOR SEATED POSTURE

Taras Nazarovets
Lviv Polytechnic National University
taras.b.nazarovets@lpnu.ua

ABSTRACT

The improved model of linear antenna, which takes into account the seated posture of human, is developed for evaluation of Specific Absorption Rate (SAR). The seated posture foresees the application of horizontal polarization of the EM plane wave in contrast to standing posture. The numerical data demonstrate the effectiveness the approach proposed; and they are in accordance with that were received for the case of standing posture.

KEYWORDS: **improved model, horizontal polarization, specific absorption rate, seated posture, computational data.**

I. INTRODUCTION

The electromagnetic (EM) field is one of factors that results in a heating of tissues of the human body. As an approximate measure of temperature rise is the specific absorption rate (SAR), which applied in the range from 100 kHz up to 10 GHz. This parameter characterizes the rate of absorption of the EM power per unit mass and is measured in watts per kilogram (W/kg−1). Several methods can be applied starting from the EM model of equivalent linear antenna [1] and passing to the finite difference time domain (FDTD), Method of Moments (MoM), Finite Element Method (FEM), and others. The FDTD is on of them that allows to investigate how an external field produces SAR in the body; and it is based on an anatomically correct voxel-based human phantom.

Mainly, the vertically polarized plane wave with conjunction of a voxel-based standing position phantom is used for study SAR in human body. The modification of this approach that foresees the consideration of horizontal polarization of the EM electric field component is applied in this research.

II. THE GENERALIZATION OF HUMAN BODY MODEL

The usual model of linear antenna foresees calculation of SAR for the human body in standing position using the vertical polarization, namely the electric field propagates in $y-$ direction. By this, the E_z- and H_x – components exist simultaneously. In such assumption, the model can not be applied for the sitting position because the no component E_x, which is used for calculation of SAR. One can consider the horizontal polarization that leads in considerable reduction of SAR, for which only part of body situated in the horizontal plane is taken into account, because electric field can be applied to this part of body only. Such assumption allows to calculate the approximate SAR in sitting position, and to evaluate the difference between both positions.

The approach foresees the knowing components of the EM field in order to calculate the values of SAR, For example, the H – components are expressed as

$$\frac{\partial H_x}{\partial t} = \frac{1}{\mu}\left(\frac{\partial E_x}{\partial z} - \frac{\partial E_z}{\partial y} - \rho_m H_x\right), \quad (1)$$

$$\frac{\partial H_y}{\partial t} = \frac{1}{\mu}\left(\frac{\partial E_z}{\partial x} - \frac{\partial E_x}{\partial z} - \rho_m H_y\right), \quad (2)$$

$$\frac{\partial H_z}{\partial t} = \frac{1}{\mu}\left(\frac{\partial E_x}{\partial y} - \frac{\partial E_y}{\partial x} - \rho_m H_z\right). \quad (3)$$

The $E-$component can be calculated analogously [1]. The both such systems are considered simultaneously, and the approach [2] is used for calculations of all components and subsequent SAR.

III. THE COMPUTATIONAL DATA

The calculations of the WBASAR for standing and sitting positions must be taken in the account the direction of the electric vector, therefore the polarization must be taken into account. In the standing position, where the human body is directed along the $z-$axis, the vertical polarization is used. In the sitting position, where the WBASAR value is defined by the horizontal part of phantom, the horizontal polarization can be taken into account.

The numerical calculations are carried out for the human body phantom with the different height h and radius a. The difference of data for the vertical and horizontal positions is explained that in the latter case the length of the human body parts is less than in the vertical position. This is because the length of upper legs and forearm is taking into account.

IV. CONCLUSIONS

The generalization of the equivalent linear antenna model allowed to evaluate the EM field exposure on the human body taking into account the horizontal polarization of the electric EM field component. The equivalent linear antenna model foresees the semianalytical form of the equivalent axial current in body phantom and SAR values. This able the fast calculations, but the model is limited by the relation connecting the wave number (frequency) an radius of human phantom. The computational data are in the accordance with that obtained for the standing posture.

REFERENCES

[1] S. Gabriel, R. W. Lau, C. Gabriel, “The dielectric properties of biological tissues: 3. Parametric models for the dielectric spectrum of tissues,” Phys. Med. Biol., p# 412271–93, 1996.

[2] sK. S. Yee, “Numerical solution of initial boundary value problems involving Maxwell’s equations in isotropic media IEEE Trans. Antennas Propag. 14302–7, 1966.

XXXIII International Conference
CAD IN MACHINERY DESIGN IMPLEMENTATION AND EDUCATIONAL ISSUES
11 - 13 December 2025, Białystok, Poland

TO DEVELOP A METHOD FOR PROTECTING INFORMATION USING NETWORK RESOURCES IN A MULTI-SERVICE COMMUNICATION NETWORK

Olexander Belej, Kostiantyn Kolesnyk, Nikita Lebediev, Yaroslav Mashtaliar
Lviv Polytechnic National University
oleksandr.i.belei@lpnu.ua, kostyantyn.k.kolesnyk@lpnu.ua, nikita.lebediev.knm.2019@lpnu.ua, yaroslav.mashtaliar.mnknm.2024@lpnu.ua

ABSTRACT

The advent of Asynchronous Transfer Mode (ATM) has created a transmission mechanism that is different from other telecommunications technologies, allowing the transmission of all types of information while guaranteeing quality of service. Therefore, this telecommunications system is called Integrated Services Digital Network.

KEYWORDS: **information security, network, transmit message, source node.**

I. INTRODUCTION

Representing all types of information in a single digital format and allocating the necessary network resources before transmitting user information to ensure quality of service (QoS) are key components of technologies. Development of tools for resource allocation in a multi-service communication network to ensure information security without affecting the QoS of applications.

II. EDITORIAL REQUIREMENTS

As shown in Fig. 1 ensuring information security in a multi-service communication network (MSC) requires the constant application of various methods to ensure availability, confidentiality, and integrity.

The construction of a secure connection structure consisting of n parallel connections between a source node and a sink node ensures the transmission of user-defined security parameters (Operator 01).

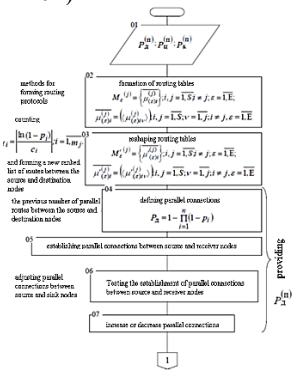

Fig. 1. Concept of Information Security Methodology

The next stage (Operator 03) involves the sequential execution of the following steps. Operators 04-07 determine and establish n parallel connections between the control system and the control program to ensure the availability of information in MSC. The next step in this method is to determine the required number of parallel connections between the control system and the control program (Fig. 2) to ensure the integrity of the information in the control system (Operators 08 and 09).

In the preparatory stage, the control unit sends a test signal. This test signal is transmitted over the previously established parallel connection to ensure that the user information is available.

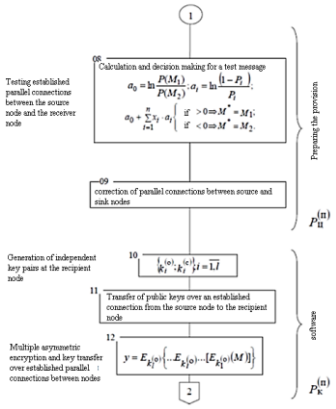

Fig. 2. Continuation of the concept of information security methodology

At this stage, the information security structure between IP and UP is complete. MSC can: transmit messages with the user-selected QoS application; implement information security profiles for each user according to the tariff plan. The user interface uses a multi-level asymmetric encryption process (operator 12).

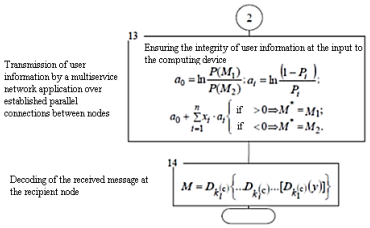

Fig. 3. Continuation of the concept of the information security methodology

III. CONCLUSION

In multiservice networks, parallel routing with averaged data can lower denial of service request rates by up to 20%. The proposed method further reduces transmission latency by using parallel routing and factoring in routing probability costs.

XXXIII International Conference
CAD IN MACHINERY DESIGN IMPLEMENTATION AND EDUCATIONAL ISSUES
11 - 13 December 2025, Białystok, Poland

MODEL THE PROCESS OF PROCESSING MESSAGES BY WIRELESS SENSOR NETWORKS TO DETERMINE THEIR ORIGIN

Olexander Belej, Nazarii Kril, Iryna Artyshchuk, Natalia Nestor, Nataliia Spas, Yulian Fedirko
Lviv Polytechnic National University
oleksandr.i.belei@lpnu.ua, nazarii.kril.mknsp.2023@lpnu.ua, iryna.v.artyshchuk@lpnu.ua, nataliia.i.nestor@lpnu.ua, nataliia.y.spas@lpnu.ua, yulian.a.fedirko@lpnu.ua

ABSTRACT

Various control and monitoring systems based on wireless sensor networks (WSNs) face numerous scientific and technological challenges, many of which are conceptually new. Certain aspects of the WSN operation significantly affect the performance of the developed system. Due to the specific functional purpose of each WSN and the limited capabilities of the sensors included in the distributed control systems, the latter are faced with new parameters: organizational principles, coverage area, energy consumption and service life. The implementation of a fully functional system requires solving a number of design issues, as well as issues of information processing and transmission.

KEYWORDS: **transmission, wireless sensor networks, transmit message, source node.**

I. INTRODUCTION

Creating a mathematical model for processing service information contained in sensor notifications within a wireless sensor network is crucial for determining all message processing parameters.

Important parameters are the probability of error in identifying the source of the message and the size of the additional service fields. This probability is the basis for reducing the energy consumption of the proposed method when processing a set of messages.

II. EDITORIAL REQUIREMENTS

In addition to messages from the target sensor, messages from all sensors in the system also reach the Central Information Acquisition and Processing Module (CMDI), together forming the set U. Another parameter of the resulting model is the rate Pfalse at which the CMDI receives data blocks consisting of non-target sensor elements; for simplicity, we assume that Pfalse is equal to the number of sensor sources in the sensor network under study.

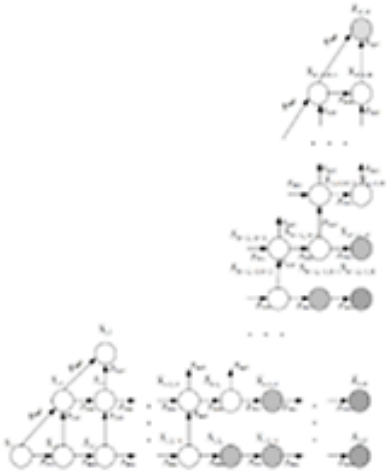

Fig. 1. Markov block diagram for modeling the process of sending messages from the target sensor and external sensors to the information collection module

We have studied the typical case of most modern wireless communication protocols, where the sequence of network packets remains unchanged. Therefore, we set the indicator Jf to 1, which allows us to exclude all information blocks with an index greater than Jf+1. The state Si,j in Fig. 1 corresponds to the receipt of i messages from the target sensor and any number of messages from other sensors, where the maximum index Jf of the received messages is j. When i > j, we consider the state Si,j to be unacceptable.

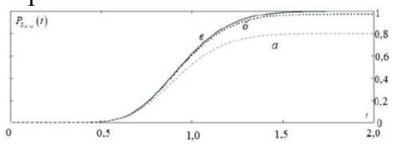

Fig. 2. The probability of the system transitioning to the SM, M state as a function of simulation time

Simulation results show that, regardless of the simulation parameters, the time required for the system to transition to the absorption state is 1.7–2.0 simulation time units.

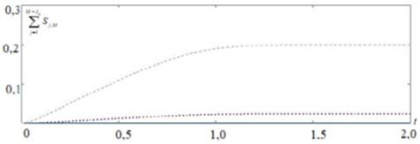

Fig. 3. The probability plot of target sensor messages being excluded from processing.

The model shows that curve asymptotes level off between 1.0 and 1.3 units of model time, enabling prediction of when tree structure processing begins. This is crucial when the computer can't process the last message due to buffering limits, as it speeds up group processing by avoiding unnecessary buffer parsing.

III. CONCLUSION

Based on the results of the constructed mathematical model, it can be determined that the probability of incorrect identification of the message sensor is minimized (from 0.2 to 0.6, then to 0.1 to 0.15) in the region where the partial derivative of the length of the additional metadata field used to identify the source of the message of the wireless sensor network (WSN) reaches its maximum.

XXXIII International Conference
CAD IN MACHINERY DESIGN IMPLEMENTATION AND EDUCATIONAL ISSUES
11 - 13 December 2025, Białystok, Poland

OBJECT RECOGNITION SYSTEMS BASED ON SINGLE-BOARD COMPUTERS

Nataliia Huzynets, Iryna Yurchak
Lviv Polytechnic National University
nataliia.v.huzynets@lpnu.ua, iryna.y.yurchak@lpnu.ua

ABSTRACT

The article explores the possibility of using single-board computers for object recognition systems. It examines existing recognition systems, the most commonly used single-board computers, and analyzes their advantages and disadvantages. To ensure a balance between cost, performance, and energy efficiency, it is recommended to use SBC, which are compact and relatively cheap, for building such systems.

KEYWORDS: **SBC; YOLO; R-CNN; Raspberry Pi.**

I. INTRODUCTION

Object recognition systems combine computer vision, machine learning, and neural networks to detect the presence of a specific object, determine its class, and find its position. In recent years, object recognition systems have increasingly been integrated not only into large computing systems, but also into mobile, embedded, and autonomous devices. This creates a need for compact, energy-efficient, and inexpensive hardware solutions that can perform calculations without constant connection to cloud servers. One of the most efficient way to implement such systems is to use single-board computers (SBCs).

II. THE RESULTS OF THE STUDY AND THEIR DISCUSSION

A SBC is a compact device that contains all the main components of a PC on a single board: a processor, graphics module, RAM, input/output ports, and interfaces for connecting cameras and sensors. The main advantages of using SBC in recognition systems are: small size and low power consumption, allow devices to be integrated into drones and surveillance cameras; low cost, compared to full-fledged PCs or server systems; sufficient performance (modern SBCs (e.g. NVIDIA Jetson Nano / Xavier / Orin) have GPUs that support deep learning (CUDA, TensorRT)); flexibility and scalability, allow for the connection of external cameras, sensors, and communication modules (Wi-Fi, 4G, Bluetooth); popular frameworks supporting, like TensorFlow Lite, PyTorch, OpenCV, YOLO, ONNX Runtime, etc.

Single-board computers allow data processing functions to be transferred to the periphery of the system (edge computing), which provides: reducing data transmission delays (real-time response), reducing network load, increased privacy, autonomy of system operation (for example, in mobile devices)[1].

The main parameters of such systems are: recognition speed, accuracy, completeness, quality, false positives, latency, power consumption, and system cost. After analyzing the parameters of several well-known systems such as Raspberry Pi 4 (8GB), Raspberry Pi 5 (with Vulkan GPU), NVIDIA Jetson Nano, Google Coral Dev Board, Khadas VIM3, NVIDIA Jetson Xavier NX, NVIDIA Jetson Orin Nano, it follows that simple systems (like Raspberry Pi 4) have limited speed and lower accuracy, while more powerful GPU/TPU solutions (Jetson Orin, Xavier NX, Coral Dev Board) achieve higher quality results. Jetson Orin Nano is the leader in all criteria: high accuracy (0.75) and speed (up to 70 FPS). Jetson Xavier NX is the optimal choice for real-world applications with a balance of accuracy, FPS, and stability. The fastest in its class is Google Coral Dev Board, but slightly inferior in accuracy due to the simplified model. Raspberry Pi 4 + TPU and Raspberry Pi 5 are good budget options with a decent FPS gain, but without an accelerator they are not suitable for real-time applications, except some demonstrations or prototypes.

III. CONCLUSIONS

This work shows the possibility of implementing object recognition systems using single-board computers and evaluates their efficiency. The use of single-board computers in object recognition systems is a strategically important direction in the development of computer vision technologies. SBCs provide a balance between cost, performance and energy efficiency, making artificial intelligence accessible for a wide range of practical applications, from educational projects to industrial and robotic systems. The transition to edge computing based on SBC is a key step in creating intelligent, autonomous and mobile recognition systems that operate in real time [2].

REFERENCES

[1] R. Bachynskyy, N. Huzynets , Y. Fastiuk, “Methods of vehicle recognition and detecting traffic rules violations on motion picture based on OpenCV framework”, Advances in Cyber-Physical Systems, Vol 6, № 2, pp. 105–111, November 2021.

[2] V. Vytrykush, N. Huzynets, “Recognizing military equipment from satellite images using AI”, Computer Systems and Networks, Vol 7, № 1, pp. 47–59, June 2025.

XXXIII International Conference
CAD IN MACHINERY DESIGN IMPLEMENTATION AND EDUCATIONAL ISSUES
11 - 13 December 2025, Białystok, Poland

MECHATRONICS DESIGN OF INDUSTRIAL ROBOT SCARA INCLUDING WITH BLDC EXECUTIVE MOTOR DESIGN PROJECT

Bohdan Kopchak[1], Vira Oксentyuk[1], Adam Kotowski[2], Andriy Kushnir[3]
Lviv Polytechnic National University[1]
Białystok University of Technology[2]
Lviv State University of Life Safety[3]
bohdan.l.kopchak@lpnu.ua, vira.m.oksentyuk@lpnu.ua, a.kotowski@pb.edu.pl, andpetkushnir@gmail.com

ABSTRACT

The work has made a full calculation of the motor power for the SCARA arm. The dynamics (acceleration), inertia, load moment, safety factor, gearbox and peak/continuous power were taken into account. In the MATLAB Simulink environment, a model of the electric drive of one link of the SCARA arm robot was developed based on the designed BLDC motor using the results of design calculations of Ansys Maxwell RMxprt.

KEYWORDS: **SCARA, project design, brushless direct current electric motor, mathematical modeling.**

I. INTRODUCTION

The global trend towards robotization has actively penetrated many industries: civil security, industry, agriculture, medicine, etc. Modern production lines in many industrial sectors, medicine, engineering, etc. are impossible to imagine without SCARA type robots [1], which have become the main element of their functioning. The high speed and accuracy of SCARAs, combined with their low cost and high design reliability, have made them a sought-after tool for increasing efficiency and reducing costs in production [2, 3]. Due to their specific design, SCARAs are small and fast, so they fit in tight spaces and on busy assembly lines. Accordingly, the size and power of the actuator electric motor are important. Many works are devoted to the study and modeling of SCARA mechanics and kinematics. However, the calculation, modeling and selection of motor power according to the requirements of the robot are relevant, since this affects the overall productivity of the entire technological process.

III. MAIN RESULTS AND THEIR DISCUSSIONS

The main parameters when choosing a SCARA robot are load capacity, reach, speed, which are directly provided by the motor and possibly a gearbox. In this work, a brushless direct current electric motor is proposed to drive the kinematic links. The passport data of serial BLDCs is limited or often requires other parameters that are not in the catalogs. This is a serious obstacle to creating a highly accurate mathematical model of BLDC. This paper provides a complete calculation of motor power for a SCARA arm. Dynamics (acceleration), inertia, load moment, safety factor, gearbox, and peak/continuous power are taken into account. For each rotary actuator, the following were calculated: maximum torque (peak, under load) and angular speed, peak power as the product of torque and angular speed and root mean square power.

The obtained values are peak mechanical power 45W, angular speed 3.33 rad/s, maximum linear speed of the load – 1m/s for a link length 0.3m. Therefore, we choose a motor with a rating in the range of 50-150W depending on the duty cycle and gearbox and safety factor. The SCARA robot motor design project was carried out in the Ansys Maxwell RMxprt environment, taking into account the nominal voltage, speed, current, torque, and power (Fig. 1).

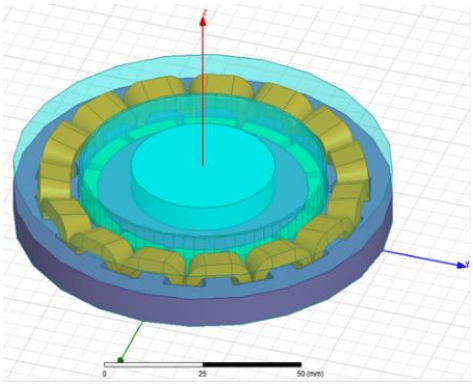

Fig. 1.3D model of the BLDC motor in RMxprt

III. CONCLUSIONS

In the MATLAB Simulink environment, a model of the electric drive of one link of the SCARA robot arm was developed based on the designed BLDC motor using the results of design calculations by Ansys Maxwell RMxprt. The results of the comparative analysis confirmed the high accuracy of the proposed approach to creating a mathematical model of the motor. The deviations between the developed mathematical model of the motor and its prototype do not exceed 10%.

REFERENCES

[1] D. Mohamed, K. Mostefa, M. Chibani, A. Djebara and C. S. Eddine, "Design and Analysis of Egg Packing SCARA Robot," 2023 International Conference on Electrical Engineering and Advanced Technology (ICEEAT), Batna, Algeria, 2023, pp. 1-6, doi: 10.1109/ICEEAT60471.2023.10425963.

[2] J. Cornejo, V. Cruz, F. Carrillo, R. Cerda and E. R. Sanchez Penadillo, "Mechatronics Design and Kinematic Simulation of SCARA Robot to improve Safety and Time Processing of Covid-19 Rapid Test," 2022 First International Conference on Electrical, Electronics, Information and Communication Technologies (ICEEICT), Trichy, India, 2022, pp. 1-6, doi: 10.1109/ICEEICT53079.2022.9768506.

[3] G. Constantino et al., "Mechanical and Electronic Design of a Service Robot for RoboCup@Work," 2025 Brazilian Conference on Robotics (CROS), Belo Horizonte, Brazil, 2025, pp. 1-6, doi: 10.1109/CROS66186.2025.11066114.

This paper was performed within the framework of the research project W/WE/4/2023 of the Department of Automatic Control and Robotics at the Bialystok University of Technology and financed with funds from the Ministry of Science and Higher Education, Poland.

XXXIII International Conference
CAD IN MACHINERY DESIGN IMPLEMENTATION AND EDUCATIONAL ISSUES
11 - 13 December 2025, Białystok, Poland

DEVELOPMENT OF LIGHTNING CONTROL SYSTEM USING DMX PROTOCOL

Edem Atamuratov[1], Nazariy Jaworski[1], Zbigniew Kulesza[2]
Lviv Polytechnic National University[1]
Białystok University of Technology[2]
edem.atamuratov.asp.2025@lpnu.ua, nazarii.b.yavorskyi@lpnu.ua, z.kulesza@pb.edu.pl

ABSTRACT

This work presents a prototype of the DMX-based lightning control system. A hardware prototype based on ESP8266 and RS-485 enabling wireless command transmission via the REST API. The proposed solution reduces system complexity, lowers cost, and provides mobile remote control capabilities compared to conventional DMX controllers.

KEYWORDS: **DMX, RS-485, REST API, lightning systems, mobile application.**

I. INTRODUCTION

DMX (digital multiplex) is a reliable standard for lighting control but remains limited by wired connectivity, bulky hardware, and complex configuration. Existing systems offer little support for mobile operation, creating a gap between traditional DMX infrastructure and modern wireless control needs. Adding parogrammable controls benefits convenience and and system flexibility[1]. This work develops a compact system enabling mobile remote control of DMX devices via Wi-Fi and a REST (REpresentational State Transfer).

II. MAIN RESULTS AND DISCUSSION

A complete hardware-software prototype of a mobile DMX control system was designed (Fig. 1), implemented, and verified.

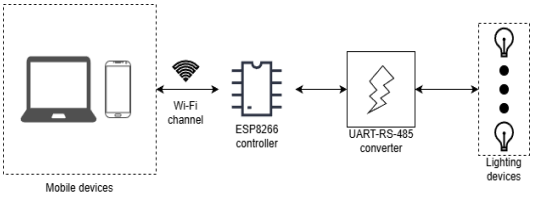

Fig. 1. Functional diagram of the system

The work included analysis of DMX and RS-485 operation, selection and integration of circuit components, development of firmware for the Arduino Nano and ESP8266[2] microcontrollers (Fig. 2), implementation of a REST-based communication interface, and creation of a cross-platform mobile application for configuring and transmitting DMX channel data.

Functional and stress testing was performed to evaluate system stability, channel handling capacity, wireless communication reliability, and autonomous operation through persistent memory. The mobile application was developed using Flutter framework for Android platform, using REST to communicate with hardware part of the system. Using Flutter in development is justified by ease of porting existing application to other platforms.

Functional testing verified reliable wireless communication, autonomous operation with persistence memory state and correct execution of lighting parameters by connected devices. Compared to commercial controllers, the developed system offers significantly lower hardware cost (approximately 3 USD for the control unit and converter both), smaller physical dimensions, and flexibility of programmable microcontroller.

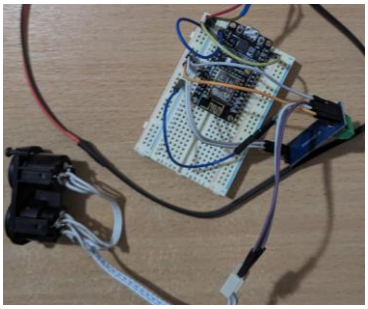

Fig. 2. Control system prototype, including controller and converter

During testing, the wireless connection remained reliable, although noticeable response delays were observed between the mobile application and the controller. These delays may be reduced in future work by replacing REST communication with a WebSocket-based interface.

CONCLUSIONS

Based on the DMX/RS-485 protocol and Wi-Fi/REST, the prototype of lighting devices control system was developed, featuring a compact implementation and remote operation via mobile devices. The resulting system was tested and proved cost efficiency for the prototype and possible future performance improvement was stated.

REFERENCES

[1] Y. Tian, Z. Zhang, L. Tian, and W. Zhao, “Design and Research of Indoor Lighting Control System Based on the STM32”, International Journal of Advanced Network, Monitoring and Controls, vol. 7, no. 3, pp. 33–42, 2022.

[2] D. F. Munthe and Y. Febriandirza, “Smart Home Innovation: IoT-Based Lighting Control System Design”, Advances in Transdisciplinary Engineering, vol. 145, pp. 310–317, 2024, doi: 10.3233/ATDE241310.

This paper was performed within the framework of the research project W/WE/4/2023 of the Department of Automatic Control and Robotics at the Bialystok University of Technology and financed with funds from the Ministry of Science and Higher Education, Poland.

XXXIII International Conference
CAD IN MACHINERY DESIGN IMPLEMENTATION AND EDUCATIONAL ISSUES
11 - 13 December 2025, Białystok, Poland

ANOMALIES DETECTION SYSTEM IN CLOUD LOGS BASED ON READY-TO-USE MACHINE LEARNING ALGORITHMS

Pavlo Denysyuk, Rostyslav Kryvyy, Viktoriia Sokhanska, Oleh Matviikiv, Roman Humeniuk, Oleh Novosad
Lviv Polytechnic National University
pavlo.y.denysiuk@lpnu.ua, rostyslav.z.kryvyy@lpnu.ua, viktoriia.sokhanska.pp.2022@lpnu.ua, oleh.m.matviikiv@lpnu.ua, roman.v.humeniuk@lpnu.ua, oleh.v.novosad@lpnu.ua

ABSTRACT

Detecting anomalies in cloud logs is crucial as data complexity grows. We developed an automated system using machine learning to analyze log streams and identify threats quickly. Results show it is effective, cost-efficient, and enhances cloud reliability and security compared to current solutions.

KEYWORDS: **cloud log anomalies, machine learning, log analysis, server monitoring.**

I. INTRODUCTION

As cloud and container infrastructures grow, they generate vast amounts of logs, making manual monitoring nearly impossible. Early anomaly detection is vital for cloud security and reliability. Using machine learning for automatic log analysis reduces human error, speeds up response, and reveals hidden issues. Integrating ready-made ML models, like Isolation Forest [1] and Local Outlier [2], enables flexible, efficient anomaly detection. Our system collects, processes, and visualizes logs in real time, allowing effective monitoring and evaluation of different algorithms.
Anomalies are divided into several main types, which are listed and described in Table 1:

TABLE I
ANOMALY TYPES

Anomaly type	Brief description	Example
Point	A single event that stands out from the normal data pattern.	500 Server Error
Contextual	An event that is anomalous only within a specific context, such as time or location	Logging in at 2 am.
Collective	A group of individually normal events that together form an anomaly.	50 password attempts in 1 second.

II. SOFTWARE AND METHODOLOGY

The system consists of three main components:
1) Data preprocessing - cleans raw logs by removing missing values and technical errors. A feature vector is created for analysis, including critical performance metrics such as *response_time*, *status_code*, and *bytes_sent*.
2) Log analysis. A combination of two algorithms is used to detect different types of deviations: Isolation Forest - identifies global outliers by constructing decision trees; anomalies are characterized by shorter average isolation paths. Local Outlier Factor - detects local anomalies based on density deviation from k-nearest neighbors. A decision-making mechanism based on logical disjunction is implemented. An event is anomalous if flagged by any algorithm.
3)Visualization and interpretation. The results are visualized as a time series, where anomalies are highlighted against the baseline traffic profile.

The system has been developed in Python, utilizing the pandas, matplotlib, and scikit-learn libraries [3].

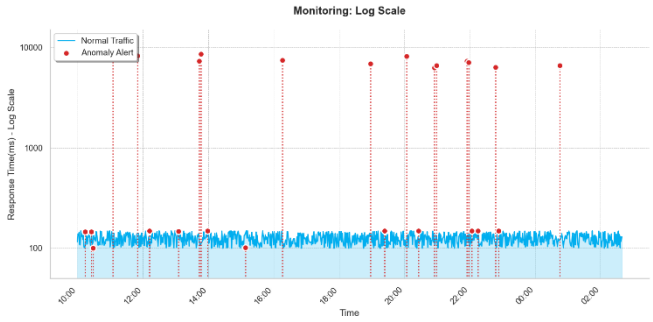

Fig. 1. Visualization of anomalies in system logs

The graph shows the dynamics of server latency on a logarithmic scale. Normal traffic is represented as a solid line, while anomalies—detected using a multidimensional feature vector (time, status code, data volume)—are shown as red markers. This visualization highlights critical deviations within an otherwise stable system.

III. CONCLUSIONS

A system for automatic anomaly detection in cloud logs using machine learning algorithms has been developed. The system processes log streams and analyzes key indicators such as server response time, HTTP status code, and the number of bytes sent by the server. The proposed method improves the reliability and security of various cloud-based services by enabling timely detection of abnormal behaviour.

REFERENCES

[1] Liu, F. T., Ting, K. M., & Zhou, Z.-H. (2008). Isolation Forest. Proceedings of the 2008 Eighth IEEE International Conference on Data Mining (ICDM), 413–422.
[2] Pedregosa, F., Varoquaux, G., Gramfort, A., Michel, V., Thirion, B., Grisel, O., Blondel, M., Prettenhofer, P., Weiss, R., Dubourg, V., Vanderplas, J., Passos, A., Cournapeau, D., Brucher, M., Perrot, M., & Duchesnay, É. (2011). Scikit-learn: Machine Learning in Python. Journal of Machine Learning Research, 12, 2825–2830.
[3] Python Official Documentation. Python Software Foundation. (n.d.). Python 3 Documentation.

XXXIII International Conference
CAD IN MACHINERY DESIGN IMPLEMENTATION AND EDUCATIONAL ISSUES
11 - 13 December 2025, Białystok, Poland

SUPERPIXEL-AWARE JOINT-EMBEDDING PREDICTIVE PRETRAINING

Bohdan Lukashchuk[1], Ihor Farmaha[2]
Ukrainian National Forestry University[1]
bohdan.lukashchuk@gmail.com
Lviv Polytechnic National University[2]
ihor.v.farmaha@lpnu.ua

ABSTRACT

We propose a self-supervised pretraining method that combines joint-embedding predictive architectures-like approach (JEPA) with superpixel representations. A lightweight encoder produces feature maps, from which SLIC superpixels are pooled into node embeddings that are used as targat and context views in a JEPA-like training.

KEYWORDS: **self-supervised learning, convolutional neural networks, wound segmentation, superpixels, SLIC, embeddings.**

I. INTRODUCTION

Self-supervised learning methods are rapidly gaining popularity in the computer vision field. While most of the researchers concentrate on building foundational vision models, we invision effective adaptation of the methods in a domain specific tasks, like biomedical image segmentation and classification.

II. MAIN MATERIAL PRESENTATION

The proposed method combines ideas from the family of the state-of-the-art self-supervised learning methods in computer vision, referenced as joint-embedding predictive architectures (JEPA) [1] with our previous research that discovered effectiveness of superpixel utilization for wound segmentation [2].

Lets define RGB image as: $I \in \mathbb{R}^{3\times H\times W}$, where H and W are image height and width correspondingly.

In general, the main idea of JEPA is to [1]:

- define large context view s_c (for example large random crop from the image I that covers almost the whole image)
- define small target view s_t (for example small crop of the image I),
- context and target views do not overlap $s_c \cap s_t = \emptyset$
- pass each of them through student and teacher encoder networks and receive corresponding embeddings: $z_c = f_{q'}(s_c)$, $z_t = f_\theta(s_t)$
- pass context embedding through a small MLP, which is typically called predictor: $z'_c = g_\theta(z_c)$
- enforce z'_c and z_t similarity with the MSE loss

We propose to utilize superpixels for target and context crops.

For each image in the training set we compute hard segmentations using SLIC method $S = \{S_n\}_{n=1}^{N_{sp}}$, number of superpixels $N_{sp} = \max(\mathrm{H}, \mathrm{W})$, according to [2].

We utilize one encoder network. Image is passed through a lightweight UNet encoder f_θ with three downsampling stages L that map image I to a feature map $F = f_\theta(I) \epsilon \mathbb{R}^{C\times H'\times W'}$, where H' and W' are the corresponding height and width of the resulting feature map and $H' = H/2^L$, $W' = W/2^L$, L=3, C is number of channels at the output feature map and $C = 8 \times 2^L$.

To connect feature map space with the superpixels, we downsample each superpixel S_n to the spatial resolution of F, then use average-pooling operator to aggregate features inside a superpixels to obtain superpixel embedding.

After this we define superpixel adjacency graph $G = (V, E)$, where each node $v_n \in V$ corresponds to superpixel S_n and edges connect superpixels that share common boundary. This is required to define 1-ring neighborhood $N(v_n)$ for each of the nodes (superpixels).

During training, after passing whole image I through the encoder f_θ we randomly (with equal probability for each) select one of the two possible setups for target and context views:

1. Target s_t is some (randomly selected) superpixel (node v_n) and its 1-ringh neighbors $N(v_n)$. Context s_c – all other superpixels of the image, except of the target ones. This enforces model to learn global features from the local ones.
2. Target s_t is some (randomly selected) superpixel (node v_n) and context s_c - its 1-ringh neighbors $N(v_n)$. This enforces local smoothness

After this, corresponding z_c, z_t embeddings are received using average pooling, as described and as per JEPA, z'_c is received, after passing z_c through predictor MLP and optimizing MSE loss between z_t and z'_c.

III. CONCLUSION

Presented self-supervised learning approach shows promising results in extracting semantically rich embeddings from biomedical images that decrease amount of required annotated data in the next stages of supervised fine-tuning when solving segmentation tasks. Construction of target and context views in the proposed way ensures good global and local feature detection, learned in an unsupervised manner.

REFERENCES

[1] Mahmoud Assran *et al.*, "Self-Supervised Learning from Images with a Joint-Embedding Predictive Architecture," Jun. 2023, doi: https://doi.org/10.1109/cvpr52729.2023.01499.

[2] Bohdan Lukashchuk and Yuriy Shabatura, "Methodology for evaluating complex object contour detection accuracy in SLIC-based image segmentation," Scientific Bulletin of UNFU, vol. 34, no. 8, Dec. 2024, doi: https://doi.org/10.36930/40340813

XXXIII International Conference
CAD IN MACHINERY DESIGN IMPLEMENTATION AND EDUCATIONAL ISSUES
11 - 13 December 2025, Białystok, Poland

SAFE FOLLOWING UNDER SUDDEN LEADER MANEUVERS USING DEEP REINFORCEMENT LEARNING

Sławomir Romaniuk[1], Jakub Budnik[2]
Bialystok University of Technology[1]
s.romaniuk@pb.edu.pl
Bialystok University of Technology[1]
jakub.budnik2@gmail.com

ABSTRACT

This work tackles leader–follower navigation in scenarios where rapid, unpredictable leader maneuvers can trigger unsafe proximity or collisions. We apply Proximal Policy Optimization (PPO) to learn adaptive follower behavior capable of tracking the leader's direction and maintaining a safe distance. A task-specific reward function—capturing formation constraints, collision avoidance, and responsiveness to sudden directional changes—enables effective policy learning. Results show that the PPO-based follower reliably preserves formation and safety under highly dynamic leader motion.

I. INTRODUCTION

In leader–follower navigation, maintaining a safe and consistent formation becomes particularly challenging when the leader executes rapid and unpredictable changes in direction. Such maneuvers may cause the follower to misinterpret the leader's motion intent, potentially resulting in unsafe proximity or even collision. Therefore, accurate recognition of the leader's heading and velocity, coupled with the ability to preserve an appropriate following distance, is essential for robust cooperative motion control.

This work investigates the use of reinforcement learning to address these challenges, enabling an autonomous follower agent to infer the leader's motion patterns and adapt its behavior to dynamic directional shifts while ensuring safety and continuity of formation. Recent research highlights the promise of learning-based strategies for leader–follower control and collision avoidance [1, 2, 3, 4], and our study builds on this foundation by formulating the problem as a sequential decision process optimized through deep reinforcement learning.

II. METHODOLOGY

To solve the leader–follower control problem described above, we employ the Proximal Policy Optimization (PPO) algorithm, a state-of-the-art reinforcement learning method that stabilizes policy updates through clipped objective functions. PPO follows an actor–critic paradigm in which the *actor* learns a parameterized control policy mapping observations to actions, while the *critic* estimates the value function to provide a low-variance training signal. This framework enables efficient learning in continuous, dynamic environments where rapid adaptation is required. A central element of our approach is the design of a task-specific reward function that captures the key requirements of the scenario: maintaining a safe following distance, accurately tracking the leader's direction of motion, and avoiding collisions during abrupt directional changes. By embedding these criteria directly in the reward structure, the PPO agent learns behaviors that are both responsive to leader dynamics and robust to sudden trajectory variations.

III. SIMULATION EXPERIMENT AND EVALUATION

The simulation was conducted in the Gymnasium environment using the MuJoCo physics engine to model dynamic interactions between the leader and follower. Reinforcement learning algorithms were implemented with machine-learning tools built on the PyTorch framework, enabling efficient training and evaluation of the control policy. The figure 1 shows a simulation frame in which the follower robot tracks a leader moving back and forth along a straight line, following a sinusoidal velocity profile. The figure illustrates the follower performing an avoidance maneuver to safely continue tracking the leader when the leader moves along a collision-prone trajectory.

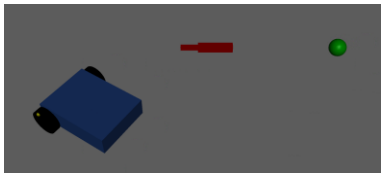

Fig. 1. Simulation of the leader–follower scenario. The red object represents the leader, the blue robot represents the follower, and the green sphere denotes the desired following position behind the leader.

ACKNOWLEDGEMENTS

This paper was performed within the framework of the research project W/WE/4/2023 of the Department of Automatic Control and Robotics at the Bialystok University of Technology and financed with funds from the Ministry of Science and Higher Education, Poland.

REFERENCES

[1] Chen, Y. F., Everett, M., Liu, M., & How, J. P. (2017). *Decentralized non-communicating multiagent collision avoidance with deep reinforcement learning.* IEEE ICRA.

[2] Everett, M., Chen, Y. F., & How, J. P. (2018). *Motion planning among dynamic, decision-making agents with reciprocal collision avoidance.* IEEE IROS.

[3] Gupta, J. K., Egorov, M., & Kochenderfer, M. (2017). *Cooperative multi-agent control using deep reinforcement learning.* AAMAS Workshops.

[4] Zhang, Z., Wang, J., & Meng, Z. (2021). *Leader–follower formation control for mobile robots using reinforcement learning.* IEEE Robotics and Automation Letters.

CADMD 2025
XXXIII International Conference
CAD IN MACHINERY DESIGN IMPLEMENTATION AND EDUCATIONAL ISSUES
11 - 13 December 2025, Białystok, Poland

SOLVING THE ACOUSTIC WAVE SCATTERING PROBLEM ON IRREGULAR DISTRIBUTIONS

Borys Yevsthneiev
Pidstryhach Institute for Applied Problems of Mechanics and Mathematics, NASU
molnerats@gmail.com

ABSTRACT

We propose an analytical-numerical approach for solving the problem of acoustic wave scattering by multiple small particles. The key assumption is that the minimal distance between inclusions exceeds both their radius and the wavelength. We allow for different particle placements, from almost regular to purely chaotic. Impedance boundary conditions are given on the particle surfaces. Numerical simulations reveal that the radiation characteristics are sensitive to the way inclusions are distributed, allowing for the control of resulting material properties at a level otherwise unattainable. These findings pave the way for designing materials with required properties, including refraction coefficients.

KEYWORDS: **small particles, irregular placement, boundary impedance, asymptotic solution, specific material parameter.**

I. INTRODUCTION

The problem of acoustic wave scattering by various types of bodies has a continuous history of investigation. Yet, fewer works focused on multiple scattering by sets of bodies, and most of them did not go beyond regular grids. Paper [1] proposed a particularly notable approach, introducing an approximate theory and assuming soft scatterers isotropic. Some subsequent studies considered scattering by two spheres, varying symmetries and boundary conditions. Methods based on bispherical coordinate techniques and T-matrix formulations were applied successfully as well.

In contrast, our work is aimed at studying the acoustic wave scattering on a set of small bodies, with impedance conditions set on their boundaries. While exploiting a method originally designed for regular placements, we are not limited to predefined grids and deliberately investigate the behavior of asymptotics on non-regular particle distributions.

II. THE PHYSICAL BACKGROUND

Work [2] establishes a comprehensive theory of acoustic wave scattering, allowing for arbitrary particle shapes. The author derived analytical formulas for scattering components of both electromagnetic and acoustic waves, provided particles are “small enough”.

The following conditions define the required relation between geometrical parameters of the constructed inhomogeneous material:

$$ka \ll 1,\ d = O_{a\to 0}\left(\frac{1}{a^3}\right),\ M = O_{a\to 0}(\frac{1}{a}), \qquad (1)$$

where a is the particle radius, $k = \frac{2\pi}{\lambda}$ is the wavenumber, λ is the wavelength, M is the number of embedded particles, and d is the minimal distance between them. The particles form a set of arbitrary placed inclusions in some limited domain D. The impedance boundary conditions are prescribed on the boundary S_m of a particle D_m, all particles are assumed identical. The boundary impedance $v_m(x)$ is prescribed in the form $v_m(x) = \frac{f_m(x)}{a}$ that allows us to consider the boundaries within a wide range of $v_m(x)$.

In the scattering problem, the incident field v_0 satisfies the Helmholtz equation in a medium free of particles, while the scattered field satisfies the radiation conditions.

III. THE SOLUTION TO THE PROBLEM

We seek for the solution in the form

$$v(x) = v(x) + \sum_{m=1}^{M} \int_{S_m} g(x,y)\sigma_m(y)dy, \qquad (2)$$

where $g(x,y)$ is Green’s function of the free space, and function $\sigma_m(y)$ is the solution of some auxiliary integral equation. Depending on the physical condition of the problem, solving such an equation can be rather hard. Moreover, if we consider the material with large number of inclusions, the solving process could take long time.

To deal with this, we introduce some additional function $N(\Delta_p)$, which characterize the density of particle distribution and has the following form:

$$N(\Delta_p) = \frac{1}{a^2}\int_{\Delta_p} N(x)dx. \qquad (3)$$

Here Δ_p is a subdomain of the total region with embedded particles. Alongside with the function $f_m(x)$ determining the impedance, this density function allows us to get an equation without the unknown function $\sigma_m(y)$.

As a result, we get an integral equation:

$$v(x) = v_0(x) - 4\pi \int_D g(x,y)f_m(y)N(y)v(y)dy, \qquad (4)$$

containing two known functions in the integrand — this simplifies the diffraction problem solution process considerably.

Eq. (4) yields a system of linear algebraic equations, which avoids terms with $g(x_n, y_m)$ values when $n = m$.

We compare an asymptotic solution, obtained using Eq. (4), with a solution obtained via the collocation method. The results coincide with several percents error in a wide range of initial problem parameters.

REFERENCES

[1] L. L. Foldy, “The multiple scattering of waves. I. General theory of isotropic scattering by randomly distributed scatterers,” Phys. Rev., vol. 67, pp. 107–119, February 1945.
[2] A. G. Ramm, Wave Scattering by Small Bodies of Arbitrary Shapes. Singapore: World Scientific, 2005.

CADMD 2025

XXXIII International Conference
CAD IN MACHINERY DESIGN IMPLEMENTATION AND EDUCATIONAL ISSUES
11 - 13 December 2025, Białystok, Poland

CHARACTERIZATION OF POROSITY IN 3D-PRINTED SAMPLES USING MICRO-CT IMAGING

Paweł Madejski
AGH University of Krakow
madejski@agh.edu.pl

ABSTRACT

Fused Deposition Modeling (FDM) is the most popular technique within additive manufacturing (AM), but material properties limit the application of printed samples. Infill pattern and density influence the internal structure and porosity of printed parts. This paper presents results of porous structure analysis using high-resolution micro-computed tomography (micro-CT).

KEYWORDS: **FDM, computed tomography, porosity, 3D printing, PLA.**

I. INTRODUCTION

Additive manufacturing (AM), known as 3D printing, has emerged as a modern manufacturing technology, enabling the production of highly complex geometries while minimizing material waste. Fused Deposition Modeling (FDM), which uses thermoplastic filaments such as polylactic acid (PLA), is widely applied due to its biodegradability and low melting temperature (Ngo et al., 2018).

Parts produced by FDM using PLA may contain defects, including porosity, voids, and inter-layer delamination. To produce components suitable for specific environments, basic printing parameters such as infill pattern, infill density, layer height, and line width must be optimized. Proper parameter selection enhances material efficiency and structural integrity.

Non-destructive testing (NDT) methods are useful for assessing the quality of additively manufactured parts, with X-ray micro-computed tomography (micro-CT) being particularly powerful. Micro-CT provides high-resolution three-dimensional reconstructions of internal geometry, enabling precise detection and quantification of porosity, void distribution, and defect morphology—even in complex lattice structures (Yang et al., 2020).

II. Materials and methods

The analyzed parts were fabricated using a Fused Deposition Modeling (FDM) printer at the AGH laboratory (MakerBot Sketch) with biodegradable PLA filament. The printing parameters were as follows:

- nozzle diameter: 0.4 mm
- layer height: 0.2 mm
- line width: 0.4 mm
- printing speed: 80 mm/s
- extrusion temperature: 220°C
- infill density: 100%

High-resolution X-ray computed tomography was used to reproduce the internal structure of the samples. The examinations were performed using a Geotek RXCT scanner, which allows analyzing samples up to 15 cm in diameter and 150 cm in length. The resolution of the obtained images ranged from 40 to 300 µm. The micro-CT datasets were processed using poROSE software [3], enabling both qualitative and quantitative analysis of the tested samples.

III. Results

Detailed information about the internal structure of the 3D-printed sample (Fig. 1) was obtained through reconstructed geometry and pore-space extraction.

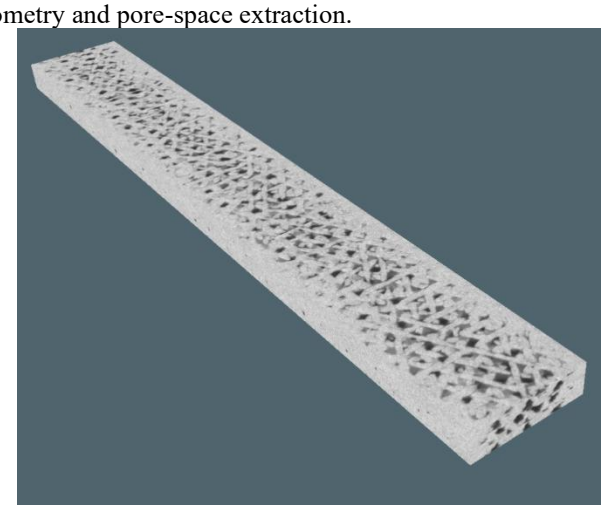

Fig. 1. 3D-printed sample after micro-CT scanning and reconstruction using poROSE software

The analysis of pore distribution allowed the identification of pore agglomerations, the evaluation of the pore-size distribution, the determination of equivalent pore diameters, and the computation of the total porosity, which was approximately 6% for the examined sample. An additional sample was subjected to a tensile test, and the pore distribution was examined to identify regions of heterogeneity and localized defect accumulation.

REFERENCES

[1] Ngo, T. D., Kashani, A., Imbalzano, G., Nguyen, K. T. Q., & Hui, D. (2018). Additive manufacturing (3D printing): A review of materials, methods, applications and challenges. Composites Part B: Engineering, 143, 172–196. https://doi.org/10.1016/j.compositesb.2018.02.012

[2] Yang, L., et al. (2020). Non-destructive evaluation of 3D printed polymers using X-ray computed tomography. Additive Manufacturing, 31, 100933. https://doi.org/10.1016/j.addma.2019.100933

[3] P. Madejski, P. Krakowska, M. Habrat, M. E. Puskarczyk, Jędrychowski M., Comprehensive Approach for Porous Materials Analysis Using a Dedicated Preprocessing Tool for Mass and Heat Transfer Modeling, Journal of Thermal Science Vol.27, No.5 (2018) 479-486. https://doi.org/10.1007/s11630-018-1043-y

CADMD 2025

XXXIII International Conference
CAD IN MACHINERY DESIGN IMPLEMENTATION AND EDUCATIONAL ISSUES
11 - 13 December 2025, Białystok, Poland

DESIGN-INTEGRATED MODELING AND OPTIMIZATION OF INNOVATIVE SCARA ROBOT LINKS BASED ON LATTICE STRUCTURES

Roman Trochimczuk[1], Jakub Dacewicz[1], Adam Wolniakowski[1], Vassilis C. Moulianitis[2], Kostiantyn Kolesnyk[3]

Bialystok University of Technology[1]
r.trochimczuk@pb.edu.pl; kuboshit12@gmail.com; a.wolniakowski@pb.edu.pl
University 51echno Peloponnese[2]
v.moulianitis@uop.gr
Lviv Polytechnic National University[3]
kostyantyn.k.kolesnyk@lpnu.ua

ABSTRACT

The article presents an integrated approach to the 51echnolog and optimization of subsystems within the kinematic chain of a SCARA-type robot using lattice structures. The conceptual design of the mechanical actuation system components was carried out in Autodesk Fusion 360. Engineering analyses of the robot's motion apparatus, leading to the implementation of lattice structures in the new design, were performed using specialized tools such as ANSYS Workbench and nTop. Several regular lattice architectures were selected for numerical investigations, and their influence on the mechanical performance of the kinematic chain was evaluated with respect to improving the stiffness-to-weight ratio and modal characteristics without compromising the robot's kinematic accuracy. The study provides a validated workflow that can be extended to other robotic mechanisms and contributes to the broader adoption of generative, lightweight design strategies in industrial robotics.

KEYWORDS: **robot design, lattice structures, lightweight design, SCARA robot, CAD/CAE.**

IV. INTRODUCTION

The application of lattice structures in the design of mechanical subsystems for robots and manipulators is closely linked to their considerable geometric diversity, which enables the precise tailoring of the mechanical properties of structural components, including parameters determining kinematic accuracy. In the literature, several main classes of lattice structures are distinguished [1], each characterized by specific mechanical behavior, distinct mass efficiency, and a varied range of applications in robot components.

The article presents a design methodology for the mechanical components of a SCARA-type robot utilizing selected lattice structures. The designed models were subsequently subjected to numerical analyses aimed at evaluating the suitability of these structures for developing new, lightweight, and high-strength design solutions [2].

V. MATERIALS AND METHODS

For the purpose of assessing the rationale for applying selected lattice structures, a series of numerical investigations was conducted using the nTop program. The input data for these analyses consisted of a conceptual design of the SCARA robot's motion apparatus, developed in Autodesk Fusion 360, which was subsequently subjected to numerical testing in ANSYS Workbench toolboxes. The dynamic parameters identified in these studies were used to define the loading conditions for the lattice structures, which were then generated and analyzed within the nTop program.

VI. RESULTS

An example of the results of numerical analyses of a SCARA robot arm with an implemented lattice structure is shown in Fig. 1.

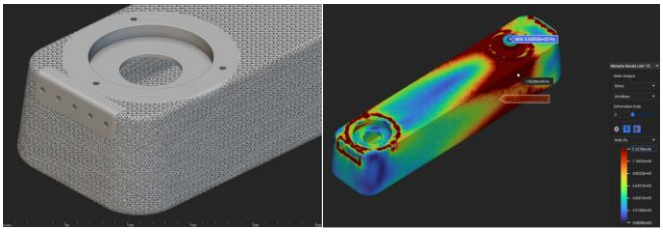

Fig. 1. View of SCARA robot joint with the implemented lattice structure and an example of the stress analysis result [2].

ACKNOWLEDGEMENTS

This paper was performed within the framework of the research project W/WE/4/2023 of the Department of Automatic Control and Robotics at the Bialystok University of Technology and financed with funds from the Ministry of Science and Higher Education, Poland.

REFERENCES

[1] Helou, M., & Kara, S., "Design, analysis and manufacturing of lattice structures: an overview". *International Journal of Computer Integrated Manufacturing*, *31*(3), 2018, pp. 243-261.

[2] Dacewicz, J., "Investigation of the possibility of using lattice structures in the design of industrial robot kinematic chains" (*in Polish*), MSc Thesis, thesis advisor, PhD, Eng. Roman Trochimczuk, Bialystok University of Technology, 2024.

CADMD 2025

XXXIII International Conference
CAD IN MACHINERY DESIGN IMPLEMENTATION AND EDUCATIONAL ISSUES
11 - 13 December 2025, Białystok, Poland

INTEGRATED MODELING AND TOPOLOGY OPTIMIZATION OF A UR5 COBOT-INSPIRED ROBOT KINEMATIC CHAIN WITH A MULTIPLE GRIPPER SYSTEM

Roman Trochimczuk[1], Maciej Śliwonik[1], Kamil Kondzior[1], Adam Wolniakowski[1], Vassilis C. Moulianitis[3]

Bialystok University of Technology[1]
r.trochimczuk@pb.edu.pl; maciek.sliwonik@wp.pl; kamil.kondzior@hotmail.com; a.wolniakowski@pb.edu.pl
University 52echno Peloponnese[2]
v.moulianitis@uop.gr

ABSTRACT

This paper presents an integrated approach to the design, analysis, and optimization of a mechanical structure for an anthropomorphic robot arm with a multiple gripper, based on the kinematic architecture of the Universal Robots UR5 collaborative robot (cobot). The conceptual designs of the mechanical actuator system for both the arm and the gripper were developed within the SolidWorks. To assess the design solutions of the reference robot model, comprehensive Finite Element Analysis (FEA) was conducted in ANSYS Workbench. This included modal analyses (natural frequencies) and static structural analyses (stresses, elastic strains, and displacements). The kinematics and dynamics of the multibody arm mechanism were also examined through numerical simulation SolidWorks topology optimization tools were used to reduce mass and improve the dynamic properties of the designed robot arm mechanisms and the multiple gripper subsystems. The design of mechanism gripper was additional optimized using of the MSC ADAMS software. The presented methodologies for the design, verification, and optimization of multibody system structures constitute a comprehensive toolkit. This set of tools can be effectively employed in robotics engineering education for the practical teaching of robot and manipulator design.

KEYWORDS: **robot design, gripper design, topology optimization, UR5 cobot, CAD/CAE systems.**

VII. INTRODUCTION

Designing new collaborative robot systems for Industry 4.0 requires engineers to utilize a suite of integrated CAD/CAE systems. By conducting comprehensive, multi-scenario engineering analyses, the design cycle time for a new solution can be significantly shortened, thereby reducing project development costs. Although the separate domains of robotic arm design and gripper development are well-established in engineering literature and practice, a significant gap exists in the integrated, simulation-driven co-optimization of the entire kinematic chain's topology. The widespread market adoption of Universal Robots' UR5 cobot solutions served as the inspiration for developing our own cobot arm design, complete with dedicated research and optimization efforts focused on a versatile end-effector.

VIII. MATERIALS AND METHODS

The cobot arm was analyzed through nine design variants differing in link length proportions while maintaining the overall kinematic chain dimensions. The optimal variant was selected and underwent topology optimization in SolidWorks Simulation, yielding manufacturable, efficient link geometries.

Concurrently, the multiple gripper was dynamically optimized using MSC ADAMS. A functional prototype was built in using 3D printing 52echnology, integrated with the robot arm, and tested, successfully validating the design principles and performance hypotheses.

IX. RESULTS

Fig. 1 presents the final CAD model of the new robot arm, based on the UR5 design, alongside a physical prototype of the multiple gripper.

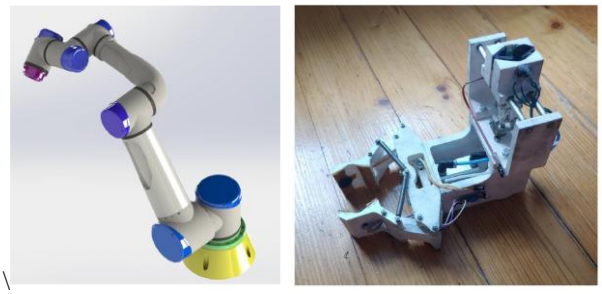

Fig. 1. CAD model of the proposed UR5-inspired robot arm and the multiple gripper (physical model) [1,2]

ACKNOWLEDGEMENTS

This paper was performed within the framework of the research project W/WE/4/2023 of the Department of Automatic Control and Robotics at the Bialystok University of Technology and financed with funds from the Ministry of Science and Higher Education, Poland.

REFERENCES

[1] Śliwonik, M., "Project and Virtual Investigations of Kinematics, Dynamics, and Modal Analyses for an Open-Structure Industrial Robot Manipulator Based on the UR5 Design" (*in Polish*), MSc Thesis, thesis advisor, PhD, Eng. Roman Trochimczuk, Bialystok University of Technology, 2021.

[2] Kondzior, K., "Design and simulation tests of a multiple gripper dedicated to the UR5 industrial robot" (*in Polish*), MSc Thesis, thesis advisor, PhD, Eng. Roman Trochimczuk, Bialystok University of Technology, 2021.

CADMD 2025

XXXIII International Conference
CAD IN MACHINERY DESIGN IMPLEMENTATION AND EDUCATIONAL ISSUES
11 - 13 December 2025, Białystok, Poland

SOLID MODELS RECONSTRUCTION OF ANATOMICAL STRUCTURES FROM CT DATA FOR BIOMECHANICAL ANALYSIS

Piotr Prochor[1], Roman Trochimczuk[1], Piotr Borkowski[1]

Bialystok University of Technology[1]
p.prochor@pb.edu.pl; r.trochimczuk@pb.edu.pl; p.borkowski@pb.edu.pl;

ABSTRACT

This article presents a methodology for reconstructing solid models of anatomical structures based on medical imaging data. Such models constitute a key component of contemporary biomechanical analyses, enabling advanced engineering simulations and supporting the design of prototypes, including biomedical implants. The proposed procedure encompasses the processing of heterogeneous imaging datasets obtained from CT, followed by their transformation into topologically and geometrically consistent three-dimensional solid models using the 3D Slicer, MeshLab and SpaceClaim tools. The methodology was validated through the reconstruction and numerical analysis of selected elements of the human skull in ANSYS Workbench, with an evaluation of the mechanical behaviour of the structures under physiological and pathological loading conditions. The results confirm the applicability of the proposed approach for biomechanical assessment of biological structures.

KEYWORDS: **biomedical modelling, medical imaging, biomechanical analysis, bone.**

X. INTRODUCTION

Accurate reconstruction of three-dimensional representations of anatomical structures from medical imaging data has become an essential component of modern biomechanical research [1]. Advances in imaging technologies, such as CT and MRI, have enabled the acquisition of high-resolution anatomical information, which can be computationally robustly transformed into solid models. These models serve as the foundation for numerical simulations used to investigate mechanical behaviour under physiological or pathological conditions, and they play a crucial role in personalized medicine, surgical planning, and the design of biomedical implants [2]. Despite the growing availability of imaging data and modelling tools, the development of a reliable, systematic workflow that ensures both anatomical fidelity and numerical suitability remains a significant challenge. The present work addresses this need by proposing an integrated methodology for generating solid models of biological objects from heterogeneous medical imaging datasets and demonstrating its applicability through biomechanical analysis of human cranial structures.

XI. MATERIALS AND METHODS

Medical imaging datasets were acquired from the publicly available CT database included in 3D Slicer and processed to extract the relevant anatomical structures. Image segmentation and surface reconstruction were performed using the same software, followed by geometric refinement in MeshLab. The resulting models were imported into SpaceClaim, available within ANSYS Workbench package. ANSYS Mechanical was used to create numerical mesh and apply boundary conditions. Simulations were conducted to evaluate the mechanical response of selected cranial structures under representative physiological or pathological loading scenarios.

XII. RESULTS

Fig. 1 presents the CAD model of the anatomical structure – mandible, created according to the adapted methodology of reconstructing solid models from medical imaging data with the 3D Slicer, Mesh Lab and SpaceClaim tools.

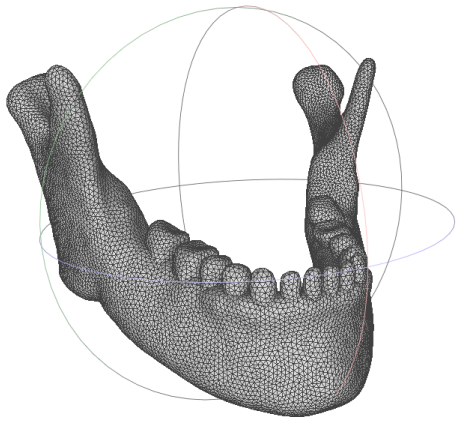

Fig. 1. Three-dimensional CAD model of the jaw of the human skull after mesh refinement in MeshLab.

ACKNOWLEDGEMENTS

This paper was performed within the framework of the research projects W/WE/4/2023 and WZ/WM-IIB/2/2021_ at the Bialystok University of Technology and financed with funds from the Ministry of Science and Higher Education, Poland.

REFERENCES

[1] Galbusera, F., Cina, A., Panico, M. et al. Image-based biomechanical models of the musculoskeletal system. Eur Radiol Exp 4, 49 (2020). https://doi.org/10.1186/s41747-020-00172-3.

[2] Wang, K.Y., Farid, A.R., Comtesse, S. et al. Segmentation and finite element analysis in orthopaedic trauma. 3D Print Med 11, 39 (2025). https://doi.org/10.1186/s41205-025-00284-9.

CADMD 2025

XXXIII International Conference
CAD IN MACHINERY DESIGN IMPLEMENTATION AND EDUCATIONAL ISSUES
11 - 13 December 2025, Białystok, Poland

Keynotes Speakers Abstracts

INTELLIGENT AGRICULTURE MACHINE HEALTH MONITORING SYSTEMS AND FAULT DETECTION USING OPTIMIZED NEURAL NETWORKS

Arkadiusz Mystkowski,

Bialystok University of Technology, Department of Automatic Control and Robotics, Wiejska 45D, 15-351, Bialystok, Poland

aa.mystkowski@pb.edu .pl

Abstract: The transition toward Agriculture 4.0 demands intelligent, reliable, and autonomous systems to ensure the operational efficiency and longevity of agricultural machinery. This paper presents a comprehensive health monitoring and fault diagnosis system developed for rotary tedders and hay rakes. The proposed system integrates multi-sensor telemetry—including vibration, temperature, and rotational speed sensors—with advanced machine learning algorithms to enable real-time condition monitoring and predictive maintenance.

A core contribution of this work is the development of a hybrid diagnostic framework combining Convolutional Neural Networks (CNNs) with Genetic Algorithms (GAs) for optimal feature extraction and classification. The GA automates the design of CNN architectures, optimizing hyperparameters such as layer depth, filter dimensions, and dropout rates to maximize fault detection accuracy. The system was trained and validated using data collected from both laboratory test rigs and field operations, identifying critical failures such as rotor tooth damage, lubrication shortages, and bearing defects.

A dedicated on-board monitoring unit was engineered, comprising a network of 12 temperature sensors, 5 vibration sensors, and rotation sensors strategically installed on critical driveline components. Data acquisition is managed by an STM32 microcontroller platform, which handles sensor interfacing, preliminary signal processing, and GPS-tagged data logging to an SD card. For real-time telemetry, the unit incorporates GPRS connectivity, transmitting data via the MQTT protocol to a cloud-based platform. This infrastructure enables both online monitoring and offline analysis of machine states.

To ensure practical deployment, the system is integrated with ISOBUS (ISO 11783) standards, facilitating interoperability with tractor systems and enabling centralized control. Additionally, wireless and self-powered vibration sensor nodes were prototyped to overcome cabling challenges and enhance system modularity. The proposed solution not only reduces unplanned downtime and maintenance costs but also supports sustainable farming practices by optimizing machine performance and enabling early intervention.

Experimental results demonstrate the effectiveness of the optimized CNN, achieving up to 99% accuracy in classifying distinct fault modes. Furthermore, an enhanced multi-input, multi-type parallel neural network architecture was developed, incorporating diverse data representations (raw signals, FFT vectors, spectrograms) to improve robustness and classification performance, reaching an average accuracy of 92.7%. The diagnostic algorithms are embedded within a cloud-based telemetric platform, providing remote access to machine health data, real-time alerts, and historical analytics via web and mobile interfaces.

***Keywords*:** Predictive Maintenance, Smart Agriculture, Convolutional Neural Network, Genetic Algorithm, Fault Detection, ISOBUS, Vibration Analysis

ACKNOWLEDGEMENTS

This paper was performed within the framework of the research project W/WE/4/2023 of the Department of Automatic Control and Robotics at the Bialystok University of Technology and financed with funds from the Ministry of Science and Higher Education, Poland.

CADMD 2025

XXXIII International Conference
CAD IN MACHINERY DESIGN IMPLEMENTATION AND EDUCATIONAL ISSUES
11 - 13 December 2025, Białystok, Poland

DEEP LEARNING-BASED METHODS AND BIOLOGICALLY INSPIRED ALGORITHMS FOR SECURING CYBER-PHYSICAL MANUFACTURING SYSTEMS

Milica Petrović,

University of Belgrade, Faculty of Mechanical Engineerning, Department of Production Engineering, Laboratory for Industrial Robotics and Artificial Intelligence (ROBOTICS&AI),
Kraljice Marije 16, 11120 Belgrade 35, Serbia

mmpetrovic@mas.bg.ac.rs

Abstract: Driven by the principles of Industry 4.0, modern manufacturing systems increasingly rely on intelligent mobile robots that require a high degree of autonomy to meet contemporary market demands. While industrial robots are already widespread, mobile robotics introduces new challenges that call for advanced cognitive capabilities, particularly for small and medium-sized enterprises seeking global competitiveness. Deep learning–based autonomous subsystems enable industrial mobile robots to make more flexible, accurate, and robust real-time decisions than traditional deterministic sensor-driven approaches. This research direction aims to develop artificial intelligence–based solutions for cognitive mobile robotics using machine learning techniques such as convolutional neural networks. The focus is on creating new ML-based cognitive mechanisms for obstacle avoidance, decision-making, and vision-based control, and on integrating these capabilities into high-level cognitive architectures that improve environmental understanding and enhance the overall adaptability of mobile robotic systems within intelligent manufacturing environments.
At the same time, the increasing frequency of cyber-attacks on industrial systems poses significant risks, leading to machine tool failures and workflow disruptions that require rapid, adaptive responses. To address these security-driven disturbances, this research direction also investigates the flexible job shop scheduling problem under temporary machine breakdowns caused by cyber-attacks. After an attack is resolved, the affected machines must be reintegrated efficiently to restore production stability. To support real-time, adaptive rescheduling, the proposed research employs a Genetic Algorithm, a biologically inspired metaheuristic well suited to solve complex NP-hard scheduling problems. The proposed method optimizes two performance criteria: balanced machine utilization and mean flow time. Implemented in MATLAB® and validated on relevant benchmark problems, the proposed approach demonstrates improved responsiveness, resource efficiency, and system resilience under cyber-induced failures, complementing the broader goal of enabling intelligent, flexible, and secure manufacturing systems empowered by advanced cognitive robotics and AI-driven decision-making.
***Keywords*:** mobile robots, intelligent control systems, deep learning, autonomous systems, visual servoing, genetic algorithms, rescheduling, optimization, manufacturing systems, cyber-attacks.

ACKNOWLEDGEMENTS
This research was supported by the Science Fund of the Republic of Serbia, grant No. 17801, Cybersecurity of Motion Control Systems in Industry 4.0 – MCSecurity, and by the Ministry of Science, Technological Development and Innovations of the Serbian Government under the contract No. 451-03-137/2025-03/200105.

CADMD 2025

XXXIII International Conference
CAD IN MACHINERY DESIGN IMPLEMENTATION AND EDUCATIONAL ISSUES
11 - 13 December 2025, Białystok, Poland

DESIGN AND MANUFACTURE OF ACTIVE OPTICAL FIBERS WITH A RING-SHAPED CORE STRUCTURE

Piotr Miluski,

Bialystok University of Technology, Department of Photonics, Electronics and Lighting Technology, Wiejska 45D, 15-351, Bialystok, Poland

p.miluski@pb.edu.pl

Abstract: Silica optical fibers, in addition to their commercial applications in telecommunications, provide a compelling platform for the development of active photonic components such as optical amplifiers, lasers, and broadband emission sources. The high resistance of silica to large optical power densities and its low attenuation are crucial for designing rare-earth-doped fibers, especially for medium- and high-power laser applications. Variations in the refractive index of conventional step-index fibers, caused by nonlinear effects, scattering, and dispersion, can alter the modal structure and lead to instabilities in the output beam profile. These issues can be mitigated by employing fibers with advanced, structured core designs. New large-mode-area (LMA) optical fiber designs supporting Gaussian-like beam profiles will be presented. Implementing a multi-ring refractive-index structure enables a substantial increase in the effective propagation area of the fundamental mode (mode field area, MFA), in some cases by several orders of magnitude. Maintaining single-mode operation in such large-core fibers typically requires limiting the numerical aperture (NA) to below 0.1.

Moreover, new materials, doping techniques, and fiber architectures introduce new design, simulation of spectral metrological challenges related to parameter measurement and comprehensive fiber characterization.

The presentation will discuss recent designs of specialty optical fibers, including structured-core fibers, multi-ring fibers, and photonic-structure fibers intended for the transmission and generation of optical radiation with a controlled emission profile. Such fibers are used in systems ranging from narrowband laser sources to ultra-broadband generators.

Developing these fibers requires characterization of the optical, thermal, and luminescent properties of the materials. Key parameters include the refractive-index profile, dopant distribution, spectral attenuation, and absorption coefficient. In high-power fiber laser systems, it is also necessary to monitor aging effects arising from photodegradation of the glass matrix, which manifests as a reduction in output optical power.

The talk will present fundamental design, measurements and fabrication setups used for characterizing fiber preforms and specialty fibers operating in amplifier and laser configurations. It will also cover new large-mode-area (LMA) fiber designs, issues related to shaping the spatial profile of the output beam, and methods for evaluating beam quality. Additionally, selected applications of luminescent fibers with complex refractive-index profiles will be discussed, particularly new metrological uses such as atmospheric monitoring and free-space measurement systems.

***Keywords*:** Doped Optical Fibers, Lanthanides, Active Optical Fibers, Fabrication And Characterization

ACKNOWLEDGEMENTS
The research project was funded by the National Science Centre (Poland) granted on the basis of the decision no. UMO-2020/37/B/ST7/03094.

CADMD 2025

XXXIII International Conference
CAD IN MACHINERY DESIGN IMPLEMENTATION AND EDUCATIONAL ISSUES
11 - 13 December 2025, Białystok, Poland

DESIGN AND MANUFACTURE OF ACTIVE OPTICAL FIBERS WITH A RING-SHAPED CORE STRUCTURE

Zhuoqi Cheng,

University of Southern Denmark, Mærsk Mc-Kinney Møller Institute, Campusvej 55, 5230 Odense, Denmark

zch@mmmi.sdu.dk

Abstract: Every year >23M people die due to time-critical health conditions such as cardiovascular, respiratory diseases and traumatic injuries. As an estimated majority of these critical emergencies happen outside specialized hospitals, most of these deaths are a direct result of the lack of time in which emergency procedures can be delivered to these patients. Among the top life-saving procedures are heart catheters, hemorrhage control & extracorporeal membrane oxygenation (ECMO), which today are performed via the femoral artery as the standard of care. However, the femoral artery procedures can only be achieved by Specialized Physicians (SP) available in specialized hospitals.
To address this unmet need, the RAPID project aims to develop the first portable vascular robot, which provides means for the insertion of a needle into the femoral artery. By increasing early access to life-saving procedures, the RAPID project aims to decrease emergency mortality by 25%, corresponding to 1.780 lives saved annually in Denmark and 271.500 lives saved annually in the EU.
In the past 3 years, we have explored and developed robotic technologies to localize femoral artery based on a single Ultrasound element, track the needle tip and detect vessel puncture through optical scattering imaging processing. Eventually, the developed robot has been tested on pigs. In total, 13 puncture attempts were made. The system located the correct position every time within the scanned area. All punctures were successful in the end: 9 on the first try, and 4 with a small amount of human adjustment (three needed a bit of extra pressure on the device, and one required correcting the needle angle).

***Keywords*:** Portable Robot, Needle Insertion, Ultrasound Imaging, Puncture Detection, Optical Scattering, Convolutional Neural Network.

ACKNOWLEDGEMENTS
The RAPID project is a Grand Solutions research project granted by Innovation Fund Denmark in 2022 with three partners: NEURESCUE ApS, SDU Robotics and Rigshospitalet.

INDEX

2025